Epigenetic regulation via methylation on histone H3K27 is involved in leg regeneration patterning and photoperiodic responses of the circadian clock in the cricket *Gryllus bimaculatus*

フタホシコオロギの脚再生及び概日時計における

ヒストン H3K27 のメチル化を介したエピジェネティック制御

2016, March

Yoshimasa Hamada

Graduate School of Natural Science and Technology

Doctor's Course

OKAYAMA UNIVERSITY

Okayama, JAPAN

Table of contents · 2

Acknowledgement

I am grateful to my supervisor Prof. Kenji Tomioka, Graduate School of Natural Science and Technology, Okayama University, for his kind guidance, continuous help and constant inspiration throughout the progress of this work and in preparation of the thesis.

I thank Dr. Tetsuya Bando and Prof. Hideyo Ohuchi, Graduate School of Medicine, Dentistry and Pharmaceutical Sciences, Okayama University, for technical advice, helpful discussion and excellent comments especially about chapter 2.

I am thankful to all professors of the Graduate School of Natural Science and Technology, Okayama University, especially, Dr. Taishi Yoshii, Dr. Hideki Nakagoshi and Prof. Hitoshi Ueda for valuable suggestions and technical advice.

I should acknowledge present and previous members of the Chronobiology Laboratory for their support for my research activities, especially, Dr. Outa Uryu for technical advice and helpful discussion.

Abstract

Epigenetics is defined as heritable changes in gene expression that are not caused by changes in the DNA sequence. It is well known that epigenetic modifications, such as methylation, acetylation, ubiquitination and phosphorylation, on DNA, RNA or histone tail of core histones including H2A, H2B, H3 and H4. It is involved in various biological phenomena including pluripotency of iPSc, tumor suppression, pathogenesis of gene disorder, repression of allergy, seasonality of blooming, and behavioral learning. Methylation of lysine residue at 27th aa of histone H3 (H3K27) is a well-known epigenetic regulation that represses expression of neighboring genes via induction of heterochromatin formation by recruiting Polycomb group proteins. Conversely, demethylation of trimethylated histone H3K27 (H3K27me3) derepresses and promotes gene expression to switch the heterochromatin to euchromatin. To understand details in epigenetic mechanisms, I analyzed the function of methylation on H3K27 in leg regeneration processes and photoperiodic responses in circadian rhythms in the cricket *Gryllus bimaculatus*. The results showed that in the leg regeneration process, upregulation of histone H3K27me3 level regulates leg segment repatterning by alteration of the expression pattern of leg patterning genes and that in the circadian clock system, histone H3K27me3 is involved photoperiodic modulation of circadian locomotor rhythms via daily expression profiles of clock component genes. These results suggest that histone H3K27me3 is involved in the modulation of gene expression triggered by specific cues such as leg amputation and photoperiodic changes in the cricket.

List of abbreviations

ALM, accessory limb model
Am, *Apis mellifera*
ANOVA, analysis of variance
AP axis, anterior-posterior axis
BarH, *Bar homeobox*
β-cat, *beta-catenin*
bHLH, basic helix-loop-helix
dUTX, Drosophila UTX
Clk, *Clock*
CLK, CLOCK
cl, claw
cry, *cryptochrome*
CRY, CRYPTOCHROME
Cry2, *cryptochrome2*
CRY2, CRYPTOCHROME2
CT, circadian time
cyc, *cycle*
CYC, CYCLE
dac, *dachshund*
DD, constant darkness
DIG, digoxigenin
Dll, *Distal-less*
Dm, *Drosophila melanogaster*
Dnmt, *DNA methyltransferases*
dome, *domeless*
dpa, days post amputation
Ds, Dachsous
ds, *dachsous*
dsRNA, double-stranded RNA
DV axis, dorsovental axis
Egfr, *Epidermal growth factor receptor*
E(z), Enhancer of zeste
Fe, femur
Ft, Fat
ft, *fat*
Gb, *Gryllus bimaculatus*
H3K27, lysine residue 27th of histone H3
H3K27me3, trimethylated histone H3K27
hop, *hopscotch*
Hs, *Homo sapiens*
iPSc, induced pluripotent stem cell
K, lysine
LD, light-dark cycle
Lft, Lowfat

lft, *lowfat*
Mm, *Mus musculus*
Ms, *Modicogryllus siamensis*
PAS, stands for PER, ARNT and SINGLEMINDED
PBT, phosphate-buffered saline with Tween 20
Pc, *Polycomb*
PCP, planar cell polarity
pdf, *pigment-dispersing factor*
PDF, pigment-dispersing factor
per, *period*
PER, PERIOD
PFA, paraformaldehyde
Ph, pharyngeal
Pr, prepharyngeal
PD axis, proximodistal axis
qRT-PCR, quantitative RT-PCR
R, arginine
RISC, RNA-induced silencing complex
RNAi, RNA interference
RPKM, reads per kilobase per million reads
S, serine
SCN, suprachiasmatic nuleus
SET, Su(var)3-9, Enhancer of zeste and Trithorax
Shh, *Sonic hedgehog*
T2 leg, mesothoracic leg
Ta1, tarsomere 1
Ta2, tarsomere 2
Ta3, tarsomere 3
Ta, tarsus
Tas, tarsal super
Ti, tibia
Tis, tibial super
tim, *timeless*
TIM, TIMELESS
UTR, untranslated region
Utx, *Ubiquitously transcribed tetratricopeptide repeat gene on the X chromosome*
ZT, zeitgeber time

Chapter 1.
General introduction

Epigenetics is defined as heritable changes in gene expression without changes in the DNA sequence (Lan *et al*., 2007; Stewart *et al*., 2009; Wyngaarden *et al*., 2011). Examples of visible epigenetic regulation are aging, cancer development, lifestyle-related diseases, a calico cats manifestation, caste formation by royalactin in honeybees, variation of properties in monozygotic twins and so on (Brunet and Berger, 2014; Cridge *et al*., 2015; Dawson and Kouzarides, 2012; Herb, 2014; Hochedlinger and Plath, 2009; Kalantry, 2011). These are caused by changes in chromatin structure that is induced by various epigenetic factors chemically modifying DNA, RNA, or histone tail (Hamon and Cossart, 2008). However, it is still unknown how epigenetic regulations modulate broad biological phenomena. There is evidence that epigenetic regulation contributes to the pluripotency of stem cells in regenerating tissues although the relationship between epigenetic regulation and repatterning mechanism in regeneration process remains unresolved (Hamon and Cossart, 2008). Epigenetic regulation is implicated to regulate gene expression involved in the circadian clock and in its photoperiodic responses, but the mechanism remains to be explored (Asher *et al*., 2008). The aim of this study is to clarify the role of epigenetic regulations and its commonality and diversity in leg regeneration and circadian rhythm.

1.1. The boundaries between regenerative and non-regenerative animals

An organ regeneration therapy is one of the biggest dreams of human. It is well known that regenerative ability of mammalian is extremely limited; human can regenerate hair, nail, skin, liver, erythrocyte and muscle (Fig. 1-1A). Additionally, common experimental model animals, such as mice and flies, also show lower regenerative ability: neonatal and adult mice can only regenerate the distal part of the finger when amputated from the first joint, and skin, muscle and bone (Borgens, 1982; Miura *et al*., 2015; Muneoka *et al*., 2008; Neufeld and Zhao, 1995) and *Drosophila* can regenerate only imaginal discs but not their legs or wings (Bryant, 1975; Campbell and Tomlinson, 1995; Gibson and Schubiger, 1999; Meinhardt, 1982; Strub, 1979). Accordingly, the regeneration process has been dissected by using high regenerative models. In amphibians, newts can regenerate

lost part of tissues such as limbs, optical tissues (lens, retina and cornea), brain, spinal cord, intestine, and heart (Hayashi *et al*., 2013) (Fig. 1-1B). Axolotls also show high regenerative ability, and they can produce ectopic limb (called "accessory limb") (Fig. 1-1C). The accessory limb model proposed a stepwise model for limb regeneration that regeneration requires nerve and polarity (Endo *et al*., 2004; Satoh *et al*., 2015). Interestingly, tadpoles regenerate complete limbs without non-regenerative stage, but the regenerative ability is gradually lost in association with growth: flogs regenerate incomplete rod like limbs (called "spike") (Mitogawa *et al*., 2015; Miura *et al*., 2015) (Fig. 1-1D). The boundary between regenerative and non-regenerative animals is across animal phyla. For example, planarians, *Dugesia japonica*, show highly regenerative ability so that they can regenerate head region from amputated tail fragment and regenerate tail region from amputated head fragment (Fig. 1-1E). Of the other planarian species, *Phagocata kawakatsui*, also can regenerate tail region from amputated head fragment, but they cannot regenerate head region from amputated tail fragment (Fig. 1-1E). These facts indicate difficulty in defining boundary between regenerative and non-regenerative animals (Agata and Inoue, 2012). Umesono *et al.* (2013) discussed the difference in regenerative profiles between the two planarians species. In *Dugesia japonica,* they demonstrated that interaction between reciprocally gradient ERK signaling and Wnt/beta-catenin (β-cat) signaling in anterior-posterior axis modulates regenerative manner of head, prepharyngeal (Pr), pharyngeal (Ph), and tail regions. When planarian stem cells, called neoblast, are stimulated by ERK signaling, the cells differentiate into head cell. Then, the cells are transformed into Pr, Ph or tail cell as Wnt/β-cat signaling represses the ERK signaling level. Further investigation, based on this model, demonstrated that overexpression of Wnt/β-cat signaling caused defect in regenerative ability of head region from amputated tail fragment in *Phagocata kawakatsui*, and that head region is regenerated from amputated tail fragment by RNAi against *beta-catenin* (Umesono *et al*., 2013). These findings provided an insight into fundamental regeneration mechanisms in high regenerative animals, such as newts, axolotls, flogs and crickets (Hayashi *et al*., 2015b; Makanae *et al*., 2014a; Makanae *et al*., 2014b; Mitogawa *et al*., 2014; Tsutsumi *et al*., 2015).

In the future, it is expected that the regeneration mechanism from regenerative animals is applied to non-regenerative animals, such as human, mice and flies, to regenerate the lost part of tissue.

1.2. The process of leg regeneration in the cricket *Gryllus bimaculatus*

Leg regeneration study of insect has been used cockroach, cricket and *Tribolium* (French, 1976; Mito and Noji, 2008; Shah *et al*., 2011). To understand the regeneration mechanism, I selected the two-spotted cricket, *Gryllus bimaculatus*, which has high regenerative ability and can be used as regenerative emerging model animal for various experiments, such as leg regeneration, transplantation, quantitative RT-PCR, *in situ* hybridization, immunostaining, RNA interference (RNAi), genome editing, and production of transgenic strains (Bando *et al*., 2013; Hamada *et al*., 2015; Ishimaru *et al*., 2015; Matsuoka *et al*., 2015; Nakamura *et al*., 2010; Watanabe *et al*., 2012). The cricket leg is composed of six segments that are arranged along the proximodistal (PD) axis, i.e., coxa, trochanter, femur, tibia, tarsus, and claw. The tarsus is further subdivided into three tarsomeres. When the tibia of the third-instar nymph is amputated, the leg regenerates and recovers its allometric size and proper shape by the sixth instar (i.e., within 20 days of amputation), being restored to almost normal adult size and shape. Soon after healing, the blastema (which is a mass of proliferative cells) develops in the distal region of the amputated leg. Blastemal cells have most distal positional identity (called ‘distalization’), proliferate and form the missing structures by intercalary processes between the most distal region and the remaining part of the continuous positional value of the leg (Agata *et al*., 2007). Previously, Bando *et al*., 2013 performed comparative transcriptome analysis of regenerating and normal amputated legs of crickets to profile mRNA expression associated with leg regeneration (Bando *et al.*, 2013). The one of the upregulated genes in the transcriptome analysis, the Jak/Stat pathway genes, which is linked to the immune system, were focused on. RNAi of the Jak/Stat signal pathway component genes, the regenerated leg was induced leg regeneration disruption. In contrast, RNAi against *Gryllus* homologue of *Socs* (*Gb’Socs*), a suppressor of cytokine signaling, resulted in leg elongation. Additional experiments

showed that the Jak/Stat pathway promotes cell proliferation downstream of the Dachsous/Fat (Ds/Fat) pathway (Bando *et al*., 2011; Bando *et al*., 2009). The Ds/Fat pathway is downstream of Hippo pathway that regulates planar cell polarity (PCP), cell proliferation and tumor suppressors. RNAi against *Gryllus* homologue of *ds* (*Gb'ds*) or *fat* (*Gb'fat*), resulted in the regenerated legs were shorter and thicker than control ones. Following, Lowfat (lft) is the only molecule that has been shown to interact with the intracellular domains of both Ds and Fat in *Drosophila* (Mao *et al*., 2009). In the crickets treated with RNAi against *Gryllus* homologue of *lft* (*Gb'lft*), the length of regenerated tibia was shorter than control one, but the overproliferation that observed in regenerated legs of *Gb'fat* and *Gb'ds* were not caused by RNAi against *Gb'lft*. Dual RNAi against *Gb'ds* and *Gb'lft* or *Gb'fat* and *Gb'lft* resulted in regeneration legs were not distinguishable from $Gb'lft^{RNAi}$ crickets. These findings demonstrated that Ds/Fat pathway regulates positional value and cell proliferation in regenerating legs (Bando *et al*., 2011).

1.3. Epigenetics for tissue regeneration

When a leg is amputated at distal tibia of third-instar nymph, the amputated surface is first covered by wound epidermis, and then blastema cells are formed. Blastema cells are the mass of undifferentiated cells that emerge from differentiated cells losing their cell fate by cell division ('dedifferentiation'), and differentiate into several types of unipotent cells ('redifferentiation') to restore the lost tissue part following the expression of tissue patterning genes ('repatterning'). These differentiated cells and blastema cells display different gene expression patterns. During the dedifferentiation and repatterning processes, epigenetic factors may play a key role in changing gene expression in both cell types (Hayashi *et al*., 2015a; Yakushiji *et al*., 2007; Yakushiji *et al*., 2009; Yakushiji-Kaminatsui *et al*., 2016). For instance, the regenerative ability of zebrafish fin was interfered by knock down of *Kdm6b1* which is a histone H3K27 tridemethylase (Stewart *et al*., 2009). To clarify the molecular basis of epigenetic regulation on these prosesses during leg regeneration in the cricket, the function of the *Gryllus bimaculatus* homologues of *Enhancer of*

zeste (*Gb'E(z)*) and *Ubiquitously transcribed tetratricopeptide repeat gene on the X chromosome* (*Gb'Utx*) homologues were highlighted. *Gb'E(z)* and *Gb'Utx* regulate methylation and demethylation of histone H3 lysine 27 (H3K27), respectively (Hamada *et al*., 2015; Matsuoka *et al*., 2015) and were found to be upregulated in regenerating legs compared with non-regenerating legs by transcriptome analysis (Bando *et al*., 2013). To analyze the role of *Gb'E(z)* and *Gb'Utx* regulation, their dsRNA treated ($Gb'E(z)^{RNAi}$ and $Gb'Utx^{RNAi}$) crickets were dissected the phenotype and gene expression in leg regeneration.

1.4. Observations on circadian rhythms of insects

The majority of insects show daily activity rhythms that synchronize to daily environmental cycles such as light dark cycles (LD) caused by the Earth's rotation. They are nocturnal, diurnal or crepuscular. For example, cockroaches show nocturnal locomotor activity rhythms in LD conditions. Under constant conditions of light and temperature the rhythm persist for several months (Roberts, 1960). The fly, *Drosophila melanogaster*, shows bimodal locomotor activity rhythms with peaks around dawn and before dusk under LD condition. When the flies are transferred from LD to DD, they show free-running rhythms with a period of approximately 24 h (Konopka and Benzer, 1971). Humans also show rhythms with an approximately 24 h period (Wright *et al*., 2012). Thus, there is the common circadian rhythm system conserved from insects to mammals to adapt to the cyclic environment. In mice, the length of activity phase was altered depending on the length of dark phase (Refinetti, 2002), and the phenomenon was also observed in the cricket *Gryllus bimaculatus* (Koga *et al*., 2005). The physiological responses to seasonal changes in light cycles are called photoperiodic responses. The cricket *Modicogryllus siamensis* shows photoperiodic responses in their nymphal development and the photoperiodic sensitive stage is limited during the first and second instar nymphal stages (Tamaki *et al*., 2013; Taniguchi and Tomioka, 2003). But, the detailed mechanism of the photoperiodic response still remains elusive. The cricket *G. bimaculatus* shows nocturnal locomotor activity with the activity concentrating

during night and the rhythm persists in constant conditions in the laboratory (Tomioka and Chiba, 1982). It is expected that elucidation of the mechanism for photoperiodic response of circadian rhythms in *G. bimaculatus* will promote dissection of the mechanism underlying the photoperiodic response of *M. siamensis*.

1.5. Localization of the circadian pacemaker in insects

The pacemakers regulating the circadian rhythm have been studied and localized to separate regions of the brain. The central clock organ of insects is divided into two classes, i.e. the optic lobe and the central brain. The optic lobes are bilaterally paired structure residing between the compound eye and the brain and receive light information from the compound eye (Fig. 1-2A). In crickets and cockroaches, the clock has been localized in the optic lobe. Removal of the two optic lobes resulted in a loss of locomotor rhythms in the cockroach *Leucophaea maderae* and the cricket *G. bimaculatus* (Page *et al*., 1977; Tomioka and Chiba, 1984; Tomioka and Chiba, 1989b). These insects have been used for circadian rhythm research using many of the modern experimental techniques, such as RNAi, quantitative RT-PCR, and *in situ* hybridization. In contrast to cockroaches and crickets, studies on flies and moths indicated importance of the central brain as the site of the circadian pacemaker. In silkmoths (*Antheraea pernyi* and *Hyalophora cecropia*) extirpation of the optic lobes had no effect on the persistence of the flight activity rhythm, but removal of the cerebral lobes resulted in arrhythmic flight activity (Truman, 1974). Locomotor activity rhythms of the house fly *Musca domestica* continued after surgical lesion of the optic lobes but disappeared after lesions of the cerebral lobe (Helfrich *et al*., 1985). The importance of the cerebral lobe in the rhythm generation was also shown by a transplantation experiment in the fruit fly *D. melanogaster* (Handler and Konopka, 1979).

1.6. Molecular oscillatory mechanism of the insect circadian clock

The oscillatory mechanism of the circadian clock is based on transcriptional/translational molecular feedback loops (Dunlap, 1999). In insects, the clock machinery has been most profoundly studied in the fruit fly *Drosophila melanogaster* (Fig. 1-2B). The major players of the clock machinery are *Clock* (*Clk*) and *cycle* (*cyc*). Their product proteins CLK and CYC contain a basic helix-loop-helix (bHLH) region that allows them to bind to a short DNA sequence called E-box in the promoter region of *period* (*per*) and *timeless* (*tim*) (Kyriacou and Rosato, 2000). PER and TIM proteins increase during the night and heterodimerize in the cytoplasm and enter the nucleus to repress their own transcription by inhibiting the CLK-CYC (Allada *et al*., 1998; Rutila *et al*., 1998; Williams and Sehgal, 2001). Similar clock component genes have been found in the cricket *G. bimaculatus* (Moriyama *et al*., 2008; Uryu *et al*., 2013).

1.7. The epigenetic regulation of circadian rhythms

Epigenetics is defined as heritable changes in gene expression that are not caused by changes in the DNA sequence (Lan *et al*., 2007; Stewart *et al*., 2009; Wyngaarden *et al*., 2011). It becomes evident that the regulation of circadian gene expression is at least in part regulated by epigenetic modifications, especially deacetylation and phosphorylation on DNA or histone tail of H3 (Asher *et al*., 2008). In fact, recent studies revealed that the cycling of the circadian clock is precisely controlled by a mechanism including chromatin remodeling, recruitment of RNA polymerases, posttranscriptional and posttranslational modifications (Aguilar-Arnal and Sassone-Corsi, 2013; Bellet and Sassone-Corsi, 2010; Doi *et al*., 2006; Hwang-Verslues *et al*., 2013; Ripperger and Merrow, 2011; Yung *et al*., 2015). The chromatin remodeling is now recognized to play an important role in regulation of circadian clock and its response to environmental time cues. In both mammals and insects, CLK not only plays as a transcriptional activator but also at the same time recruits other transcription factors by binding E-boxes at the regulatory region of the clock

controlled genes, including *per* and *tim* (Doi *et al*., 2006; Menet *et al*., 2014; Taylor and Hardin, 2008). Although the involvement of epigenetic regulation in the circadian clock machinery was found in various organisms from *Neurospora crassa* to mice, the detailed mechanism of epigenetic control of the molecular machinery of the circadian clock still remains largely unknown.

1.8. The objective of this study

The leg regeneration process and the photoperiodic response of the circadian clock are both long-lasting and gradually changing phenomena and most likely include epigenetic regulation. In this study, I addressed the following four issues: (1) effects of H3K27me3 level for cricket leg regeneration, (2) modulation of leg patterning genes by H3K27me3 levels, (3) photoperiodic modulation of locomotors rhythms by *Gb'E(z)*, (4) function of *Gb'E(z)* in the photoperiodic regulation of molecular oscillatory mechanism of the circadian clock. The epigenetic gene *E(z)* was cloned based on transcriptome data base of the cricket *G. bimaculatus* and its function in leg regeneration and circadian rhythm modulation was analyzed with RNAi mediated gene silencing method. I first attempted to determine the optimal concentration of dsRNA for systemic RNAi of epigenetic gene because high dsRNA concentration used for knocking-down genes related to development caused lethal. To investigate the relationships between the epigenetics and leg regeneration or circadian system in the crickets, expression of leg patterning genes and circadian clock genes were examined by *in situ* hybridization and quantitative real-time reverse transcribed PCR (qPCR) (Fig. 1-3). The goal of this study was to obtain the fundamental knowledge on the function of *Gb'E(z)* in the cricket *G. bimaculatus* and to establish the cricket as a good emerging model insect for molecular study of epigenetics.

Figures and Figure legends

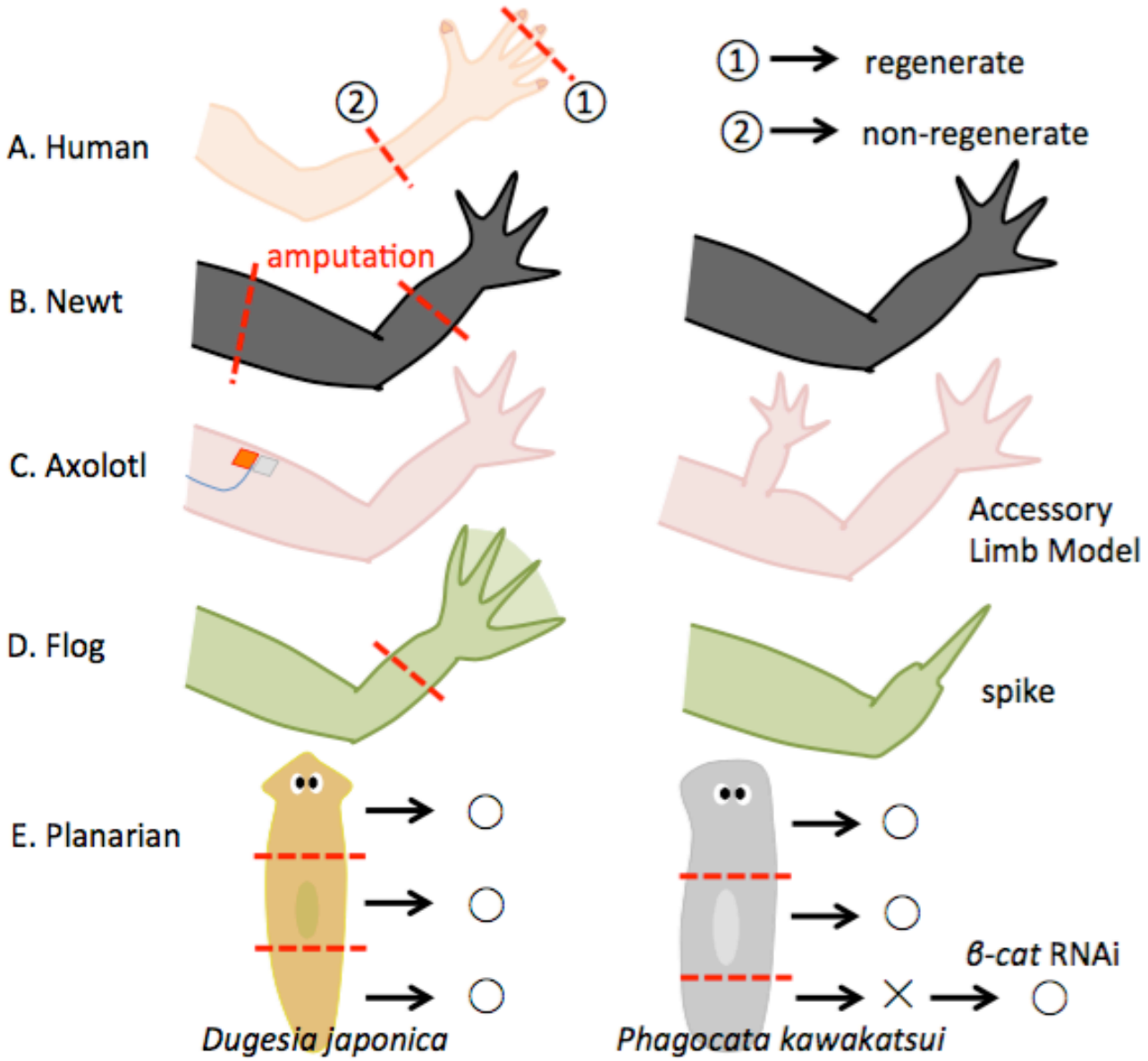

Fig. 1-1. Regenerational diversity in regenerative animals and non-regenerative animals. (A) Mammalian animals such as humans or mice show partially regenerative ability that can only regenerate some internal organs and distal tips. (B) Newts can regenerate whole body or structure such as limb and tentacles in adult. (C) Axolotls can induce bumps and accessory limbs in response to wounding and nerve provision A piece of skin from the opposite side of the contralateral limb (red panel) is transplanted beside the wound skin (gray panel) to which a nerve (blue line) is deviated. (D) Tadpoles can regenerate the completely limb, but flogs can regenerate rod like structure "called spike". (E) Planaria *Dugesia japonica* can regenerate whole body from head, middle (prepharyngeal and pharyngeal) and tail fragment, while *Phagocate kawakatsui* cannot regenerate head region from tail fragment, but *β-cat* RNAi induce regeneration of head region.

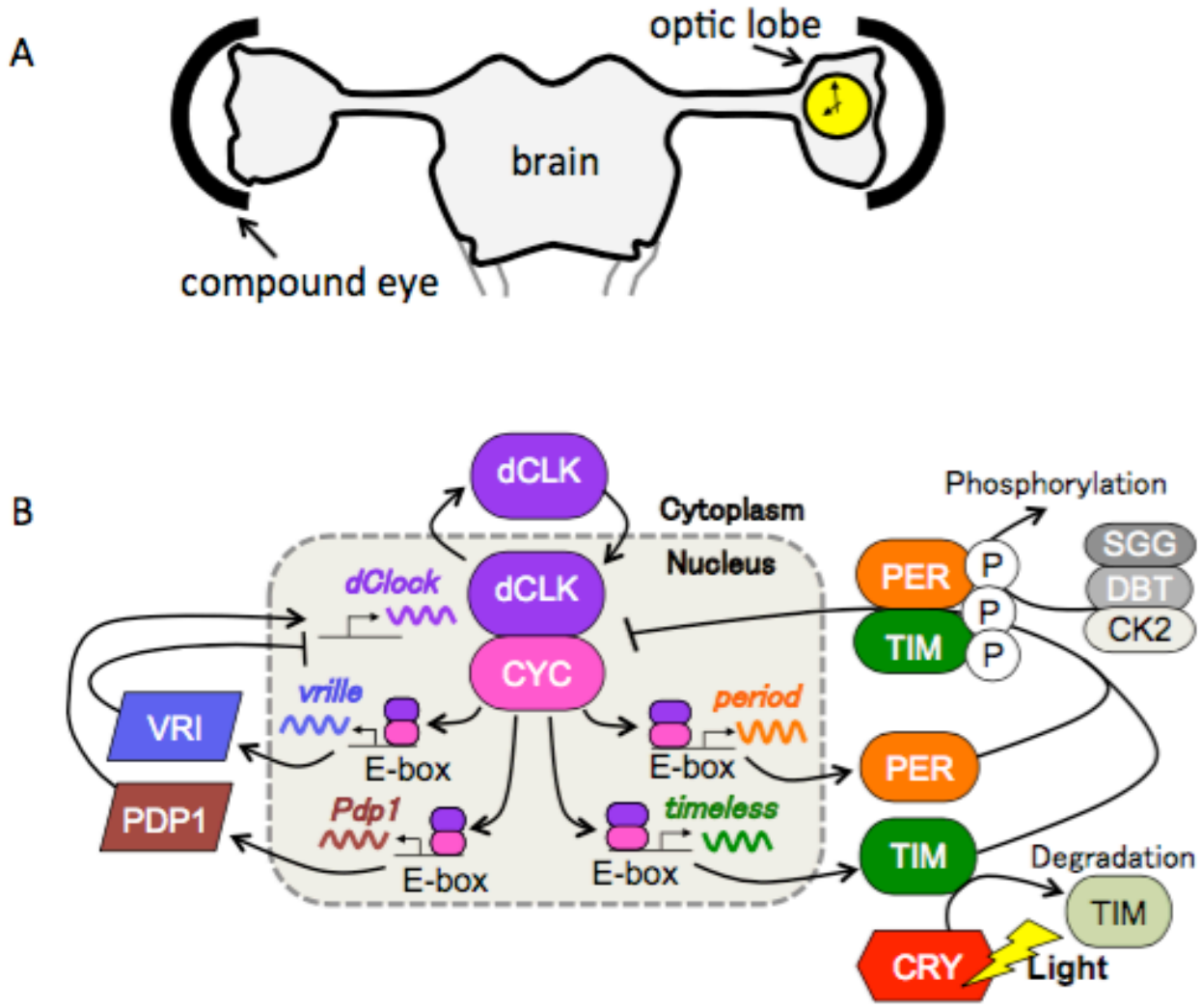

Fig. 1-2. The central clock structure and clock oscillatory mechanism in the cricket and the fly. (A) The central clock structure in the cricket, *Gryllus bimaculatus*. The central clock localized in optic lobe which is located between compound eye and brain. (B) The molecular oscillatory mechanism of the *Drosophila* circadian clock. CLK and CYC form a heterodimer that promotes transcription of *per*, *tim*, *vri* and *Pdp1ε* through E-box. During the day, translated TIM proteins are degraded by light-activated CRY. PER and TIM form a complex that is capable of moving into the nucleus. The complex represses transcription of *per* and *tim* through inhibitory action on CLK-CYC. Phosphorylated PER and TIM are degraded by the proteasome system. The CLK-CYC heterodimer is thus released from suppression to reactivate *per* and *tim* transcription, starting the next cycle. VRI and PDP1ε repress and activate *Clk* transcription, respectively, leading to a rhythmic expression of CLK.

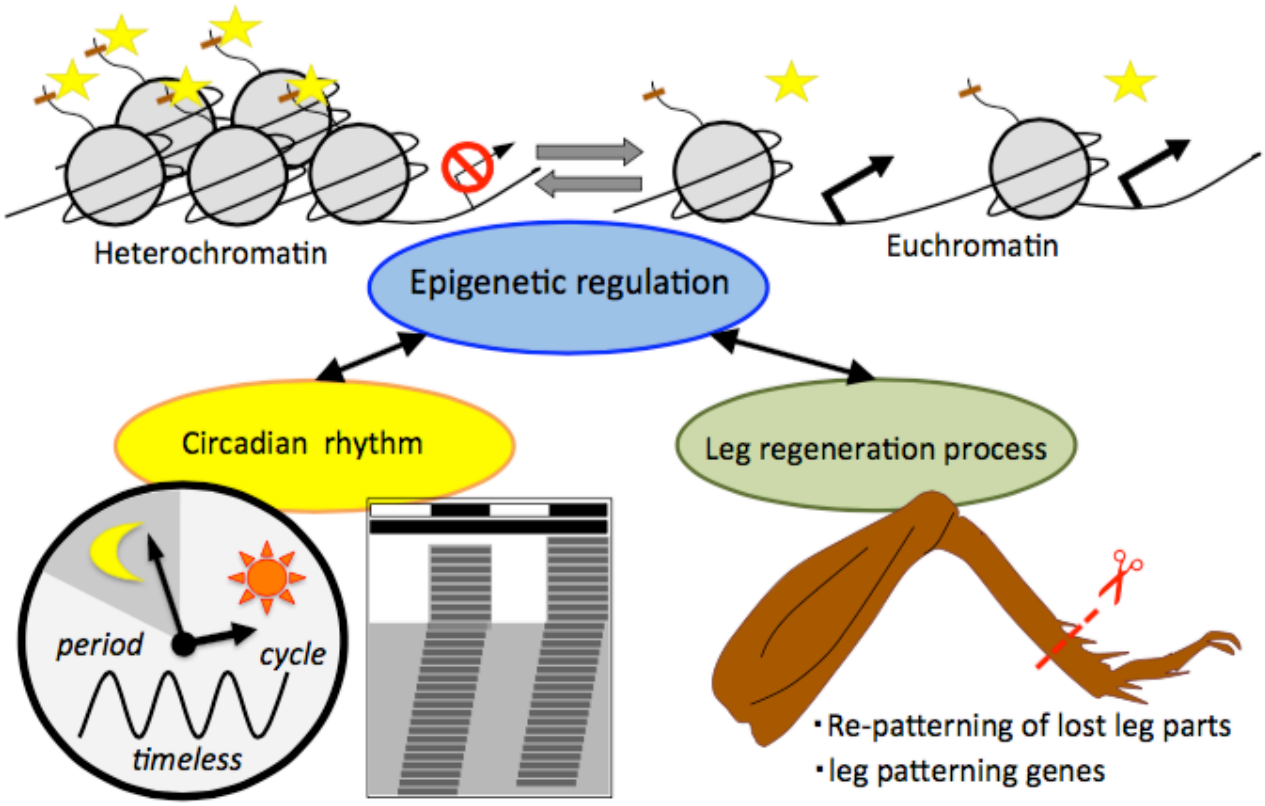

Fig 1-3. The landscape of this study. The upper image shows the epigenetic regulation based on reversible changes of chromatin structure by chemical modifications on DNA, RNA or histone tail. The lower image shows subjects of this study, i.e., epigenetic regulation of circadian rhythm and leg regeneration.

Chapter 2.

Leg regeneration is epigenetically regulated by histone H3K27 methylation

2.1. Abstract

Hemimetabolous insects such as the cricket *Gryllus bimaculatus* regenerate lost tissue parts using blastemal cells, which is a population of dedifferentiated-proliferating cells. The gene expression of several epigenetic factors is upregulated in the blastema compared with the expression in differentiated tissue, suggesting that epigenetic changes in gene expression may control the differentiation status of blastema cells during regeneration. To clarify the molecular basis of epigenetic regulation during regeneration, in this report focused on the function of the *Gryllus Enhancer of zeste* (*Gb'E(z)*) and *Ubiquitously-transcribed tetratricopeptide repeat gene on the X chromosome* (*Gb'Utx*) homologues that regulate the methylation and demethylation on histone H3 27th lysine residue (H3K27), respectively. Methylated histone H3K27 in the regenerating leg was diminished by *Gb'E(z)*^{RNAi} and was increased by *Gb'Utx*^{RNAi}. Regenerated *Gb'E(z)*^{RNAi} cricket legs exhibited extra leg segment formation between the tibia and tarsus, and regenerated *Gb'Utx*^{RNAi} cricket legs showed leg joint formation defects in the tarsus. In the *Gb'E(z)*^{RNAi} regenerating leg, the *Gb'dac* expression domain expanded in the tarsus. In contrast, in the *Gb'Utx*^{RNAi}-regenerating leg, *Gb'Egfr* expression in the middle of the tarsus was diminished. These results suggest that regulation of the histone H3K27 methylation state is involved in the repatterning process during leg regeneration among cricket species via the epigenetic regulation of leg patterning gene expression.

2.2 Introduction

Regeneration is a phenomenon in which animals restore lost tissue parts using remaining cells. This phenomenon is observed in various organisms ranging from the sponge to vertebrates, including planarians, insects, fishes and urodeles; however, the regenerative capacity of humans, mice and chicks is limited (Agata and Inoue, 2012). When regenerative animals lose tissue sections, a wound epidermis immediately covers the wound surface. Subsequently, a population of proliferating multipotent cells or pluripotent stem cells develops into a blastema beneath the wound

epidermis. The lost tissue is restored using the blastema cells via a repatterning process that depends on positional information and pattern formation genes. In planarians, blastema cells originate from stem cells called neoblasts (Handberg-Thorsager *et al*., 2008). In other regenerative animals, including insects, differentiated cells lose their cell fate to produce blastema cells (i.e., the "dedifferentiation" process) (Konstantinides and Averof, 2014; Tamura *et al*., 2010; Truby, 1985; Tweedell, 2010). Blastema cells differentiate into several types of unipotent cells (i.e., the "redifferentiation" process) to restore the lost tissue part following the expression of tissue patterning genes, so-called "repatterning". These differentiated cells and blastema cells display different gene expression patterns, although the genome sequences of these cells are not different. Therefore, during the dedifferentiation and redifferentiation processes, epigenetic factors may play a key role in modulating gene expression in both cell types.

Epigenetics is defined as heritable changes in gene expression that are not caused by changes in the DNA sequence (Lan *et al*., 2007; Stewart *et al*., 2009; Wyngaarden *et al*., 2011). The epigenetic regulation of gene expression is primarily mediated by the methylation of specific DNA nucleotides and posttranslational histone modification. Methylation of the cytosine DNA base is an irreversible reaction that represses the expression of neighboring genes via the formation of inactive chromatin. Other epigenetic events include chemical modifications such as methylation, acetylation, phosphorylation and ubiquitination of specific amino acid residues of the N-terminal tail of histones H2A, H2B, H3 and H4. Methylation of the 27th lysine residue on histone H3 (H3K27) is a well-known epigenetic mark that represses the expression of neighbouring genes via the induction of heterochromatin formation by recruiting Polycomb group proteins. Conversely, demethylation on trimethylated histone H3K27 (H3K27me3) derepresses and promotes gene expression to change heterochromatin into euchromatin.

During tissue regeneration, epigenetic modifications may change during the dedifferentiation and redifferentiation processes (Katsuyama and Paro, 2011; McCusker and Gardiner, 2013; Tamura *et al*., 2010; Tweedell, 2010). In the frog *Xenopus laevis*, the regenerative capacity gradually

decreases during development, and this decrease is caused by the downregulation of *Sonic hedgehog* (*Shh*) expression mediated by epigenetic mechanisms (Tamura *et al*., 2010; Yakushiji *et al*., 2007; Yakushiji *et al*., 2009). In contrast, the regenerative capacity of the newt *Cynops pyrrhogaster* is not limited by growth because epigenetic modification of the newt *Shh* locus does not change throughout growth (Yakushiji *et al*., 2007). In zebrafish, a lost part of the caudal fin is regenerated from the blastema, and the lost fin part is not regenerated in *kdm6b1* morphant fish, which encodes a histone H3K27me3 demethylase (Stewart *et al*., 2009). Jmjd3 and Utx, which also encode histone H3K27me3 demethylases, are required for murine skin repair (Shaw and Martin, 2009). The SET/MLL family of histone methyltransferases is essential for stem cell maintenance in the planarian *Schmidtea mediterranea* (Hubert *et al*., 2014; Robb and Sanchez, 2014). In *Drosophila* imaginal disc regeneration, the expression of Polycomb group genes is downregulated in the blastema of amputated discs, which suppresses methylation on histone H3K27 (Lee *et al*., 2005; Repiso *et al*., 2011; Sun and Irvine, 2014; Worley *et al*., 2012). Epigenetic regulation of gene expression affects stem cell plasticity in mammals, and the expression of stem cell-related and differentiated cell-related genes (Barrero and Izpisua, 2011) is epigenetically changed during the differentiation process from stem cells to differentiated cells via the histone H3K4 and H3K27 methylation states (Barrero and Izpisua, 2011). Histone H3K27 methylation by Ezh2 in mammals affects the reprogramming efficiency of iPS cells derived from fibroblasts *in vitro* (Ding *et al*., 2014; Hochedlinger and Plath, 2009). These early studies imply that epigenetic regulation of gene expression plays a key role in dedifferentiation and redifferentiation during regeneration.

The two-spotted cricket *Gryllus bimaculatus,* a hemimetabolous insect, has a remarkable regenerative capacity to restore a missing distal leg part. The cricket leg consists of six segments arranged along the proximodistal (PD) axis in the following order: coxa, trochanter, femur, tibia, tarsus, and claw (Fig. 2-1A). When a metathoracic leg of a *Gryllus* nymph in the third instar is amputated at the distal position of the tibia, the distal missing part is restored after one month during four molts that occur subsequent to the amputation. After the amputation of a leg, a blastema

forms beneath the wound epidermis, similar to other regenerative organisms. The lost part of the tissue is regenerated using blastemal cells and is dependent on the expression of signalling molecules such as the *Gryllus wingless*, *decapentaplegic* and *hedgehog* homologues, and leg patterning genes including *dachshund* (*Gb'dac*), *Egf receptor* (*Gb'Egfr*), *Distal-less* (*Gb'Dll*), and *BarH* (*Gb'BarH*) (Ishimaru *et al*., 2015; Mito *et al*., 2002; Nakamura *et al*., 2008a; Nakamura *et al*., 2008b; Nakamura *et al*., 2007). The blastemal expression of these genes is activated during regeneration and may be epigenetically regulated during this process. However, the underlying mechanisms regulating gene expression during dedifferentiation and redifferentiation processes in tissue regeneration remain elusive.

In a previous study to identify the molecules that undergo expression changes in the blastema, the comparative transcriptome analysis revealed the several epigenetic factors that is upregulated in the blastema (Bando *et al*., 2013). In this study, the function of *Gb'E(z)* and *Gb'Utx* was focused on the leg regeneration process. Here, this report show that *Gb'E(z)* and *Gb'Utx* are involved in the repatterning process during regeneration via gene expression regulation of leg patterning genes.

2.3. Materials and methods

Animals

All two-spotted cricket *Gryllus bimaculatus* nymphs and adults were reared under standard conditions (L: D = 12 hour: 12 hour, 28°C) (Mito and Noji, 2008). Field crickets *Modicogryllus siamensis* were reared under long-day conditions (L: D = 16 hour: 8 hour, 25°C) (Tamaki *et al*., 2013).

Cloning of the *Gryllus* homologues

Gryllus E(z) and *Utx* homologues were cloned by PCR with LA-taq or Ex-taq in GC buffer (TaKaRa, Kyoto, Japan). Primers were designed based on the nucleotide sequence determined by

the transcriptome data. Template cDNAs were synthesised using SuperScript III reverse transcription kit with random primes (Invitrogen, Carlsbad, CA, USA) from total RNA extracted from regenerating legs at third instar nymphs or late stage embryos (Bando *et al*., 2009). *Gb'E(z)* and *Gb'Utx* nucleotide sequences were deposited in GenBank under the LC012934 and LC012935 accession numbers, respectively.

RNAi

Double stranded RNAs (dsRNAs) were synthesised using the MEGAScript T7 Kit (Ambion, Carlsbad, CA, USA) and adjusted to 20 μM for RNAi. In total, 200 nL of dsRNA was injected into the abdomens of the cricket nymphs. The cricket that injected dsRNA for exogenous genes *DsRed2* or *Egfp* was used as a negative control.. After dsRNA injection, the legs of the crickets were amputated at the appropriate positions (Mito and Noji, 2008).

Whole-mount *in situ* hybridization

Regenerating legs were cut off and fixed with 4% paraformaldehyde (PFA) in phosphate-buffered saline with Tween 20 (PBT) for 6 min at 55°C with a microwave oven. The scab and cuticle were removed using tweezers under dissecting microscopy. The regenerating legs were refixed in 4% PFA/PBT. Whole-mount *in situ* hybridization of regenerating legs was conducted as previously described (Bando *et al*., 2011; Bando *et al*., 2009). Antisense and sense probes were labelled with digoxigenin (DIG).

Immunostaining

Fixed regenerating legs were washed with PBT and blocked with 1% bovine serum albumin (BSA) in PBT for 1 hour. Blocked samples were incubated with primary antibody (rabbit polyclonal anti-trimethylated H3K27 antibody (Millipore 07-449, Billerica, MA, USA)) at 1:500 in 1% BSA in PBT overnight at 4°C. Next, the samples were blocked with 1% BSA in PBT and incubated with

secondary antibody (AlexaFluor488 conjugated anti rabbit IgG antibody (Molecular Probes A-11008, Carlsbad, CA, USA)) at 1:500 in 1% BSA/PBT for 3 hour at 25°C. Samples were washed with PBT and incubated with DAPI at 1:1000 in PBT for 15 min (Nakamura *et al*., 2008b).

2.4. Results

Gb'E(z) and *Gb'Utx* are expressed in regenerating legs

Previous study reported that the expression of several epigenetic factors was upregulated in the blastema during cricket leg regeneration based on comparative transcriptome analysis. The highest RPKM (reads per kilobase per million reads) ratio observed between the blastema and non-regenerative tissue was 8.9 for *Gb'Utx*, which encodes a histone H3K27 demethylase. The expression of *Gb'E(z)*, which encodes a histone H3K27 methyltransferase, and *Gb'Polycomb* (*Gb'Pc*), which encodes a histone H3K27me3-binding protein, is also upregulated in the blastema (Bando *et al*., 2013).

To further analyze the significance of epigenetic regulation via methylation on histone H3K27 during regeneration, *Gb'E(z)* and *Gb'Utx* full-length transcripts was identified from transcriptome data. *Gb'E(z)* encodes a 746 amino acid residue protein, and a histone methyltransferase (SET, Su(var)3-9, Enhancer of zeste and Trithorax) domain was found in the *Gb'*E(z) C-terminus. Amino acid sequence comparison of the *Gb'*E(z) SET domain compared with *Drosophila melanogaster* E(z) and *Homo sapiens* EZH2 showed 96% and 95% identity, respectively (Fig. 2-1B). In *Gryllus* and *Drosophila,* a single *E(z)* gene was found in their genomes; however, two paralogous genes, *EZH1* and *EZH2*, were found in the mouse and human genomes (Fig. 2-1C). *Gb'Utx* encodes a 1,443 amino acid residue protein, and a histone demethylase (JmjC) domain was found in the *Gb'*Utx C-terminus. Amino acid sequence comparison of the *Gb'*Utx JmjC domain compared with *Drosophila melanogaster* Utx and *Homo sapiens* KDM6A showed 91% and 83% identity, respectively (Fig. 2-1B). In *Gryllus* and *Drosophila,* a single *Utx* gene was

found in their genomes; however, three paralogous genes, *Kdm6A*, *Kdm6B* and *Uty*, were found in the mouse and human genomes (Fig. 2-1C).

To determine whether *Gb'E(z)* and *Gb'Utx* are expressed during leg regeneration, regenerating legs, whose cuticle had been removed, was analyzed by whole-mount *in situ* hybridization. *Gb'E(z)* and *Gb'Utx* were expressed in ubiquitously regenerating legs at 6 dpa (days post amputation, Fig. 2-1D). No significant signal was observed in the negative controls. Ubiquitous expression of *Gb'E(z)* and *Gb'Utx* in regenerating legs at 6 dpa was similar to the expression patterns in developing limb buds and regenerating legs at 2 dpa (Fig. 2-2).

Gb'E(z) and *Gb'Utx* regulate the histone H3K27 methylation state

To clarify *Gb'E(z)* and *Gb'Utx* functions, the expression level of these genes was reduced by RNAi against its genes, respectively. Immunostaining experiment investigated histone H3K27me3 patterns whether *Gb'E(z)*^{RNAi} and *Gb'Utx*^{RNAi} alter the histone H3K27 methylation state during leg regeneration. In the control crickets, histone H3K27me3 was detected in the blastema and host stump at 2 dpa and the regenerating tibia and tarsus at 6 dpa (Fig. 2-3A). In the *Gb'E(z)*^{RNAi} crickets, fluorescence intensities of histone H3K27me3-positive nuclei were decreased in the blastema and regenerating tarsus at 2 and 6 dpa, respectively. In the *Gb'Utx*^{RNAi} crickets, histone H3K27me3-positive nuclei appeared increased in the regenerating legs at 2 and 6 dpa. These histological results suggest that *Gb'*E(z) and *Gb'*Utx are necessary for histone H3K27 methylation and histone H3K27me3 demethylation, respectively (Fig. 2-3A).

To confirm the knockdown of the endogenous *Gb'E(z)* and *Gb'Utx* mRNA levels by RNAi, the mRNA ratio of these genes was estimated in the *Gb'E(z)*^{RNAi} and *Gb'Utx*^{RNAi} crickets compared with the control crickets (n = 15) using quantitative PCR (qPCR). The average ratio of the *Gb'E(z)* and *Gb'Utx* mRNA levels at 3 dpa decreased to 0.52±0.01 (Fig. 2-3B) and 0.56±0.02 (Fig. 2-3C) (in triplicate, ± standard deviation) in regenerating *Gb'E(z)*^{RNAi} and *Gb'Utx*^{RNAi} tibiae, respectively, indicating that the RNAi did indeed lower the mRNA levels of these genes.

***Gb'E(z)* is involved in segment patterning during leg regeneration**

To examine the function of *Gb'E(z)* during leg regeneration, the third instar nymphs was performed RNAi and the metathoracic legs was amputated at proximal tibia. In the control cricket adults, regenerated legs were indistinguishable from contralateral-intact legs. Three pairs of tibial spurs and several pairs of spines were reconstructed on the tibia. Three tarsomeres and a claw were regenerated adjacent to the tibia. One pair of tarsal spurs (arrowheads in Fig. 2-4A) was reconstructed at the anterior and posterior ends of tarsomere 1 (Ta1). Notably, no decorative structures were formed on the small tarsomere 2 (Ta2) and middle-sized tarsomere 3 (Ta3) in both regenerated and contralateral-intact legs (Fig. 2-4A).

Gb'E(z)^{RNAi} crickets were viable, and the lost parts of their amputated legs were regenerated. In the *Gb'E(z)*^{RNAi} cricket adults, the lost sections of the tibia, tarsus and claw were regenerated; however, the leg segment patterns were abnormal (Fig. 2-4A). *Gb'E(z)*^{RNAi} regenerated legs were categorized into three classes based on leg morphology abnormalities during the sixth instar stage. The class 1 phenotype was mild (23%, n = 11/49); both anterior and posterior tarsal spurs were lost in Ta1, and Ta2 was not regenerated. Most *Gb'E(z)*^{RNAi} regenerated legs were classified as class 2 (55%, n = 26/49); three tarsomeres were regenerated; however, the tarsal spurs were abnormal. In class 2-regenerated legs, several spurs were reconstructed in Ta1 at the ventral side in addition to the anterior and posterior sides where tarsal spurs were formed in the controls (red arrows in Fig. 2-4A). The regenerated leg class 3 phenotypes, which showed the most severe morphological abnormalities (13%, n = 7/49), consisted of four leg segments in the tarsus; however, the controls consisted of three tarsomeres. The second leg segment morphology of the class 3-regenerated tarsus appeared to be the Ta1 of the control; one pair of tarsal spurs was reconstructed at the end of the tarsomere (black arrowheads in Fig. 2-4A). The third and fourth segments of the class 3-regenerated tarsus were estimated the Ta2 and Ta3 of the control based on the segment size of each segment. The first segment of the class 3-regenerated tarsus was ambiguous (red bracket in Fig. 2-4A, Fig. 2-

4C); more than two spurs were formed at the end of the leg segment (red arrows in Fig. 2-4A), which is characteristic of the tibia; and, several spines were formed at the dorsal side in this extra leg segment. Regenerated legs of the other 9% of *Gb'E(z)*^{RNAi} cricket adults (n = 5/49) showed normal morphology, and the morphologies of the regenerated tibiae were normal in all classes. These phenotypes were also observed the crickets that were performed RNAi against the *Gb'E(z)_C* region (Fig. 2-4B, Fig. 2-5), suggesting that these phenotypes were not caused by an off-target effect.

Regenerated legs in *Gb'E(z)*^{RNAi} crickets exhibit an extra tibia segment

To identify the origin of extra leg segments formed in class 3 *Gb'E(z)*^{RNAi} crickets, I performed further morphological observation of the extra leg segment, which appeared to be a tibia-like structure. The mesothoracic (T2) leg regeneration process was observed in the control and *Gb'E(z)*^{RNAi} crickets, because the tibia and Ta1 morphologies were different in the T2 leg. Specifically, in the T2 legs, tibial spurs formed on the tibia; however, tarsal spurs did not form at Ta1, which differed from the metathoracic (T3) leg. In the control cricket (n = 20), the lost part of the T2 leg was regenerated after amputation of the leg on the tibia. Two pairs of tibial spurs, three tarsomeres and the claw were regenerated, and no tarsal spurs formed in the tarsus (Fig. 2-6A). In *Gb'E(z)*^{RNAi} crickets (n = 39), regenerated T2 legs had an extra leg segment between the tibia and tarsus, and two pairs of spurs formed on both ends of the tibia and extra leg segment (72%, n=28/39), indicating that the extra leg segment observed in the T2-regenerated leg of *Gb'E(z)*^{RNAi} crickets was the tibia (Fig. 2-6A, B). Morphologies of the T2-regenerated leg of the *Gb'E(z)*^{RNAi} crickets indicated that *Gb'E(z)*^{RNAi} induced extra tibia segment formation during regeneration. When the amputation position was changed from the tibia to femur, and after the amputation of the cricket leg at the distal position of the femur, the lost parts of the femur, tibia, three tarsomeres and claw regenerated in the control adult (Fig. 2-6C). In contrast, the morphologies of the regenerated legs of *Gb'E(z)*^{RNAi} cricket adults were abnormal. In class 1, the tibia, Ta1 and Ta2 regenerated as a

single short and thick leg segment without joints. Small Ta3 and claws were regenerated at the end of joint-less leg segment (25%, n = 4/16). In class 2-regenerated legs, the tibia, tarsus and claw regenerated, and a short-extra leg segment formed between the tibia and Ta1 (25%, n = 4/16). In class 3-regenerated legs, the tibia with tibial spurs regenerated adjacent to the regenerated femur. An extra tibia segment, which was assessed by spur reconstruction, formed between the tibia and tarsus. Thick and short Ta1, and the Ta3 and claw regenerated following the extra tibia segment (38%, n = 6/16) (Fig. 2-6C). These morphological observations of *Gb'E(z)*^{RNAi} regenerated legs after amputation at the femur suggest that *Gb'*E(z) may suppress extra tibia formation during regeneration regardless of amputated positions.

Next, to induce supernumerary leg formation, the grafting experiments was performed in control and *Gb'E(z)*^{RNAi} crickets. After the transplantation of the left mesothoracic tibia onto the right metathoracic tibia, resulted in the inversion of the anteroposterior (AP) polarity of the graft to the host, two supernumerary legs were formed at the anterior and posterior sides of the tibia (Mito *et al*., 2002). In the control cricket (n = 22), supernumerary legs formed at both sides of tibia consist of tibia, tarsus and claw. In the *Gb'E(z)*^{RNAi} cricket (n = 23), supernumerary legs formed on both sides of the tibia, and again, consisted of a tibia, extra tibia segment (depicted by red arrows in Fig. 2-6D), tarsus and claw (26%, n = 6/23, Fig. 2-6D, E), indicating that *Gb'E(z)* regulates leg segment pattern along PD axis but did not regulate the polarities along AP and dorsoventral (DV) axes.

Amputated position affects the *Gb'E(z)*^{RNAi} phenotype

To elucidate whether the amputated position along PD axis of tibia affects the *Gb'E(z)*^{RNAi} phenotype, the *Gb'E(z)*^{RNAi} nymphs was amputated at the distal, middle or proximal position in tibia. In the control crickets, morphologies of regenerated legs amputated at any position were similar (Fig. 2-7A); however, in the *Gb'E(z)*^{RNAi} crickets, the phenotypic rate of class 3 was elevated after amputation at the more proximal position (Fig. 2-7B). After amputation of the *Gb'E(z)*^{RNAi} cricket leg at the proximal position, 62% (n = 21/34) of regenerated legs were

categorized into class 3; however, 14% (n = 7/49) and 25% (n = 10/40) of regenerated legs were categorized into class 3 after amputation at the distal and middle positions, respectively (Fig. 2-7B). In addition, the length of the extra segment normalized to the femur length also extended after proximal amputation compared with the amputation at the middle or distal positions (Fig. 2-7A, C). Conversely, the normalized length of the regenerated tibia was shortened after proximal amputation compared with the middle or distal amputation (Fig. 2-7A, C). These results are assumed that *Gb'*E(z) target genes may be expressed in a region-specific manner along the PD axis because the amputated position affects the *Gb'E(z)*^{RNAi} phenotype ratios.

E(z) function during regeneration is conserved among two cricket species

Tarsus structures and tarsomere numbers are strictly determined depending on insect species (Tajiri *et al*., 2011). To confirm whether extra tibia segment formation caused by *E(z)*^{RNAi} is a species-specific phenotype, *E(z)*^{RNAi} during leg regeneration in the field cricket *Modicogryllus siamensis* was tested (Fig. 2-8B). *M. siamensis* regenerated the lost part of the metathoracic leg after amputation at the distal tibia, similar to *G. bimaculatus* (Fig. 2-8A, C). Next, *Ms'E(z)*, an *M. siamensis E(z)* homologue, was cloned, and *M. siamensis* nymphs were performed RNAi against *Ms'E(z)*. In *Ms'E(z)*^{RNAi}-regenerated legs, an extra tibia segment was formed between the tibia and tarsus (red bracket in Fig. 2-8A, D), similar to the *Gb'E(z)*^{RNAi} phenotype, suggesting that suppression of extra tibia formation during regeneration mediated by E(z) is a conserved mechanism at least among two cricket species.

***Gb'Utx* is involved in tarsus joint formation during leg regeneration**

Utx demethylates histone H3K27me3 and which is mediated by E(z); therefore, RNAi against *Gb'Utx* was performed the third cricket nymphs, to analyse its function during leg regeneration. In the *Gb'Utx*^{RNAi} cricket adults, the lost leg segments regenerated; however, the regenerated tarsomeres showed various morphological abnormalities in the formation of tarsal spurs

(arrowheads in Fig. 2-9A) or Ta2. In most cases, the tarsal spur at the anterior side was not reconstructed, and the anterior tarsal spur size was smaller compared with the control. In several cases, tarsal spurs on both the anterior and posterior sides were not reconstructed. In addition, leg joint formation defection was also observed between Ta1 and Ta2 in class 2-regenerated legs. These phenotypes were observed when RNAi was utilised against the *Gb'Utx_C* region, suggesting that these phenotypes were not caused by off-target effects (Fig. 2-9B).

Expression of *Gb'dac* and *Gb'Egfr* is epigenetically regulated via histone H3K27me3

These series of RNAi experiments suggests that *Gb'E(z)* suppresses extra tibia segment formation between the tibia and tarsus and that *Gb'Utx* promotes leg joint and spur formation at the tarsus during repatterning. To clarify whether *Gb'E(z)* and *Gb'Utx* epigenetically regulate leg patterning gene expression involved in tibia and/or tarsus formation, the *Gb'dac*, *Gb'Egfr*, *Gb'BarH* and *Gb'Dll* expression patterns were observed in the regenerating legs of RNAi crickets by whole-mount *in situ* hybridization. In the control regenerating legs at 6 dpa, *Gb'dac* was expressed in the tibia and tarsus proximal region (Fig. 2-10A), and *Gb'Egfr* was expressed at the distal position of tibia and the middle and distal positions of the tarsus (shown by arrowheads, Fig. 2-10A) (Nakamura *et al*., 2008b). In the tarsus, *Gb'BarH* and *Gb'Dll* were expressed in the middle section (shown by arrowhead) and the entire tarsus, respectively. In the *Gb'E(z)*^{RNAi}-regenerating legs at 6 dpa, the *Gb'dac* expression domain in the proximal tarsal region was expanded (Fig. 2-10A). *Gb'dac* expression in the distal tarsal region (red arrowhead in Fig. 2-10A) was observed in both the *Gb'E(z)*^{RNAi} and control regenerating legs (Nakamura *et al*., 2008b). The *Gb'Egfr*, *Gb'BarH* and *Gb'Dll* expression patterns were not altered in the *Gb'E(z)*^{RNAi}-regenerating legs. In the *Gb'Utx*^{RNAi}-regenerating legs, *Gb'Egfr* was expressed at the distal position of the tibia and tarsus (shown by arrowheads); however, *Gb'Egfr* was not expressed in the middle position of the tarsus (shown by the blue arrowhead), which becomes the Ta1 and Ta2 leg joint. The *Gb'dac*, *Gb'BarH* and *Gb'Dll* expression patterns were not altered in the *Gb'Utx*^{RNAi}-regenerating legs.

Overall, these results suggest that *Gb'E(z)* and *Gb'Utx* epigenetically regulate *Gb'dac* and *Gb'Egfr* expression, respectively, in regenerating legs (Fig. 2-10A).

The *Gb'dac* expression patterns were analyzed in the control and *Gb'E(z)*^{RNAi}-regenerating legs after amputation at the middle or proximal positions, because the *Gb'E(z)*^{RNAi} phenotypic rate was altered depending on the amputated positions. *Gb'dac* was expressed in the tibia and proximal region of the tarsus of the control regenerating legs amputated at the middle or proximal positions (Fig. 2-10B). In the *Gb'E(z)*^{RNAi}-regenerating legs, *Gb'dac* was expressed in tibia and entire region of the tarsus after amputation at the middle and proximal positions (Fig. 2-10B). The *Gb'dac* expression domain ratios in the tarsi were calculated (Fig. 2-10C). *Gb'dac* expression in the tarsi was significantly expanded in the *Gb'E(z)*^{RNAi}-regenerating legs compared with the control-regenerating legs (*** $P < 0.01$, Fig. 2-10C). In *Gb'E(z)*^{RNAi} crickets, *Gb'dac* expression was significantly expanded in the regenerating leg amputated proximally compared with the legs amputated middle or distally (Fig. 2-10C), correlating with the *Gb'E(z)*^{RNAi} phenotype ratios (Fig. 2-7).

Gb'E(z) and *Gb'Utx* regulate repatterning but are not involved in dedifferentiation

To determine the effective time window of RNAi against *Gb'E(z)* and *Gb'Utx*, crickets were performed RNAi after cricket leg amputation and were observed the RNAi phenotypes. In the control, regenerated legs with RNAi against exogenous gene *Egfp* at any time point were similar to the contralateral intact leg. In the *Gb'E(z)* cases, the phenotype ratios of *Gb'E(z)*^{RNAi} at 4 and 8 hpa were 80%, which is similar to the phenotypic ratio at 0 hpa, and subsequently, decreased to 50% when treated dsRNA against *Gb'E(z)* at 48 hpa (Fig. 2-11A). Regarding *Gb'Utx*, the phenotype ratios gradually decreased depending on the timing of RNAi after amputation; the ratio was 60% when the RNAi was performed at 0 hpa, and the ratios were 40% at 4 or 8 hpa and 20% at 12, 24 and 48 hpa (Fig. 2-11A). No additional phenotypes were found by employing *Gb'E(z)*^{RNAi} or *Gb'Utx*^{RNAi} at any time point.

If *Gb'E(z)* and/or *Gb'Utx* contribute to dedifferentiation during blastema formation, *Gb'E(z)*^{RNAi} and/or *Gb'Utx*^{RNAi} would exhibit a regeneration defective phenotype when RNAi is performed prior to amputation. The RNAi phenotype was observed by applying RNAi at the third instar and amputation at fourth instar nymphs, allowing a 72 hours incubation period prior to amputation. In the other group, RNAi and amputation were performed simultaneously at the fourth instar stage. In control crickets with RNAi against *Egfp*, regeneration occurred in both groups (data not shown). In *Gb'E(z)*^{RNAi} crickets, approximately 80% of RNAi crickets showed RNAi phenotypes in the regenerated legs in both groups (Fig. 2-11B). In *Gb'Utx*^{RNAi} crickets, 30% and 50% of crickets showed RNAi phenotypes in the regenerated legs following RNAi at third and forth instar, respectively (Fig. 2-11B). No additional phenotypes were observed. No regeneration defects were observed when utilising RNAi 72 hours before amputation (Fig. 2-11B), suggesting that *Gb'E(z)* and *Gb'Utx* are involved in the repatterning process but not in the dedifferentiation process to form the blastema.

2.5. Discussion

Using an RNAi knockdown approach, the epigenetic factors *Gb'*E(z) and *Gb'*Utx were determined that they mediate the methylation and demethylation, respectively, of histone H3K27 during *Gryllus* leg regeneration. Regenerated *Gb'E(z)*^{RNAi} and *Gb'Utx*^{RNAi} legs exhibited extra tibia segment formation and defects in leg joint formation, respectively, caused by the epigenetic regulation of leg patterning gene expression during regeneration.

Gb'E(z) regulates segment pattern of the lost leg section via histone H3K27me3 during leg regeneration

After amputation, differentiated cells in the tissue lose their differentiation status and dedifferentiate into blastema cells. Blastema cells proliferate rapidly, then redifferentiate into several types of differentiated cells (Nye *et al*., 2003; Tamura *et al*., 2010; Truby, 1985; Tweedell,

2010; Worley *et al*., 2012). During the dedifferentiation and redifferentiation processes, the expression profiles of differentiation- and undifferentiation-related genes change epigenetically (Barrero and Izpisua, 2011; Katsuyama and Paro, 2011; Tamura *et al*., 2010). Previous study showed that the expression levels of the epigenetic factors *Gb'E(z)* and *Gb'Utx* are upregulated during cricket leg regeneration (Bando *et al*., 2013). Therefore, in this study, the role of these epigenetic factors was examined in the leg regeneration.

The extreme cases such as the class 3 phenotype of *Gb'E(z)*^{RNAi}-regenerated legs exhibited extra tibia segment formation between the tibia and Ta1 (Fig. 2-4A), implying that *Gb'*E(z) epigenetically regulates leg patterning gene expression during tibia regeneration. Previous RNAi experiments showed that *Gb'dac* mediates tibia and Ta1 formation during leg regeneration (Ishimaru *et al*., 2015; Nakamura *et al*., 2008b). In contrast, *Dll* and *BarH* expression is involved in tarsus formation in *Drosophila* limb development (Kojima, 2004), and *Gb'Dll* expression is involved in *Gryllus* tarsus regeneration (Ishimaru *et al*., 2015; Nakamura *et al*., 2008b). The *Gb'dac* expression domain in Ta1 expanded in *Gb'E(z)*^{RNAi} regenerating legs (Fig. 2-10, 2-12A); therefore, the ectopic derepression of *Gb'dac* expression in the Ta1 distal region by *Gb'E(z)*^{RNAi} would lead to the formation of an extra tibia segment (Fig. 2-12B). In contrast, *Gb'BarH* and *Gb'Dll* expression was not altered in *Gb'E(z)*^{RNAi}-regenerating legs, which may explain why the ratio of regenerated legs with extra tibia segments was less than 20% in the *Gb'E(z)*^{RNAi} crickets (Fig. 2-4B) because normal *Gb'BarH* and *Gb'Dll* expression in the *Gb'E(z)*^{RNAi}-regenerating leg induces tarsus formation and may suppress extra tibia segment formation during regeneration (Fig. 2-12A,B).

The extreme *Gb'E(z)*^{RNAi} phenotype ratio increased after amputation of the leg at the proximal position in comparison with amputation at the middle or distal position (Fig. 2-7). Aforementioned, *Gb'dac* is not expressed in the proximal region of the tibia in the developing cricket embryo (Inoue *et al*., 2002) or the stump amputated at the proximal position. In contrast, *Gb'dac* expression remained in the host stumps amputated at the middle or distal position of regenerating legs. Maintained *Gb'dac* expression in the host stump may decrease the *Gb'E(z)*^{RNAi}

phenotype ratio and may lead to normal regeneration after amputation at the middle or distal position (Fig. 2-12B). Thus, *Gb'E(z)* reuglates repatterning of the lost leg section via the *Gb'dac* expression by histone H3K27me3, which prevents malformations such as extra leg segment formation. *Gb'E(z)* may promote cell proliferation in the leg segment through the regulation of *Gb'dac* expression.

Gb'Utx promotes the joint formation via histone H3K27me3 during leg regeneration

Gb'Utx^{RNAi}-regenerated legs exhibited leg joint formation defects at Ta1 (Fig. 2-9A). The tarsal spur reconstruction defects were likely caused by joint formation defects between Ta1 and Ta2. These findings in *Gb'Utx*^{RNAi}-regenerated legs imply that *Gb'*Utx epigenetically regulates the expression of genes involved in leg joint formation. During leg regeneration, *Gb'Egfr* is expressed in leg joints and in the spur primordia (Nakamura *et al*., 2008b). In *Gb'Utx*^{RNAi} crickets, *Gb'Egfr* expression in the leg joint in the middle region of the tarsus was diminished. Epigenetic derepression problems may have resulted in *Gb'Utx*^{RNAi} altering *Gb'Egfr* expression in the tarsus, causing leg joint and spur formation defects on the tarsus (Fig. 2-12A, C). Systemic RNAi against *Gb'Egfr* has been reported to cause defects in Ta3 and claw reconstruction during regeneration (Nakamura *et al*., 2008b). In *Drosophila*, *dUTX* genetically interacts with *Notch* to regulate cell proliferation (Herz *et al*., 2010) and in *Gryllus*, systemic RNAi against *Gb'Notch* causes the formation of a short regenerated tarsus with no leg joint formation (Bando *et al*., 2011). Differences between the *Gb'Utx*^{RNAi} and *Gb'Egfr*^{RNAi} or *Gb'Notch*^{RNAi} phenotypes indicate that *Gb'*Utx regulates *Gb'Egfr* expression in the middle region of the tarsus and that *Gb'Utx* may not interact with *Gb'Notch* during regeneration nor *Gb'Egfr* in the other regions. Thus, *Gb'Utx* promotes leg joint restoration via epigenetic regulation of *Gb'Egfr* expression by histone H3K27me3 during leg regeneration.

In comparison with the extreme phenotype of *Gb'E(z)*^{RNAi}, the morphological defects caused by *Gb'Utx*^{RNAi} was limited, with the noticeable defect involving leg joint formation between Ta1

and Ta2. In embryonic development, *Gb'E(z)*^{RNAi} embryos exhibit abnormal appendage formation (see below) (Matsuoka *et al*., 2015); however, *Gb'Utx*^{RNAi} embryos exhibit minor morphological defects in the head segment (Fig. 2-13). In other organisms, Utx is essential for regeneration, wound healing (Shaw and Martin, 2009; Stewart *et al*., 2009), embryonic development (Shpargel *et al*., 2014) and embryonic stem cell differentiation (Morales Torres *et al*., 2013) via the epigenetic regulation of cell proliferation or repair genes. Since the cricket is a hemimetabolous insect, cell proliferation and production of new cuticles during the molting process are essential; therefore, the activation of cell proliferation and subsequent processes may be regulated via various redundant molecular systems in addition to Utx. Therefore, *Gb'Utx*^{RNAi} did not result in marked regeneration defects compared with the regeneration defective phenotype observed in other organisms.

Epigenetic regulation by histone H3K27me3 does not play a role in dedifferentiation

Previously study showed that *Gb'E(z)* and *Gb'Utx* expression is upregulated within 24 hours after cricket leg amputation (Bando *et al*., 2013), suggesting that *Gb'E(z)* and *Gb'Utx* may be involved early in the regeneration process such as during the dedifferentiation into blastema cells. During *Drosophila* imaginal disc regeneration, the expression of *Polycomb* group genes, including *E(z)*, is directly downregulated by JNK signalling in the wounding edge, increasing the plasticity of differentiated cells for promoting blastema formation (Lee *et al*., 2005). In addition, *dUtx* and *E(z)* expression is activated and suppressed after injury to epigenetically regulate the expression of dedifferentiation- and redifferentiation-related genes to promote blastema formation in *Drosophila* (Katsuyama and Paro, 2011; Repiso *et al*., 2011). Conversely, during murine skin repair, Utx and Jmjd3 are involved in wound healing by upregulating the expression of repair genes (Shaw and Martin, 2009). The expression of Kdm6 family genes, which encode Utx and Jmjd3 orthologues, are upregulated during amputation to promote blastema cell proliferation in zebrafish (Stewart *et al*., 2009). During the reprogramming process in which differentiated cells develop into iPS cells, the expression of differentiation-related genes is suppressed via histone H3K27me3; however,

dedifferentiation-related genes are not repressed (Meissner, 2010), possibly through the actions of mammalian Utx homologues (Mansour *et al*., 2012). These reports imply that derepression of dedifferentiation-related genes via demethylation on histone H3K27me3 is a key event in dedifferentiation and reprogramming, including in iPS cells as well as blastema cells. Blastema cells, which are dedifferentiated cells derived from differentiated cells, are essential for regeneration in multiple organisms, including the cricket. The Wg/Wnt and Jak/STAT signalling pathways are essential for blastema cell formation because the RNAi silencing of these signalling pathways cause regeneration defects (Bando *et al*., 2013; Nakamura *et al*., 2007). If *Gb'E(z)* and *Gb'Utx* are essential for the dedifferentiation process to form the blastema, RNAi against *Gb'E(z)* and *Gb'Utx* should cause complete regeneration defects. In this study, *Gb'E(z)*^{RNAi} and *Gb'Utx*^{RNAi} exhibited defects in regenerated leg repatterning (Fig. 2-4, 2-9). Furthermore, leg regeneration occurred when RNAi against *Gb'E(z)* and *Gb'Utx* was performed 72 hours before amputation. Thus, the epigenetic regulation of gene expression via histone H3K27me3 is not required for dedifferentiation into blastema cells during cricket leg regeneration which is different from the roles of epigenetic control during cell dedifferentiation in the mouse, zebrafish and *Drosophila* (Lee *et al*., 2005; Shaw and Martin, 2009; Stewart *et al*., 2009). The effective time window of *Gb'E(z)*^{RNAi} and *Gb'Utx*^{RNAi} was also determined. Both *Gb'E(z)*^{RNAi} and *Gb'Utx*^{RNAi} are effective within 8 hours after amputation (Fig. 2-11). In general, RNAi suppresses endogenous gene expression within 24 hours in the cricket (Uryu *et al*., 2013), indicating that pattern formation involved in reconstructing the lost segment in the blastema occurs within 1.3 days after amputation via histone H3K27me3. RNAi experiments targeting *Gb'E(z)* or *Gb'Utx* result in extra tibia formation and joint formation defects; therefore, *Gb'E(z)* and *Gb'Utx* may not involved in dedifferentiation but prevent malformations during leg regeneration and play a role in the fine-tuning of the tarsus shape.

Comparison of the epigenetic gene expression control between cricket and other organisms

E(z) is a component of the Polycomb Repressive Complex (PRC) and epigenetically represses gene expression during embryogenesis (Barrero and Izpisua, 2011). In mouse limb development, Ezh2 regulates pattern formation via Hox genes expression in epigenetic manner (Wyngaarden *et al*., 2011). Similarly, *Gb'*E(z) also regulates appendage development in the head, gnathal and thoracic segments and katatrepsis via the epigenetic regulation of homeotic gene expression during *Gryllus* embryonic development (Matsuoka *et al*., 2015). However, during the regeneration process, E(z) does not likely regulate homeotic gene expression because the regenerated mesothoracic or metathoracic legs maintained their identities and showed no homeotic transformations (Fig. 2-4A, 2-6A). Thus, the expression of genes regulated by E(z) appears to depend on the biological context, that is, during embryogenesis or regeneration.

Differences in the regenerative capacity between the newt and frog are attributed to the amount of methylated DNA on a *Shh cis*-regulatory element (Yakushiji *et al*., 2007; Yakushiji *et al*., 2009). In zebrafish, the status of DNA methylation is changed in the blastema during fin regeneration (Hirose *et al*., 2013; Takayama *et al*., 2014). In addition, DNA methylation has important roles in stem cells, development, tumourigenesis and other processes. However, in insects, epigenetic repression via DNA methylation is quite limited to processes such as oogenesis in *Drosophila* or caste determination in the honeybee (Glastad *et al*., 2011; Lyko and Maleszka, 2011). In *Gryllus*, RNAi against DNA methyltransferases (*Gb'Dnmt2* and *Gb'Dnmt3*) or 5-methylcytosine hydroxylase (*Gb'Tet*) does not cause a phenotype (Fig. 2-14), suggesting that the epigenetic regulation of gene expression via DNA methylation is not essential in *Gryllus* leg regeneration. Epigenetic repression of gene expression via DNA methylation is widely utilised in combination with histone H3K27 and H3K9 methylation in vertebrates; however, in insects, histone H3K27 methylation is the dominant alteration involved in epigenetic repression. Methylation on histone H3K9 is another epigenetic alteration involved in repression; therefore, inhibition against histone H3K9me3 may cause other defects during regeneration in insects.

In conclusion, these findings demonstrates that strict control of leg-patterning gene expression via histone H3K27me3 is essential for proper repatterning during regeneration: *Gb'E(z)* promotes the restoration of lost leg sections, while *Gb'Utx* promotes leg joint restoration. Previously, other epigenetic factors were identified that regulate methylation states on histones H3K4, H3K9 and H3K36 or regulate the histone acetylation state in cricket regenerating legs (Bando *et al*., 2013). Methylation on histone H3K4 is needed to maintain the stem cell population in planarians (Hubert *et al*., 2014; Robb and Sanchez, 2014), and epigenetic changes on histone H3K4 and H3K9 correlate with cell proliferation during regeneration in the polychaete worm (Niwa *et al*., 2013), suggesting that the orchestrated regulation of epigenetic histone modification may promote dedifferentiation into blastema cells in *Gryllus*. This report is the first to demonstrate the epigenetic regulation of gene expression during tissue regeneration repatterning.

Figures and Figure legends

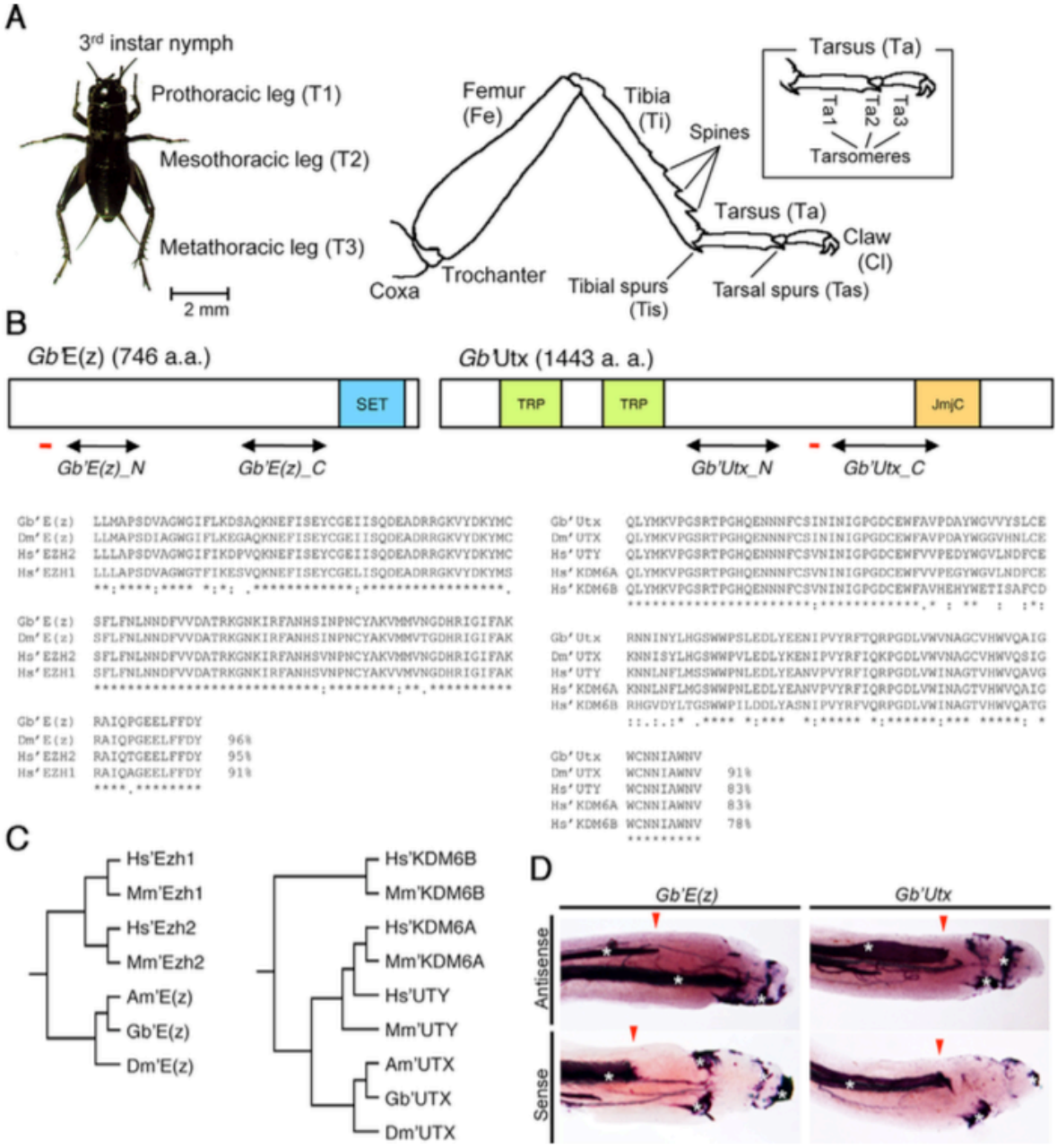

Fig. 2-1. Isolation of the *Gryllus* E(z) and Utx homologues.
(A) Dorsal view of *Gryllus* nymph at third instar and schematic diagram of *Gryllus* metathoracic leg. (B) Domain structures and corresponding regions of dsRNAs (double-headed arrow) and amplicons for qPCR (red bar) of *Gb'*E(z) and *Gb'*Utx. E(z) has a SET domain. Utx has TRP (Tetratricopeptide repeat) domains and a JmjC domain. Amino acid alignments of the E(z) SET domain and UTX JmjC domain are shown. Identical and similar amino acid residues are indicated by asterisks and dots, respectively. Sequence identities of *Gb'*E(z) and *Gb'*Utx with other homologous proteins are indicated by percentage. (C) Phylogenetic tree based on amino acid sequence alignments. Gb, *Gryllus bimaculatus*; Am, *Apis mellifera*; Dm, *Drosophila melanogaster*; Mm, *Mus musculus*; Hs, *Homo sapiens*. (D) Expression pattern of *Gb'E(z)* and *Gb'Utx* in regenerating legs at 6 dpa. Distal portion of the regenerating leg is directed towards the right. Asterisks indicate non-specific staining. Red arrowheads indicate the amputation position; therefore, the distal regions from the amputated positions are regenerated regions.

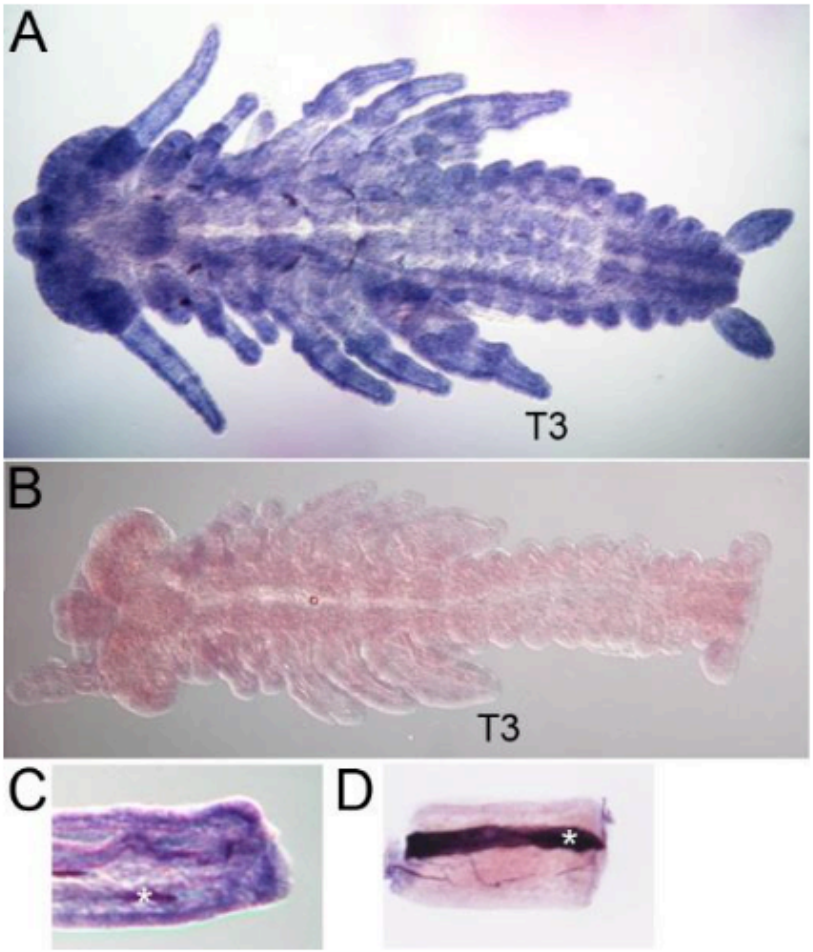

Fig. 2-2. *Gb'E(z)* and *Gb'Utx* expression patterns.
Gb'E(z) and *Gb'Utx* mRNA localization in developing embryos and regenerating legs as shown by whole mount *in situ* hybridization. (A-B) *Gb'E(z)* expression pattern in stage 10 embryos (A) and *Gb'Utx* expression in stage 9 embryos (B). (C-D) *Gb'E(z)* (C) and *Gb'Utx* (D) expression patterns in regenerating legs at 2 dpa. Asterisks indicate non-specific staining.

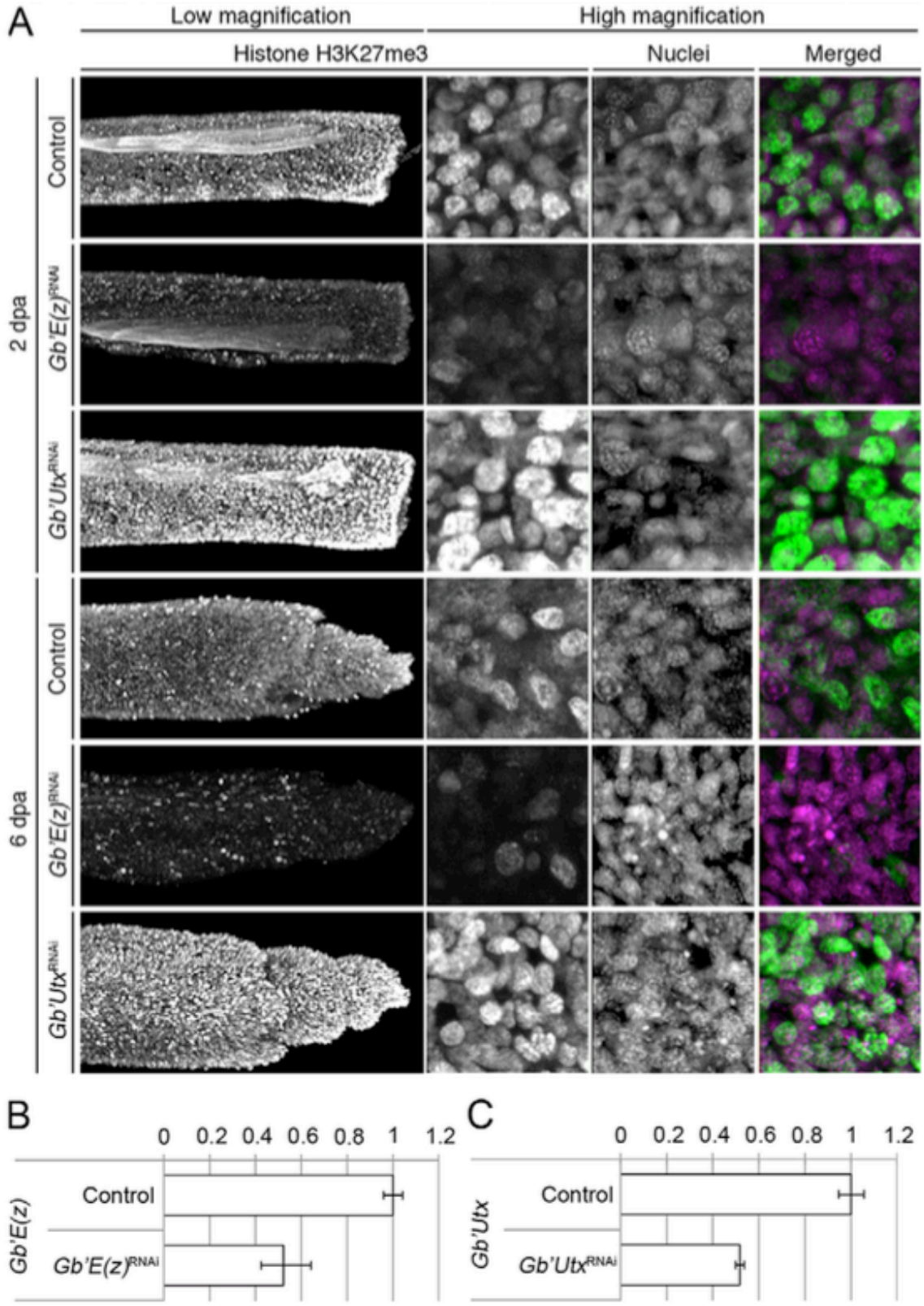

Fig. 2-3. Localization of histone H3K27me3 in regenerating legs.
(A) Localization of histone H3K27me3 (green) and DAPI (magenta) in regenerating legs of control, *Gb'E(z)*^{RNAi} and *Gb'Utx*^{RNAi} crickets at 2 and 6 dpa. Left columns show low magnification images, and the right three columns show high magnification images of the left columns. Distal portion of the regenerating leg is directed towards the right. (B) Relative *Gb'E(z)* mRNA levels in the control and *Gb'E(z)*^{RNAi}-regenerating tibias at 3 dpa. (C) Relative *Gb'Utx* mRNA levels in the control and *Gb'Utx*^{RNAi}-regenerating tibias at 3 dpa.

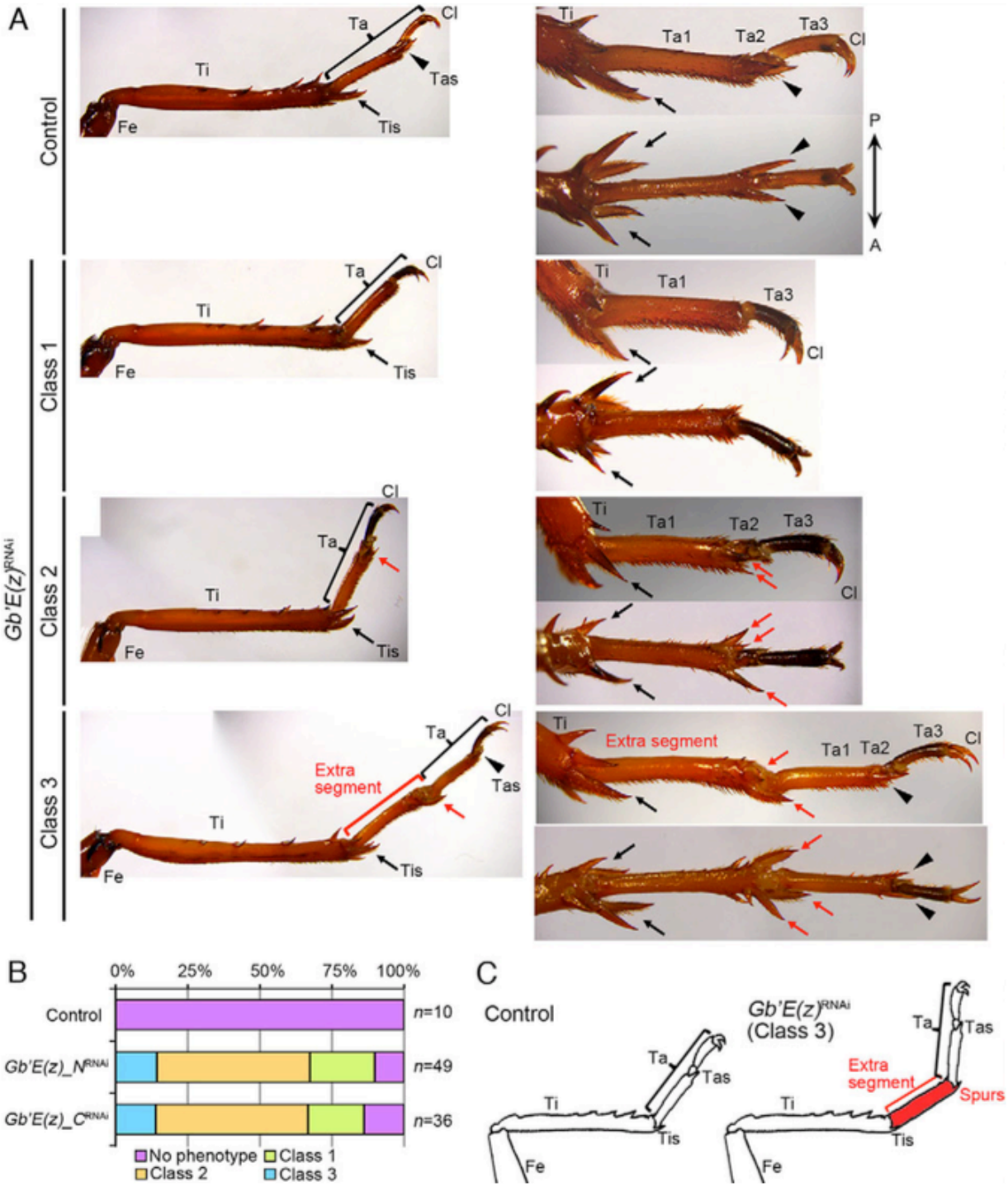

Fig. 2-4. Typical regenerated leg phenotypes in the control and *Gb'E(z)*^{RNAi} crickets.
(A) Regenerated legs in the control and *Gb'E(z)*^{RNAi} adults. Lateral views of low magnification images are shown in the left column. Lateral and dorsal views of high magnification images are shown in the right column in the upper and lower panels, respectively. Tibial spurs and tarsal spurs are denoted by the arrows and arrowheads, respectively. Tarsi are shown by brackets. Fe, femur; Ti, tibia; Ta, tarsus; Cl, claw; Tis, tibial spur; Tas, tarsal spur. Extra tibia segment and its spurs are shown by red brackets and red arrows, respectively. (B) Ratios of normal (no phenotype) and RNAi phenotypes (class 1 to 3) of control and *Gb'E(z)*^{RNAi} cricket nymphs at sixth instar. (C) Schematic diagrams of regenerating legs of control and *Gb'E(z)*^{RNAi} crickets. Extra leg segment regenerated between the tibia and tarsus of *Gb'E(z)*^{RNAi} crickets is indicated by the red color.

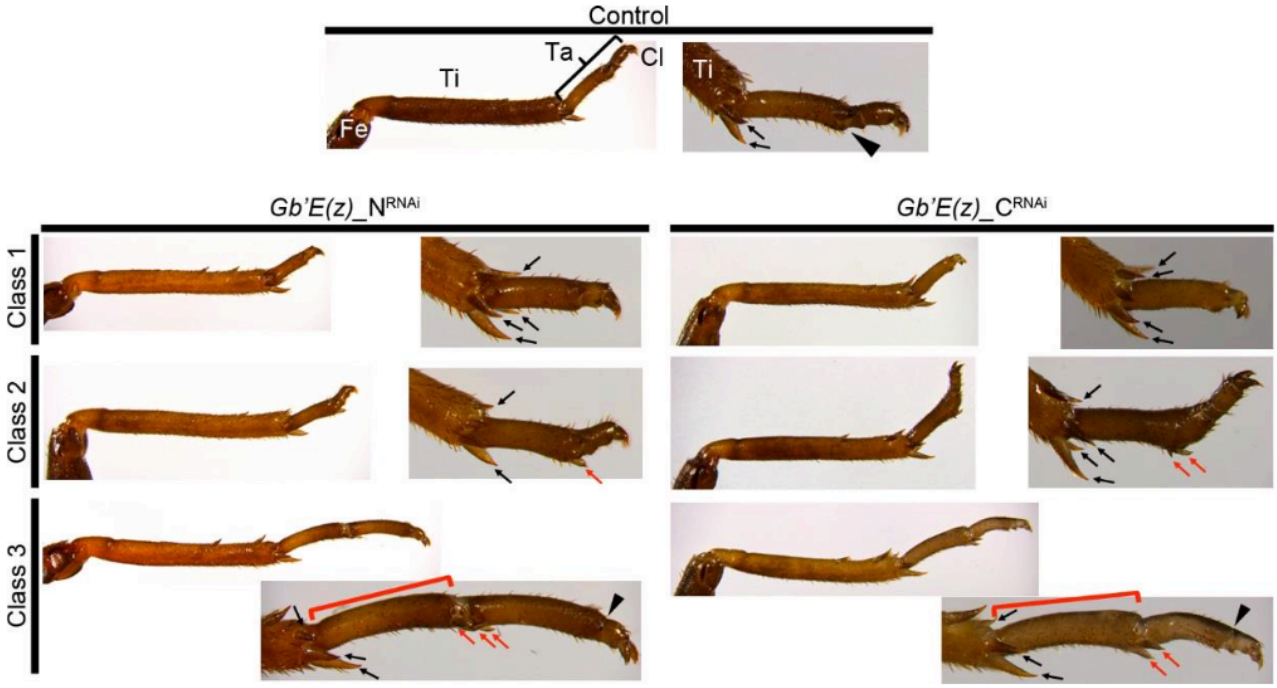

Fig. 2-5. Confirmation of *Gb'E(z)*^{RNAi} off-target effects.
Typical regenerating legs of control and RNAi crickets against *Gb'E(z)*_N (left column) and *Gb'(z)*_C (right column) at sixth instar. Tibial spurs and tarsal spurs are indicated by arrows and arrowheads, respectively, and tibial spurs on extra tibia segments are indicated by red arrows. The extra tibia segments are indicated by brackets. Fe, femur; Ti, tibia; Ta, tarsus; Cl, claw.

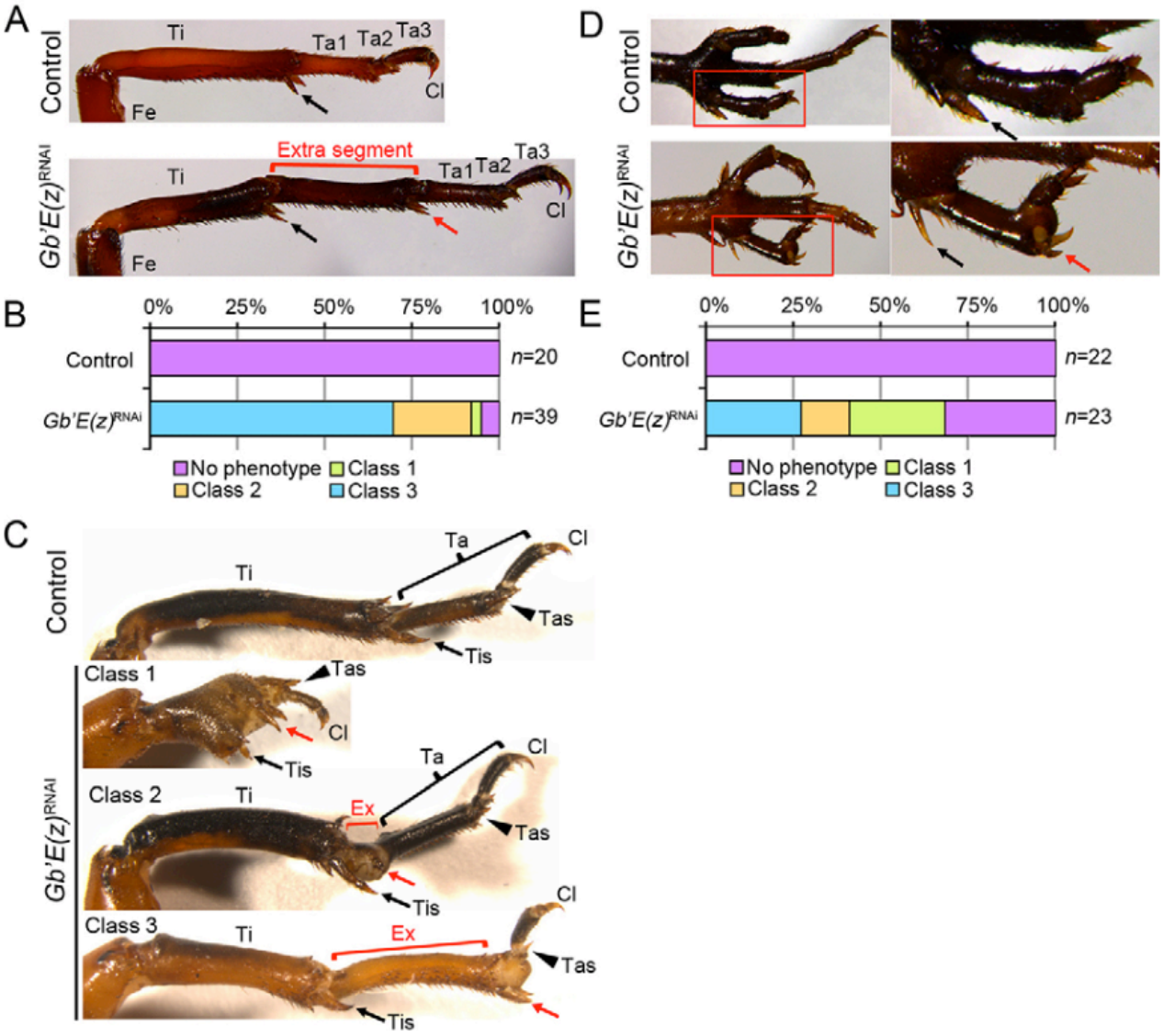

Fig. 2-6. Typical regenerated and supernumerary leg phenotypes in control and *Gb'E(z)*^{RNAi} crickets.

(A) Regenerated mesothoracic legs of control and *Gb'E(z)*^{RNAi} crickets are shown in the upper and lower panels. Tibial spars are indicated by arrows. The extra tibia segment and its spurs are denoted by a red bracket and a red arrow, respectively. (B) Ratios of normal (no phenotype) and RNAi phenotypes (class 1 to 3) of regenerated mesothoracic legs of control and *Gb'E(z)*^{RNAi} cricket nymphs at sixth instar. (C) Regenerated legs amputated at the distal femur of control (upper panel) and *Gb'E(z)*^{RNAi} (lower panels). Tibial spurs and tarsal spurs are denoted by the arrows and arrowheads, respectively. Tarsi are shown by brackets. Ti, tibia; Ta, tarsus; Cl, claw; Tis, tibial spur; Tas, tarsal spur. Extra tibia segment and its spurs are shown by red brackets and red arrows, respectively. (D) Supernumerary legs in the control (upper panels) and *Gb'E(z)*^{RNAi} (lower panels) crickets. Low magnification images are shown in the left column, and the high magnification images of the left column images (red squares) are shown in the right column. Tibial spurs are indicated by arrows. Tibial spurs on extra tibia segments are indicated by a red arrow. (E) Ratios of normal and RNAi phenotypes of supernumerary legs of control and *Gb'E(z)*^{RNAi} cricket nymphs at sixth instar.

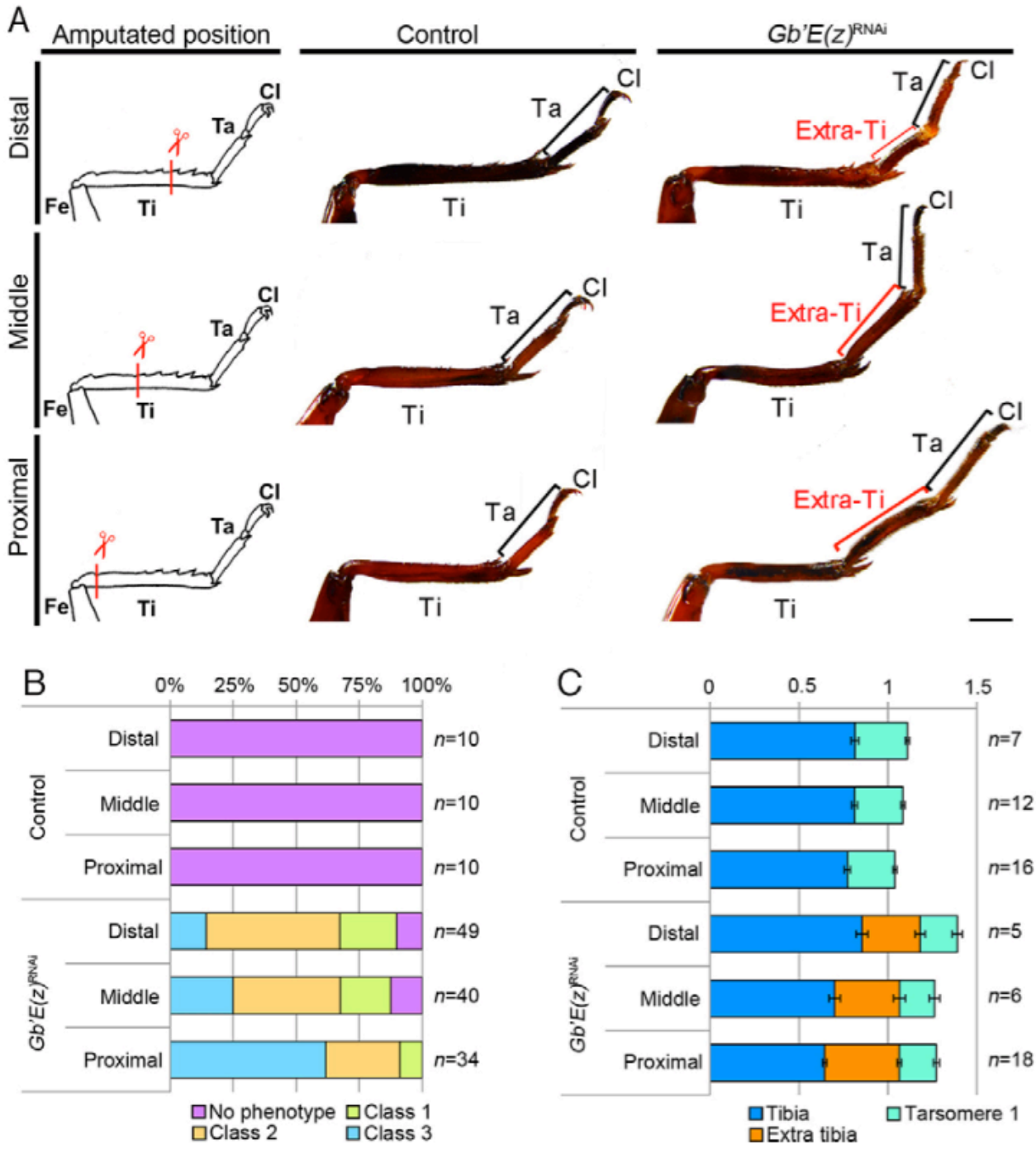

Fig. 2-7. Effect on extra tibia segment formation mediated by amputated positions in the *Gb'E(z)*^{RNAi}-regenerated legs

(A) Regenerated legs amputated at the distal (upper panels), middle (middle panels) and proximal (lower panels) positions of the control (middle columns) and *Gb'E(z)*^{RNAi} (right columns) crickets. Amputated positions are shown in the left columns. Tarsi and extra tibia segments are indicated by black and red brackets, respectively. Ti, tibia; Ta, tarsus; Cl, claw. (B) Ratios of normal and RNAi phenotypes of control and *Gb'E(z)*^{RNAi} crickets amputated at distal, middle and proximal positions at sixth instar. (C) Relative length of each leg segment of the control and *Gb'E(z)*^{RNAi}-regenerated legs normalized to the femur.

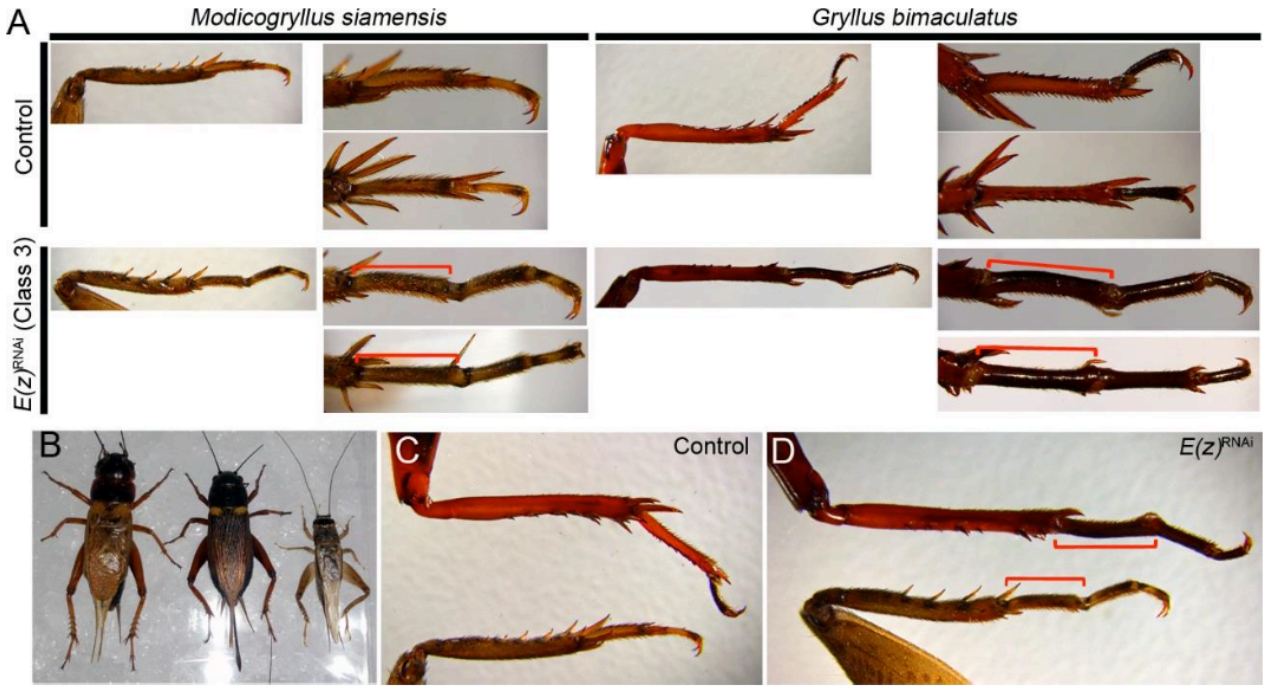

Fig. 2-8. Regenerated *Gryllus bimaculatus* and *Modicogryllus siamensis* legs.
(A) Typical phenotypes of control (upper panels) and *E(z)*^{RNAi} (lower panels) regenerated legs of *Gryllus bimaculatus* (right column) and *Modicogryllus siamensis* (left column) are shown. Lateral views of low magnification images are shown in the left columns, and lateral and dorsal views of high magnification images are shown in the upper and lower sides in right columns. The extra tibia segments are indicated by red brackets. (B) Whole bodies of male and female *Gryllus bimaculatus* (left and middle) and male *Modicogryllus siamensis* (right). (C-D) Comparison of *Gryllus* (upper) and *Modicogryllus* (lower) regenerated legs of control (C) and *E(z)*^{RNAi} crickets (D). The extra tibia segments are indicated by red brackets.

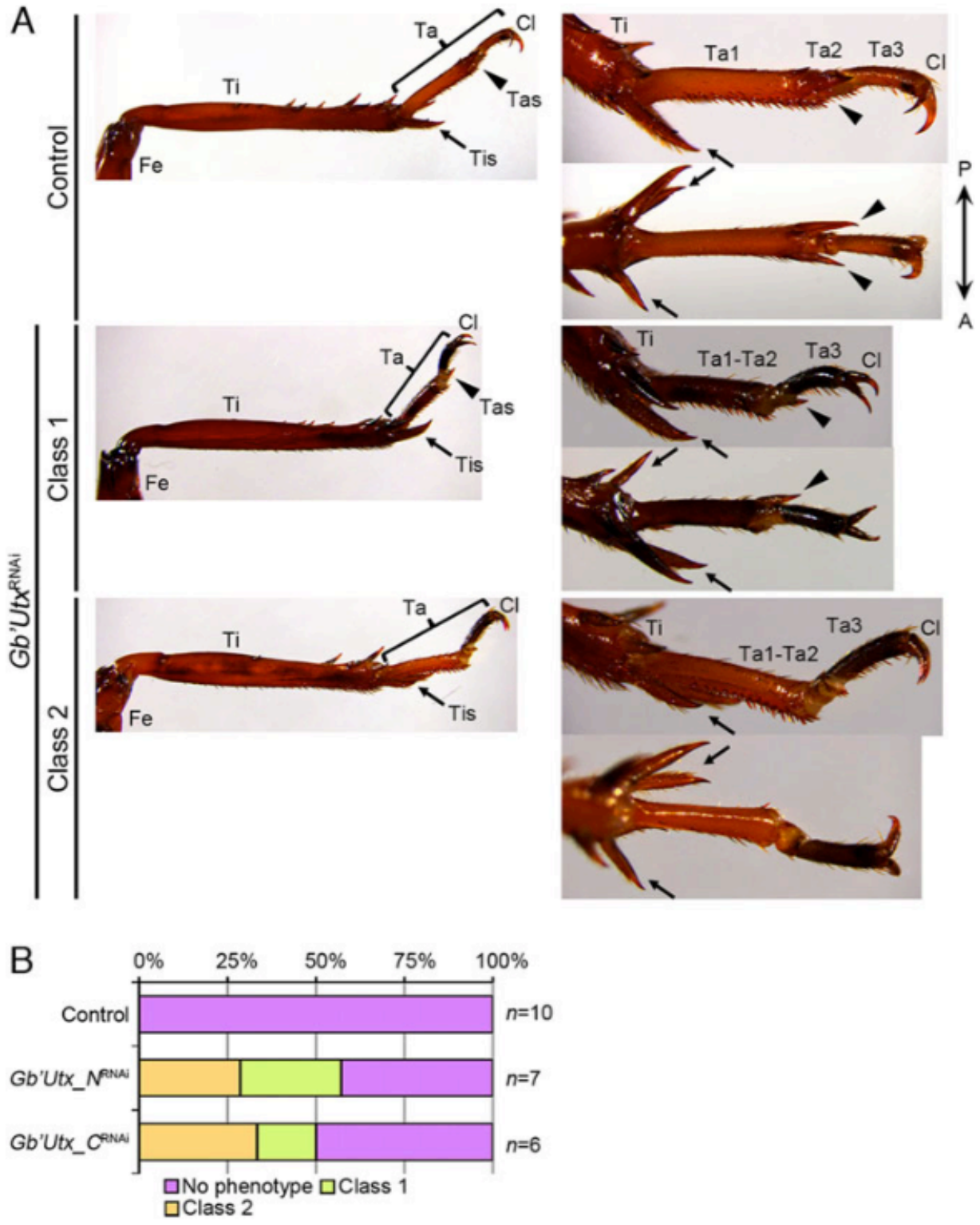

Fig. 2-9. Typical phenotypes of regenerated legs in the control and *Gb'Utx*^{RNAi} crickets.
(A) Regenerated legs in the control and *Gb'Utx*^{RNAi} adults. Lateral views of low magnification images are shown in the left column. Lateral and dorsal views of high magnification images are shown in the right column in the upper and lower panels, respectively. Tibial and tarsal spurs are denoted by arrows and arrowheads, respectively. Fe, femur; Ti, tibia; Ta, tarsus; Cl, claw; Tis, tibial spur; Tas, tarsal spur. (B) Ratio of normal (no phenotype) and RNAi phenotypes (class 1 and 2) of control and *Gb'Utx*^{RNAi} cricket nymphs at sixth instar.

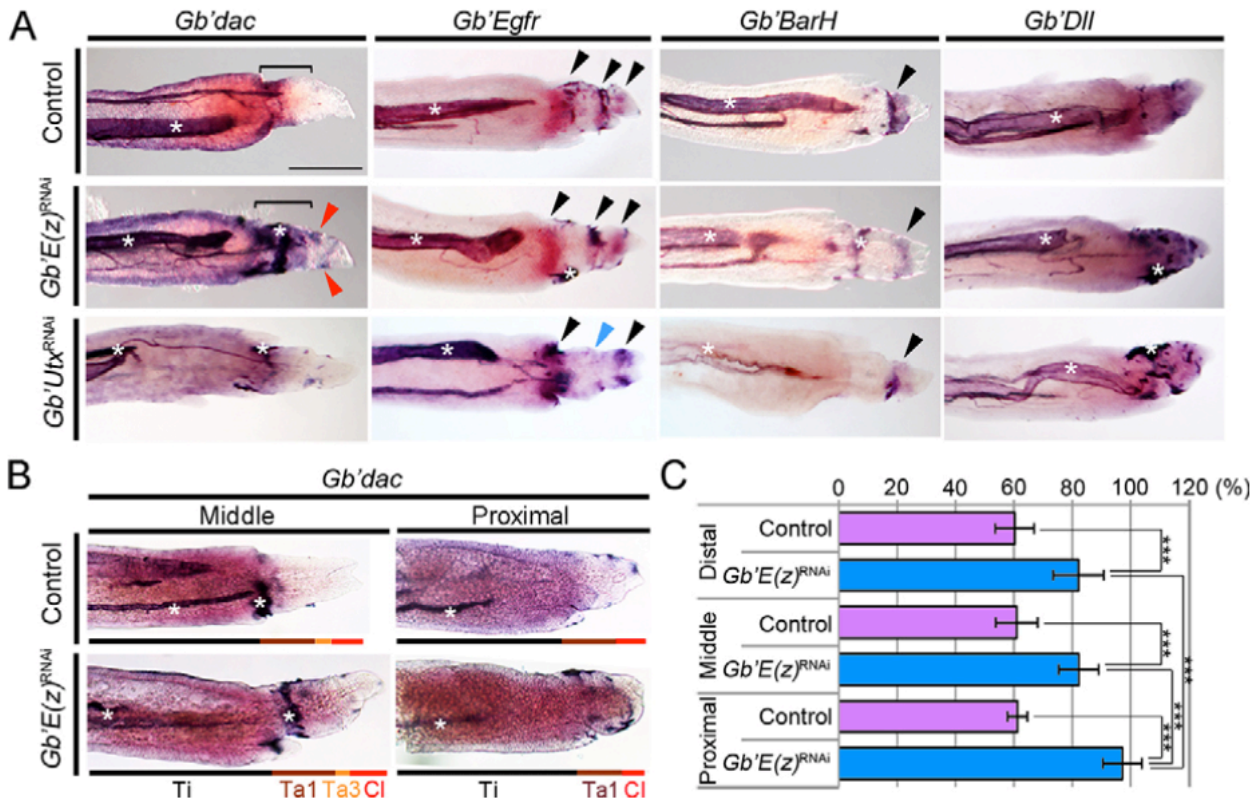

Fig. 2-10. Expression pattern of leg patterning genes in regenerating legs.
(A) *Gb'dac, Gb'Egfr, Gb'BarH* and *Gb'Dll* expression patterns in control, *Gb'E(z)*^{RNAi}- and *Gb'Utx*^{RNAi}-regenerating legs at 6 dpa. Ta1 is indicated by brackets. *Gb'Egfr* and *Gb'BarH* expression is denoted by arrowheads. Asterisks indicate non-specific staining. (B) *Gb'dac* expression patterns in control and *Gb'E(z)*^{RNAi}-regenerating legs amputated at the middle (6 dpa) and proximal positions (7 dpa). Note that the growth rate of cricket nymphs amputated proximally was slower than nymphs amputated distally or in middle; therefore, the regenerating legs was fixed when the leg amputated proximally at 7 dpa although other regenerating legs were fixed at 6 dpa. Ti, tibia; Ta1, tarsomere 1; Ta3, tarsomere 3; Cl, claw. Asterisks indicate non-specific staining. (C) The graph predicts the percentages of the *Gb'dac* expression region within Ta1 (*** $P < 0.01$).

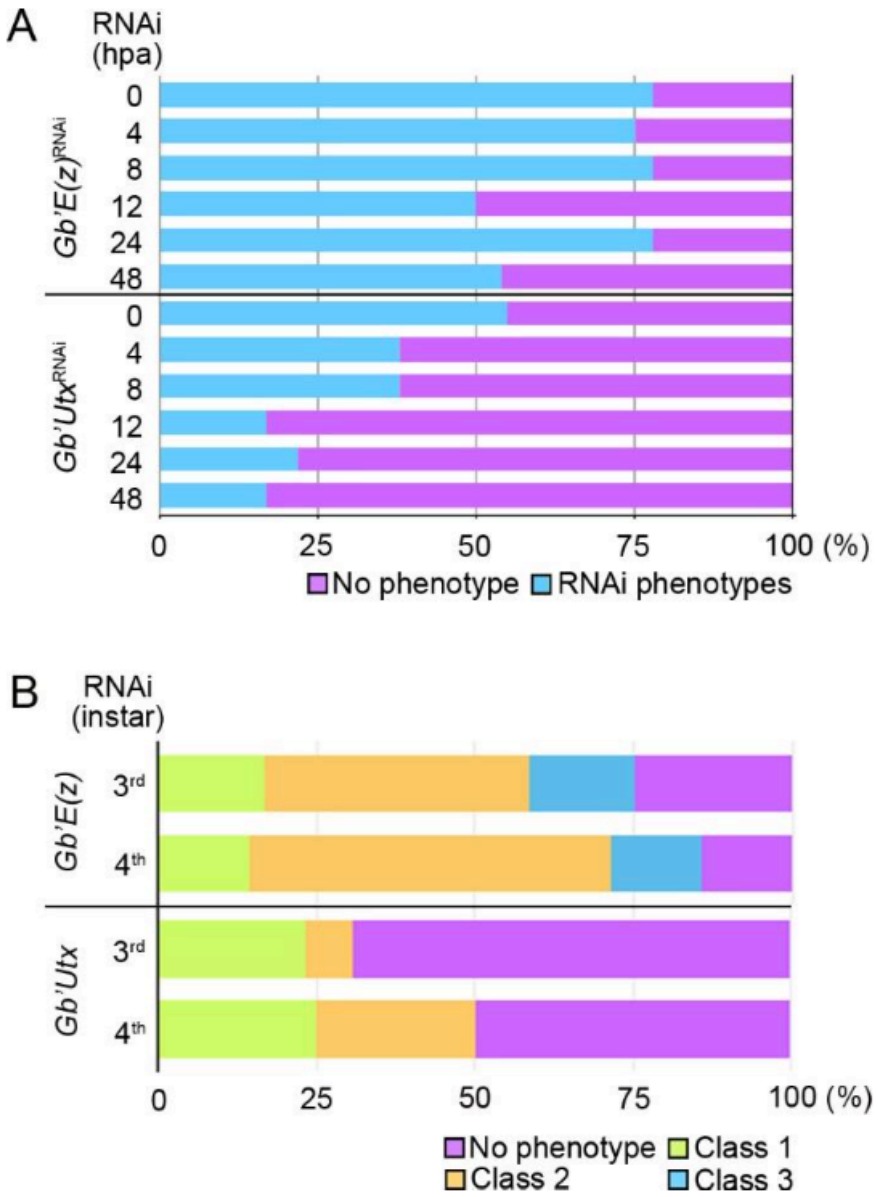

Fig. 2-11. Penetrance of regenerated leg RNAi against epigenetic factors before amputation.
(A) Graph shows the ratios (%) of abnormal regenerated legs (including phenotypes class 1, 2 and 3 of *Gb'E(z)*^{RNAi} and phenotypes class 1 and 2 of *Gb'Utx*^{RNAi}) compared with normal regenerated legs at each time point. In this graph, "hpa" means incubation period (hours) from amputation to RNAi. (B) Graph shows ratio of RNAi phenotypes against *Gb'E(z)* and *Gb'Utx*. "3rd RNAi" denotes the phenotype ratio of regenerated legs with RNAi at third instar and amputated at fourth instar. "4th RNAi" denotes the phenotype ratio of regenerated legs with RNAi and immediately amputated at fourth instar.

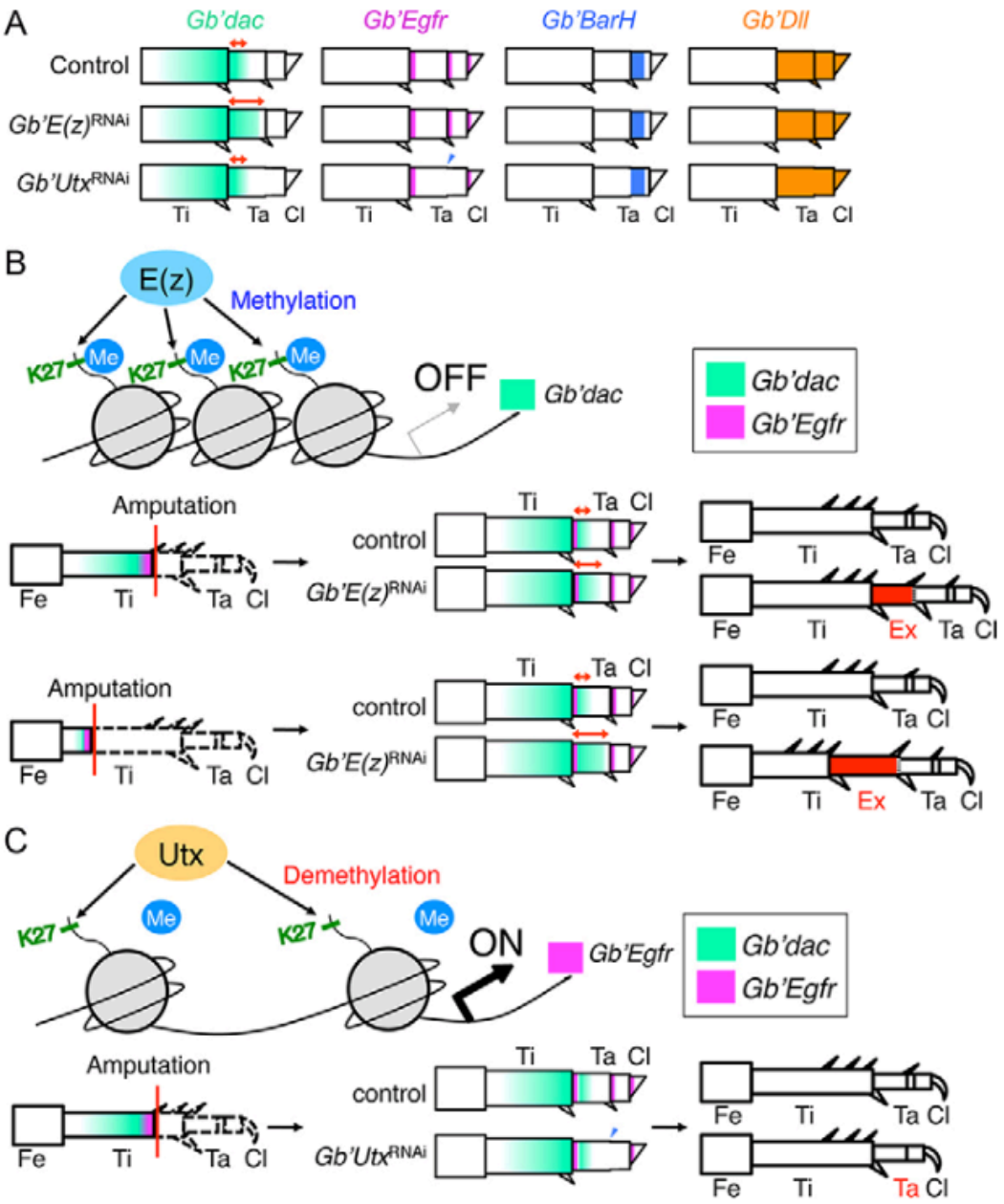

Fig. 2-12. Plausible model for the repatterning process during leg regeneration in the cricket.
(A) Schematic diagrams of *Gb'dac*, *Gb'Egfr*, *Gb'BarH* and *Gb'Dll* expression in the control, *Gb'E(z)*^{RNAi} and *Gb'Utx*^{RNAi} regenerating legs. The *Gb'dac* expression domain in Ta1 is indicated by the red double arrows. (B) E(z) methylates histone H3K27 to induce heterochromatin formation for gene expression repression. In controls, *Gb'dac* is expressed in the tibia and Ta1 to reconstruct tibia segments (indicated by the red double arrows). In *Gb'E(z)*^{RNAi} crickets, *Gb'dac* is expressed in the tibia and Ta1 to reconstruct tibia segments, however, the *Gb'dac* expression domain in Ta1 expanded, which led to the formation of extra tibia segments between tibia and Ta1. After amputation of the cricket leg at the proximal tibia, the *Gb'dac* expression domain expanded widely in comparison with the case after amputation at the distal tibia. Wider *Gb'dac* expression may lead to extra tibia segment formation at high efficiency. Ta3 and claws are normally reconstructed in *Gb'E(z)*^{RNAi} crickets because *Gb'Dll* expression in the tarsus and *Gb'BarH* expression in the tarsus center were not altered. (C) Utx demethylates histone H3K27me3 to induce euchromatin formation for derepression and activation of gene expression. In controls, *Gb'Egfr* was expressed in the distal regions of tibia and Ta1. In *Gb'Utx*^{RNAi} crickets, *Gb'Egfr* expression in the distal region of Ta1 was diminished (indicated by blue arrowheads), which caused leg joint formation and tarsal spur formation defects at Ta1. Ta3 and the claw are normally reconstructed in *Gb'Utx*^{RNAi} crickets because *Gb'Dll* expression in the tarsus and *Gb'BarH* expression in tarsus center were not altered.

Fig. 2-13. Typical embryonic phenotypes in the control and *Gb'Utx*^{RNAi} crickets.
Lateral and dorsal views of control and *Gb'Utx*^{RNAi} embryos at stage 13 are shown. *Gb'Utx*^{RNAi} embryos exhibited abnormal morphologies in the head segments.

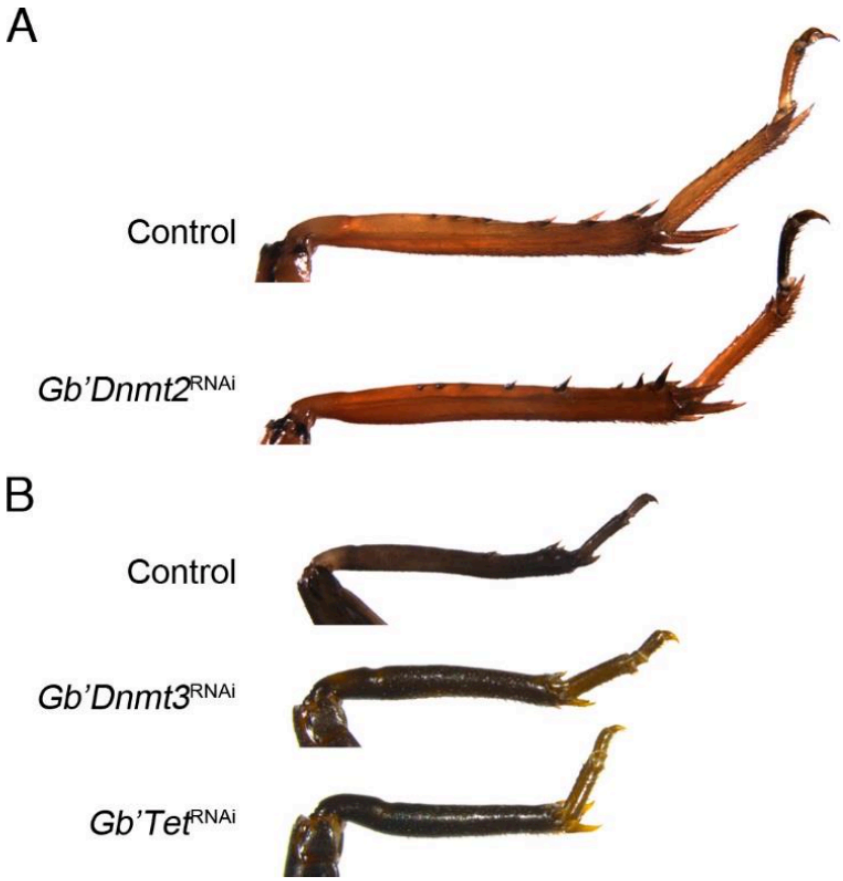

Fig. 2-14. Typical regenerated leg phenotypes in the control, *Gb'Dnmt2*^{RNAi}, *Gb'Dnmt3*^{RNAi} and *Gb'Tet*^{RNAi} crickets.
Lateral views of regenerated legs are shown. (A) Regenerated legs in the control and *Gb'Dnmt2*^{RNAi} adults. (B) Regenerated legs in the control, *Gb'Dnmt3*^{RNAi} and *Gb'Tet*^{RNAi} at sixth instar nymphs.

Chapter 3.

Epigenetic regulation via methylation on H3K27 is involved in photoperiodic responses of locomotor rhythm

3.1. Abstract

Insects show daily behavioral rhythms that are controlled by an endogenous oscillator, the circadian clock. The rhythm synchronizes to daily light–dark cycles (LD) and changes waveform in association with seasonal change in photoperiod. To explore the molecular basis of the photoperiod-dependent changes in circadian locomotor rhythm, the role of a chromatin modifier was investigated, *Enhancer of zeste* (*Gb'E(z)*), in the cricket, *Gryllus bimaculatus*. Under a 12 h: 12 h LD (LD 12:12), *Gb'E(z)* was constitutively expressed in the optic lobe, where the clock is located; active phase (α) and rest phase (ρ) were approximately 12 h in duration, and α/ρ ratio was approximately 1.0. When transferred to LD 20:4, the α/ρ ratio became significantly smaller, and the *Gb'E(z)* expression level was significantly reduced at 6 h and 10 h after light-on. This change was associated with change in clock gene expression profiles. The photoperiod-dependent changes in α/ρ ratio and clock gene expression profiles were prevented by knocking down *Gb'E(z)* by RNAi. These results indicate that epigenetic histone modification by *Gb'E(z)* is involved in photoperiodic modulation of the *G. bimaculatus* circadian rhythm.

3.2. Introduction

Most animals show daily rhythms in various physiological functions that synchronize with daily environmental cycles, such as light–dark cycles (LD), which are affected by Earth's rotation (Dunlap *et al*., 2004). The rhythm is generated by a circadian clock, which is an endogenous mechanism that oscillates over an approximately 24-h period. The circadian clock's oscillatory mechanism is based on transcriptional/translational molecular feedback loops (Aguilar-Roblero *et al*., 2015; Hardin, 2009; Tataroglu and Emery, 2015). In insects, the clock machinery is most profoundly studied in the fruit fly, *Drosophila melanogaster*, in which the major players are *Clock* (*Clk*) and *cycle* (*cyc*) (Hardin, 2009; Tataroglu and Emery, 2015); their product proteins, CLK and CYC, form heterodimers and activate the transcription of *period* (*per*) and *timeless* (*tim*) during the

late day to early night. The translated proteins PER and TIM accumulate in the cytoplasm during the night, and in the late night they heterodimerize and enter the nucleus to repress their own transcription by inhibiting CLK-CYC transcriptional activity. This feedback results in a reduction of PER and TIM levels, which leads to reactivation of *per* and *tim* transcription (Hardin, 2009; Tataroglu and Emery, 2015).

Recent studies revealed that circadian clock cycling is precisely controlled by mechanisms that include chromatin remodeling, recruitment of RNA polymerases, and posttranscriptional and posttranslational modifications (Aguilar-Arnal and Sassone-Corsi, 2015; Bellet and Sassone-Corsi, 2010; Kwok *et al*., 2015; Ripperger and Merrow, 2011). Chromatin remodeling plays an important role in regulating the circadian clock and in its response to environmental time cues. In both mammals and insects, CLK acts as a transcriptional activator and recruits other transcription factors by binding to E-boxes at the regulatory regions of clock-controlled genes, including *per* and *tim* (Doi *et al*., 2006; Menet *et al*., 2014; Taylor and Hardin, 2008).

In addition to daily time-keeping, the circadian clock plays a key role in seasonal changes in physiology, including the change in active phase to rest phase ratio (α/ρ ratio), based on seasonal change in photoperiod (Koga *et al*., 2005; Tomioka and Chiba, 1989a; Tomioka and Chiba, 1989b). The photoperiod-dependent change in α/ρ ratio persists for many days in constant darkness and is recognized as a kind of history-dependent change in the circadian clock. The history-dependent changes are also observed in the free-running period (Barrett and Page, 1989; Page, 1982; Page, 1983). However, the molecular basis of the photoperiod-dependent changes has thus far remained elusive.

In the present study, the possible was investigated that is involvement of epigenetic regulation in photoperiod-dependent changes in circadian rhythm of the cricket, *Gryllus bimaculatus*. The cricket was selected in this study for the following reasons: first, the cricket showed a clear photoperiodic response in locomotor activity rhythms (Koga *et al*., 2005; Tomioka

and Chiba, 1989b); second, the circadian clock has been localized in the optic lobe (Tomioka and Chiba, 1984; Tomioka and Chiba, 1992); and third, cDNAs were previously obtained for major clock genes (Tomioka, 2014). The role of a chromatin modifier, E(z), which trimethylates lysine 27 of histone H3 (H3K27) (Hamada *et al*., 2015), was examinated in photoperiodic modulation of the circadian rhythm, and found that knockdown by RNAi prevented photoperiodic modulation. The results are discussed relative to the role of E(z) in seasonal adaptation.

3.3. Materials and methods

Animals

Adult male crickets were purchased or taken from chronobiology laboratory colony, which is maintained under standard conditions of light-dark (LD) 12:12-h, at a constant temperature of 25 °C. The crickets were fed laboratory chow and water.

Measurement of mRNA levels

Quantitative real-time RT-PCR was used to measure mRNA levels. Total RNA was extracted from optic lobes of four to six adult males using ISOGEN (Nippon Gene, Tokyo, Japan) or TRIzol Reagent (Invitrogen, Carlsbad, CA, USA). The total RNA was treated with DNase I to remove any traces of genomic DNA. Approximately 250 ng of total RNA of each sample was reverse transcribed with random 6 mers using PrimeScript RT Reagent Kit (Takara, Tokyo, Japan). qPCR was performed with an Mx3000P Real-time PCR System (Stratagene, La Jolla, CA, USA) using Fast Start Universal SYBR Green Master (Roche, Tokyo, Japan) including SYBR Green with the following primers for respective genes: 5′-AAGGTGCGAAAACAGGCATC-3′ and 5′-TCGTCGTTTTGGTGGATGTG-3′ for *Gb'E(z)* (GenBank Accession No. LC012934), 5′-

AAGCAAGCAAGCATCCTCAT-3′ and 5′-CTGAGAAAGGAGGCCACAAG-3′ for *Gb'per* (GenBank Accession No. AB375516), 5′-GATTATGAAGTCTGTGATGATTGG-3′ and 5′-AGCATTGGAGAGAACTGAA-GAGGT-3′ for *Gb'tim* (GenBank Accession No. AB548625), 5′-GGCCGAAGCTCATAAAGTGG-3′ and 5′-AACCGCACAAAGGAACCATC-3′ for *Gb'cyc* (GenBank Accession No. AB762416), 5′-AATGACCGTAGTCGAGAAAGTGAAG-3′ and 5′-TTGCGATGATTGAGGTTGTTG-3′ for *Gb'Clk* (GenBank Accession No. AB738083), and 5′-GCTCCGGATTACATCGTTGC-3′ and 5′-GCCAAATGCCGAAGTTCTTG-3′ for *Gb'rpl18a* (GenBank Accession No. DC448653). Standard curves for the transcripts were generated by serial dilutions of amplified cDNAs and included in each qPCR run. After 40 PCR cycles, samples were subjected to melting curve analysis, and a single expected amplicon was confirmed in each sample. The results were analyzed using software associated with the instrument: quantification of mRNA levels was performed by the standard curve method, and the values were normalized to the values of *rpl18a* at each time point.

RNAi

Double-stranded RNAs (dsRNAs) were synthesized using the MEGAScript T7 Kit (Ambion, Carlsbad, CA, USA) and adjusted to 20 μM for *DsRed2* and 2 μM for *Gb'E(z)* for RNAi. For dsRNA synthesis was used the T7 primer, 5′-taatacgactcactataggg-3′, for *Gb'E(z)* and an exogenous gene, *DsRed2*; dsRNA lengths were 431 bp and 660 bp, respectively. In total, 700 nL of dsRNA was injected into the abdomens of the adult male crickets. As a negative control, the cricket were injected dsRNA for *DsRed2*.

Recording of locomotor activity

Locomotor activity of individual animals was recorded with an actograph made of a transparent plastic box (18 × 9 × 4.5 cm) with a rocking substratum, as previously described (Moriyama *et al*., 2008). A magnetic reed switch sensed rocking movements of the substratum caused by a moving cricket. The number of movements was recorded every 6 min by a computerized system. Water and food were provided ad libitum. The activity chambers were placed in an incubator in which temperature was kept at 25 ± 0.5 °C and desired lighting regimens were provided by a cool white fluorescent lamp connected to an electric timer. The light intensity was 600–1000 lux, which varied based on the animal's proximity to the lamp.

The raw data were displayed as conventional double-plotted actograms to judge activity patterns, and free-running periods were calculated using the χ^2 periodogram (Sokolove and Bushell, 1978) in ActogramJ (Schmid *et al*., 2011). If a peak of the periodogram was above the 5 % confidence level, the peak period was designated as statistically significant. The duration of the active phase, or subjective night, (α) were estimated with ActogramJ: the boundary of the active phase was defined at the time point where the moving average of activity exceeded or fell below 70 % of daily average activity; then, a linear regression line was fitted to the points for consecutive days. The rest of the time was designated as the rest phase, or subjective day, (ρ).

3.4. Results

Expression profile of *Gb'E(z)* and its suppression by RNAi in the optic lobe

First, *Gb'E(z)* was examined whether expressed in the optic lobe, which is known to harbor the circadian clock in the cricket, by using qPCR to measure *Gb'E(z)* mRNA levels in the tissue. Under LD 12:12 *Gb'E(z)* mRNA was fairly consistently expressed throughout a day in intact crickets (Fig. 3-1), and no daily fluctuation was observed (ANOVA, $F_{5, 41} = 0.34$, $P > 0.88$). To

estimate the effects of *Gb'E(z)*^{RNAi}, *Gb'E(z)* mRNA level was measured in the optic lobe of *Gb'E(z)*^{RNAi} crickets and control (*DsRed2*^{RNAi}) crickets, which were treated with ds*DsRed2*. *DsRed2*^{RNAi} crickets showed similar *Gb'E(z)* expression to that of intact crickets (Fig. 3-1) and no daily rhythm was observed (ANOVA, $F_{5, 37} = 0.52$, $P > 0.76$). The value at each time point did not differ from that of intact crickets (Tukey-test, $P > 0.05$). In *Gb'E(z)*^{RNAi} crickets, *Gb'E(z)* expression was greatly reduced compared with the control and intact crickets at all time points (Tukey-test, $P < 0.01$). Expression reduced to approximately 53% of that of intact and control crickets at zeitgeber time (ZT) 10 (ZT 0 corresponds to lights-on). These results indicate that *Gb'E(z)* is expressed rather constitutively in the optic lobe and could be knocked down by RNAi against *Gb'E(z)*, and that *DsRed2*^{RNAi} crickets can be used as a control.

Effects of *Gb'E(z)*^{RNAi} on circadian locomotor rhythms in LD 12:12

To examine the role of *Gb'E(z)* in regulation of circadian rhythms, the locomotor activity was recorded in *Gb'E(z)*^{RNAi}, intact and control crickets. Both intact and control crickets showed nocturnal activity rhythms that peaked just after lights-off under LD 12:12, and the rhythm persisted with a free-running period of 23.66 ± 0.25 (mean ± SD) h (n = 12) and 23.63 ± 0.33 h (n = 18), respectively, in constant darkness (DD) (Fig. 3-2a, b). The duration of active phase (α) and rest phase (ρ) were measured, and calculated α/ρ ratio to characterize the daily activity profile. The α/ρ ratios of intact and control crickets were 0.94 ± 0.07 (mean ± SD) (n = 13) and 0.97 ± 0.09 (n = 23), respectively, in LD 12:12, and 0.95 ± 0.23 (n = 12) and 0.97 ± 0.11 (n = 18), respectively, in DD (Table 3-1). These results were consistent with those of the previous study (Koga *et al*., 2005). The *Gb'E(z)*^{RNAi} crickets showed nocturnal locomotor rhythms similar to those of control crickets under LD (Fig. 2c); their α/ρ ratios were 0.99 ± 0.08 (n = 26) and 1.02 ± 0.11 (n = 23) in LD 12:12 and DD, respectively (Table 3-1), and were not significantly different from those of the intact and control crickets (ANOVA followed by Tukey-test, $P > 0.05$). However, their average free-running

period (23.97 ± 0.16 h, n = 23) was significantly longer than that of intact and control crickets (ANOVA followed by Tukey-test, $P < 0.01$), which indicates that methylation on H3K27 is involved in regulating the free-running period in DD.

Expression profile of clock genes in the optic lobe

Expression profiles of the clock genes *Gb'per*, *Gb'tim*, and *Gb'cyc* were investigated in the optic lobe of *DsRed2*^{RNAi} and *Gb'E(z)*^{RNAi} crickets under LD 12:12 by qPCR. The results are shown in Fig. 3. In the control crickets, the mRNA levels of *Gb'per* and *Gb'tim* showed a significant daily fluctuation, which peaked at ZT 18 under LD 12:12 (ANOVA: $F_{5, 36} = 9.01$, $P < 0.01$ for *Gb'per*, $F_{5, 17} = 67.97$, $P < 0.01$ for *Gb'tim*). *Gb'cyc* also showed a significant daily cycling, with a peak at ZT 10 in LD 12:12 (ANOVA: $F_{5, 41} = 3.62$, $P < 0.01$). Similar rhythmic expression profiles were observed for the three genes in *Gb'E(z)*^{RNAi} crickets (ANOVA: $F_{5, 20} = 15.47$, $P < 0.01$ for *Gb'per*; $F_{5, 17} = 24.25$, $P < 0.01$ for *Gb'tim*; $F_{5, 22} = 4.45$, $P < 0.01$ for *Gb'cyc*) but with slight changes in pattern or phase in comparison with those in *DsRed2*^{RNAi} crickets: *Gb'per* showed a significant reduction at ZT 6 and ZT 10 (*t*-test, $P < 0.01$), and *Gb'tim* showed a slight increase at ZT 2, a slight reduction at ZT 10 (*t*-test, $P < 0.05$), and a reduction at ZT 18 (*t*-test, $P < 0.01$) that resulted in a phase advance of the peak by 4 h. Moreover, *Gb'cyc* showed a significant increase at ZT 2 (*t*-test, $P < 0.05$).

Role of *Gb'E(z)* in photoperiodic modulation of locomotor rhythms

In the cricket, the α/ρ ratio in DD depended on the photoperiod of the preceding LD (Koga *et al*., 2005). To examine the effects of *Gb'E(z)*^{RNAi} on this photoperiodic effect on the α/ρ ratio, the locomotor activity rhythm of intact, *DsRed2*^{RNAi}, and *Gb'E(z)*^{RNAi} crickets were recorded under LD

12:12, followed by LD 20:4 for 10 cycles, and then by DD. The representative records are shown in Fig. 4, and the locomotor rhythm parameters are summarized in Table 1. The intact and control crickets showed that locomotor activity was confined to a short dark phase under LD 20:4, and the shortened active phase persisted under subsequent free-running conditions (Fig. 3-4a, b). The α/ρ ratios of intact and *DsRed2*^{RNAi} crickets were 0.53 ± 0.20 (mean ± SD) (n = 23) and 0.69 ± 0.22 (n = 33), respectively, under LD 20:4, and 0.46 ± 0.20 (n = 13) and 0.55 ± 0.19 (n = 22), respectively, under DD (Table 1). There was no significant difference between the values under DD (ANOVA followed by Tukey-test, $P > 0.05$). These results are consistent with those of Koga *et al*. [53]. Under LD 20:4 some *Gb'E(z)*^{RNAi} crickets (6/23) showed similar changes in α/ρ ratio (Fig. 3-4c). However, the other crickets (17/23) exhibited an activity pattern that consisted of a strong activity bout after lights-on in addition to the light-off peak under LD 20:4; the average α/ρ ratio was 0.84 ± 0.28 (n = 23) (Table 3-1). Interestingly, the α/ρ ratio was maintained in the ensuing DD, with an average of 0.83 ± 0.25 (n = 17), which was significantly greater than those of the intact and control crickets (ANOVA followed by Tukey-test, $P < 0.01$). Interestingly, the free-running period of the *Gb'E(z)*^{RNAi} crickets (23.99 ± 0.16 h, n = 17) was significantly longer than that of the control crickets (23.70 ± 0.23 h, n = 22) (Tukey-test, $P < 0.01$). These results indicate that H3K27 methylation is involved in photoperiodic modulation and regulation of free-running period in the circadian locomotor rhythm.

Involvement of *Gb'E(z)* in photoperiodic modulation of clock gene expression profiles

Because *Gb'E(z)* is the epigenetic factor that controls gene expression through H3K27 methylation, *Gb'E(z)* is predicted that involved in photoperiodic modulation of α/ρ ratio through alteration in clock gene expression. Consequently, endogenous *Gb'E(z)* mRNA levels in the optic lobe was examined whether altered with a change of photoperiodic condition (Fig. 3-5a). In the control crickets, *Gb'E(z)* showed no significant daily change in its expression, but a significant

reduction was found at ZT 6 and ZT 10 in LD 20:4 when compared with that in LD 12:12 (Tukey-test, $P < 0.01$). *Gb'E(z)*^{RNAi} highly reduced *Gb'E(z)* levels compared with the control at all the points in LD 20:4 (Tukey-test, $P < 0.01$). The reduced levels were significantly less at ZT 2-10 and ZT 18 than those with same treatment under LD 12:12 (Tukey-test, $P < 0.01$ for ZT 2-10 and $P < 0.05$ for ZT 18). These results indicate that *Gb'E(z)* expression level is affected by photoperiod and may be involved in photoperiodic modulation of locomotor rhythm. Then, the expression profiles of the clock genes *Gb'per*, *Gb'tim*, and *Gb'cyc* were examined in the optic lobe in the control and *Gb'E(z)*^{RNAi} crickets in LD 20:4 by qPCR (Fig. 3-5b–d). In the control crickets, *Gb'per* and *Gb'cyc* mRNA levels showed significant daily fluctuation (ANOVA: $F_{5, 26} = 3.97$, $P < 0.01$ for *Gb'per*; $F_{5, 27} = 3.48$, $P < 0.05$ for *Gb'cyc*). The peak phase occurred during the late day phase (ZT 14), which indicates that *Gb'per* and *Gb'cyc* oscillations advanced and delayed by approximately 4 h, respectively, compared with those in the preceding LD 12:12 (Fig. 5b, d). *Gb'tim* mRNA levels also showed significant daily cycling, with a peak at ZT 18 (ANOVA: $F_{5, 26} = 17.50$, $P < 0.01$), retaining the phase relationship to the lights-on similar to that was seen in LD 12:12 (Fig. 3-5c). In *Gb'E(z)*^{RNAi} crickets, mRNA levels of the three clock genes showed significant daily fluctuation (ANOVA: $F_{5, 27} = 12.09$, $P < 0.01$ for *Gb'per*; $F_{5, 18} = 37.93$, $P < 0.01$ for *Gb'tim*; $F_{5, 38} = 7.58$, $P < 0.01$ for *Gb'cy*c). *Gb'tim* showed a phase relationship with LD 20:4 similar to that in the control crickets, but the mRNA levels were significantly reduced (*t*-test, $P < 0.01$). Interestingly, the peak phase of *Gb'per* and *Gb'cyc* was delayed and advanced by approximately 8 and 4 h, respectively, relative to control crickets (Fig. 3-5b, d). These results indicate that expression profiles of *Gb'per* and *Gb'cyc* were altered by photoperiod and that this alteration was mediated at least in part by *Gb'E(z)*.

3.5. Discussions

RNAi knockdown approach revealed that the epigenetic factor *Gb'E(z)* is involved in regulating free-running period and photoperiodic modulation of the locomotor rhythm in the cricket, *G. bimaculatus.*

Gb'E(z) expression in the optic lobe

In this study, qPCR analysis revealed that the epigenetic modifier *Gb'E(z)* is constitutively expressed in the optic lobe, which is the location of the cricket's circadian clock (Tomioka and Chiba, 1992). The expression profile indicates that most of the epigenetic modifiers involved in circadian gene expression are produced and recruited when needed to regulate transcription (Hamon and Cossart, 2008). In mammals, for example, CLOCK plays a key role in the event and forms a transcriptional complex with BMAL1 to activate *Per* and *Cry* transcription by binding to the E-box in their upstream region (Stanewsky, 2003). Meanwhile, CLOCK acts as a factor that opens up chromatin, which enables other transcriptional factors to act on target genes of CLOCK (Menet *et al*., 2014). Similar molecular events may occur in transcription of *per* and *tim* in *Drosophila*, because CLK-CYC binding to upstream and/or intronic E-boxes of *per* and *tim* controls chromatin modifications through H3K9 acetylation and H3K4 trimethylation (Taylor and Hardin, 2008). Interestingly, however, the *Gb'E(z)* mRNA levels at ZT 6 and ZT 10 were higher in LD 12:12 than LD 20:4. The knowledge about these phenomena as to relationship between cricadian rhythm and epigenetic regulation, this is the first evidence for photoperiodic regulation of a clock-related epigenetic modifier in insects. Light-induced modification of chromatin is known for H3S10 in the mammalian circadian clock in the suprachiasmatic nucleus (Crosio *et al*., 2000); it is a result of phosphorylation and occurs within 5 min after lights-on, which is similar to *c-fos* induction. *Gb'E(z)* seems to be regulated by a different mechanism than immediate induction of

phosphorylation, because no apparent change was observed at lights-on in *Gb'E(z)* mRNA levels (Figs. 3-1 and 3-5). One candidate regulator for this photoperiodic regulation of *Gb'E(z)* might be KISMET, a chromatin-remodeling enzyme, because it is required for normal circadian light responses in *Drosophila* (Dubruille *et al*., 2009). *Gb'E(z)* was also shown to be induced by mechanical stimulation; when a leg was injured, the beginning of regeneration was associated with upregulation of *Gb'E(z)* (Bando *et al*., 2013; Hamada *et al*., 2015). Thus, its expression seems to be regulated by multiple pathways.

Gb'E(z) is involved in photoperiodic modulation of the circadian rhythm

Involvement of epigenetic factors in regulating the circadian clock has been shown in animals. In *Drosophila*, Brahma chromatin-remodeling protein regulates CLK binding to target promoters, and hence the free-running period of the rhythm (Kwok *et al*., 2015). Mice that lacked *Mettle3*, a factor that regulates RNA methylation, showed a delay in RNA processing that leads to circadian period elongation (Fustin *et al*., 2013). However, in the current results revealed that *Gb'E(z)* plays a different role from those previously described epigenetic regulation models. *Gb'E(z)* knockdown significantly lengthened the free-running period in DD after LD 12:12 and LD 20:4 (Table 3-1). Another important effect of $Gb'E(z)^{RNAi}$ was elimination of the photoperiod-dependent change in α/ρ ratio. In control crickets, the active phase was usually compressed during the dark phase in LD 20:4; consequently, the α/ρ ratio became much smaller (0.69 ± 0.22) than that in LD 12:12 (0.97 ± 0.09). The α/ρ ratio further decreased when transferred to DD (0.55 ± 0.19). These results are consistent with previous results (Koga *et al*., 2005). However, compression of the active phase was only observed in a few $Gb'E(z)^{RNAi}$ crickets, and the majority of them showed no compression; the average α/ρ ratio was 0.84 ± 0.28 and 0.83 ± 0.25 in LD 20:4 and in the ensuing DD, respectively. These results clearly indicate that epigenetic regulation by E(z) is required for response to changing photoperiod to modulate the duration of the active phase. The link between

regulatory mechanisms and circadian waveform or free-running period should be investigated in future studies.

Gb'E(z) contributes to response to photoperiodic changes via clock genes

This study revealed that temporal expression profiles of clock genes change in response to LD cycle. Under a long-day condition of LD 20:4, the circadian expression profile of the clock gene *Gb'tim* showed a similar pattern to that in LD 12:12, whereas *Gb'per* and *Gb'cyc* expression was advanced and delayed by 4 h, respectively (Fig. 3-5). *Gb'E(z)*^{RNAi} prevented the shift of *Gb'per* and *Gb'cyc* rhythms in response to LD 20:4 (Fig. 3-5), which indicates involvement of *Gb'E(z)* in photoperiod-dependent phase setting of daily clock gene expression. This function of *Gb'*E(z) may be mediated by trimethylation of histone H3 at K27 (H3K27me3) because H3K27me3 is known to regulate expression of *Per1* and *Per2* in the mammalian circadian clock (Etchegaray *et al*., 2006). In the mammalian clock, EZH2, a homologous protein of E(z), is recruited by the CLOCK/BMAL1 complex to bind to H3 in the promoter regions of *Per1* and *Per2* and causes di- and trimethylation of H3K27 (Etchegaray *et al*., 2006). The phase shift of *Gb'cyc* caused by *Gb'E(z)*^{RNAi} might be attributable to indirect effects through the change of *Gb'per* rhythm, because *Gb'per* is involved in the transcriptional regulation of *Gb'cyc* (Uryu *et al*., 2013). The photoperiodic regulation of daily clock gene expression may be caused by a change in *Gb'E(z)* mRNA levels (Fig. 3-5a). Because no daily rhythm is known in binding ability of EZH2 to CLOCK:BMAL1 and the promoter regions of *Per1* and *Per2* (Etchegaray *et al*., 2006), quantity of E(z) may affect the binding and eventually daily expression profiles of the clock genes. The change in *Gb'E(z)* levels may not be a simple response to a given photoperiod, because the α/ρ ratio established in a photoperiod is maintained for a long period in DD (Koga *et al*., 2005). The mechanism of this long-lasting change is an important issue that should be addressed in future studies. The long-lasting response to photoperiod is reminiscent of photoperiodism regulating the seasonal physiological adaptation in insects. Many

cricket species also show photoperiodic responses (Tauber *et al*., 1986). For example, nymphal development of *Modicogryllus siamensis* is photoperiodically regulated: nymphs grow faster under long-day conditions and become adults after seven moltings, whereas, under short-day conditions, their nymphal period is elongated, and the number of molts to adulthood increases (Taniguchi and Tomioka, 2003). Interestingly, developmental time course is determined within about 10 days after hatching (Taniguchi and Tomioka, 2003), which indicates a long-lasting effect of photoperiod. This is consistent with the finding in this study that the long-lasting change in the clock is caused by an epigenetic mechanism, and photoperiodic response is most likely underlain by the circadian clock (Goto, 2013; Saunders, 2012). How change in molecular oscillation is reflected in overt activity rhythms is still being elucidated. There are lines of evidence that molecular oscillation of the circadian clock changes in a photoperiod-dependent manner. In *Drosophila*, daily *per* expression, i.e., phase and ratio of splicing variants, changes in response to photoperiod (Collins *et al*., 2004; Majercak *et al*., 2004; Majercak *et al*., 1999). In other insects, the expression profiles of clock genes also reportedly changed based on photoperiod (Sakamoto *et al*., 2009; Syrova *et al*., 2003). This study showed that *Gb'per* and *Gb'cyc* responded differently so that the peak phases of their daily expression rhythms became closer in the long photoperiod (Fig. 3-5). Although additional research is necessary, this phase change might be somehow related to the shortening of the active phase under long-day conditions.

3.6. Conclusion

The present study discovered for the first time that methylation on H3K27 by *Gb'*E(z) is required for response to photoperiodic changes, such as length of the active phase and free-running period, which is associated with changes in expression profiles of clock component genes. These results contribute to molecular dissection of the mechanisms of insect photoperiodism and photoperiodic modulation in circadian rhythms.

Table 3-1. Effects of RNAi against *Gb'E(z)* and *DsRed2* on the locomotor rhythm of *Gryllus bimaculatus.* ANOVA revealed significant difference in both free-running period (τ) ($F_{5, 98} = 9.01$, $P < 0.01$) and α/ρ ratio ($F_{11, 230} = 22.0$, $P < 0.01$). Values with different lower case letter significantly differ from each other (Tukey-test, $P < 0.01$, except for α/ρ ratios between intact in DD following LD 20:4 and *DsRed2*^{RNAi} in LD 20:4).

Treatment	n	Light Condition	τ (mean ± SD) h	α/ρ ratio (mean ± SD)
LD12:12				
intact	13	LD	-	0.94 ± 0.07^{a}
	12	DD	23.66 ± 0.25^{a}	0.95 ± 0.23^{a}
DsRed2^{RNAi}	23	LD	-	0.97 ± 0.09^{a}
	18	DD	23.63 ± 0.33^{a}	0.97 ± 0.11^{a}
Gb'E(z)^{RNAi}	26	LD	-	0.99 ± 0.08^{a}
	23	DD	23.97 ± 0.16^{b}	1.02 ± 0.11^{a}
LD20:4				
intact	23	LD	-	0.53 ± 0.20^{cd}
	13	DD	23.80 ± 0.12^{ab}	0.46 ± 0.20^{d}
DsRed2^{RNAi}	33	LD	-	0.69 ± 0.22^{bc}
	22	DD	23.70 ± 0.23^{a}	0.55 ± 0.19^{cd}
Gb'E(z)^{RNAi}	23	LD	-	0.84 ± 0.28^{ab}
	17	DD	23.99 ± 0.16^{b}	0.83 ± 0.25^{ab}

Figures and Figure legends

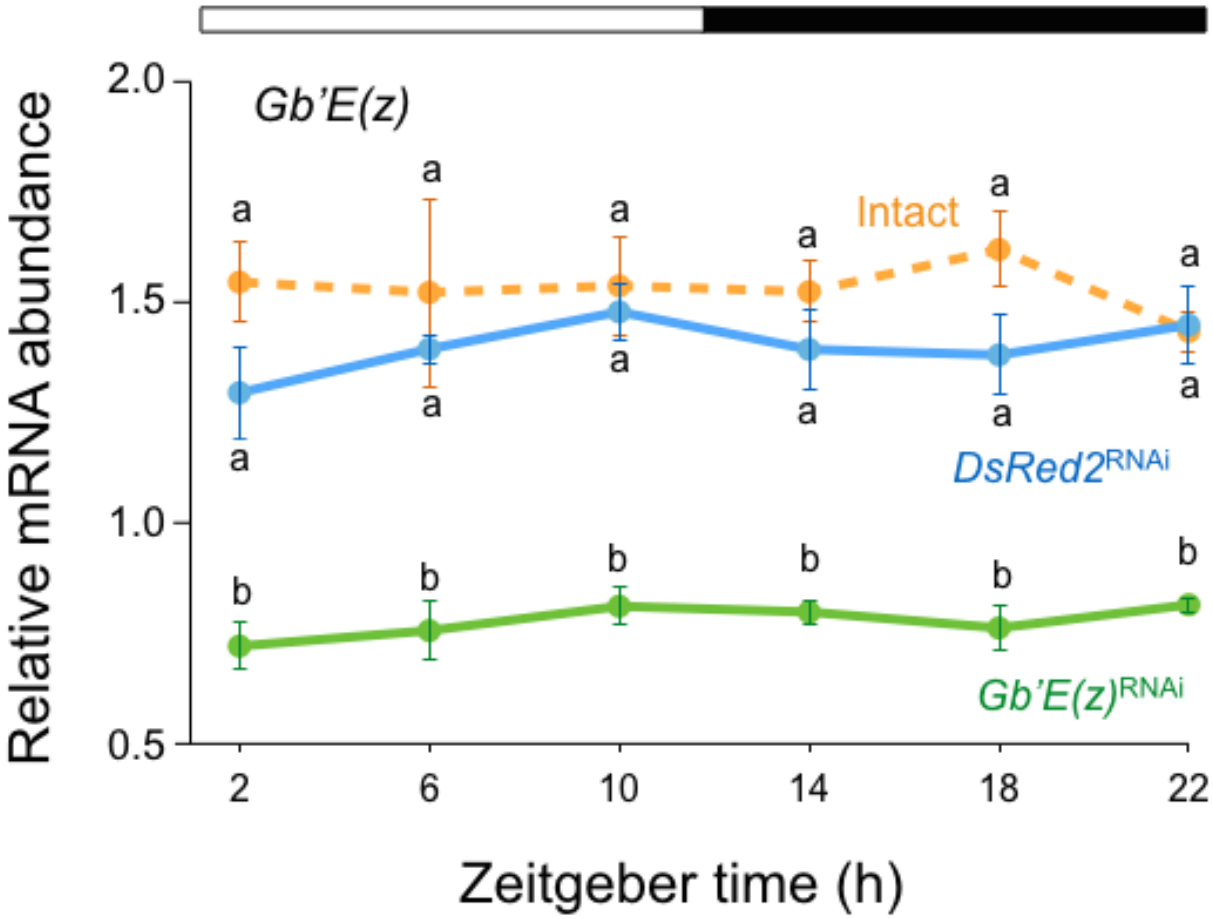

Fig. 3-1. Daily expression profile of *Gb'E(z)* in the optic lobe of crickets under LD 12:12. Blue, green, and orange symbols indicate the mRNA levels of *DsRed2*^{RNAi}, *Gb'E(z)*^{RNAi}, and intact crickets, respectively. In RNAi crickets, the optic lobes were collected 7 days after dsRNA injection. mRNA abundance was measured by qPCR with total RNA extracted from the optic lobes. Data collected from 3 to 15 independent measurements were averaged and plotted as mean ± SEM relative to the abundance of *Gb'rpl18a* mRNA, which was used as an internal reference. *Gb'E(z)* mRNA showed no daily rhythms in intact, *DsRed2*^{RNAi}, or *Gb'E(z)*^{RNAi} crickets. Values with different lower case letter at each ZT significantly differ from each other (Tukey-test, $P < 0.01$) except for those between *DsRed2*^{RNAi} in LD 20:4 and *Gb'E(z)*^{RNAi} in LD 12:12 at ZT 6 and between *Gb'E(z)*^{RNAi} in LD 12:12 and *Gb'E(z)*^{RNAi} in LD 20:4 at ZT 18 (Tukey-test, $P < 0.05$).

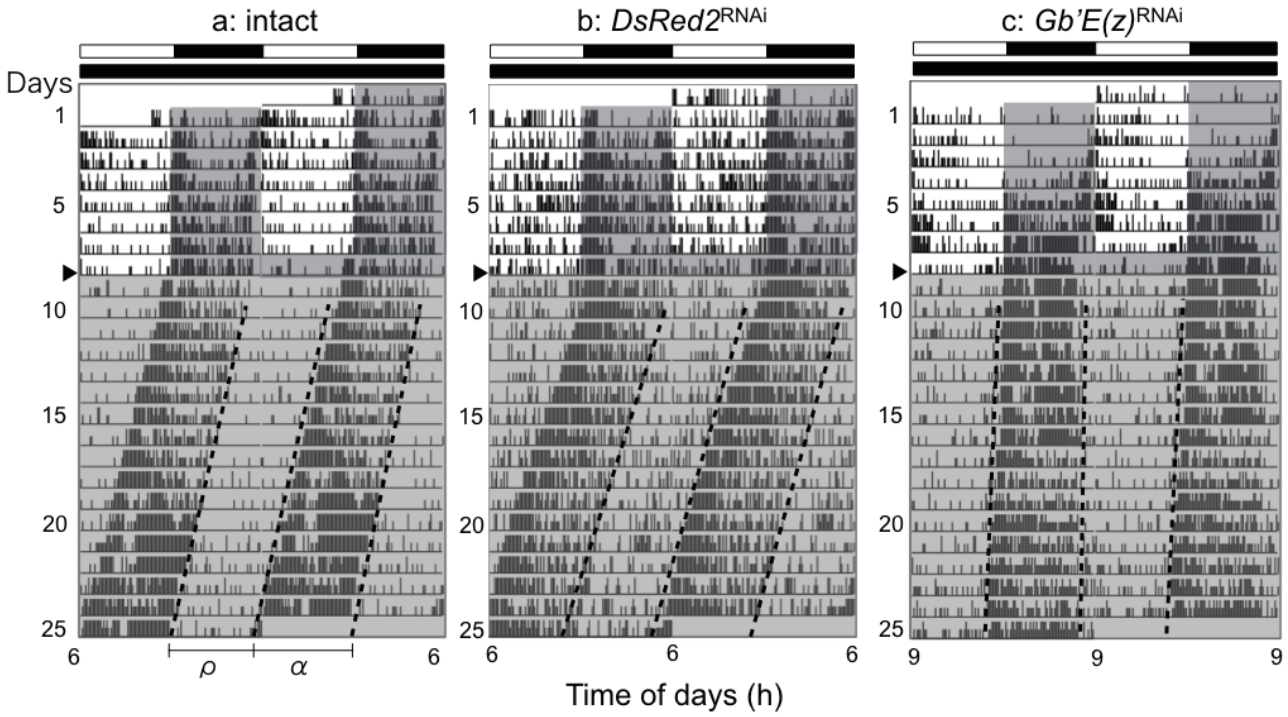

Fig. 3-2. Double-plotted actograms of locomotor activity of adult male crickets under LD 12:12 and DD. a, b, and c exemplify representative records of intact crickets (a) and those treated with dsRNA against *DsRed2* (b) or *Gb'E(z)* (c). Arrowheads indicate the day when the crickets were transferred from LD 12:12 to DD, at a constant temperature of 25 ± 0.5 °C. α and ρ indicate active phase and rest phase, respectively. Dotted lines indicate the onset and offset of the active phase. White and black bars above the actogram indicate the light and the dark phase, respectively. Gray area in the actogram indicates the dark phase.

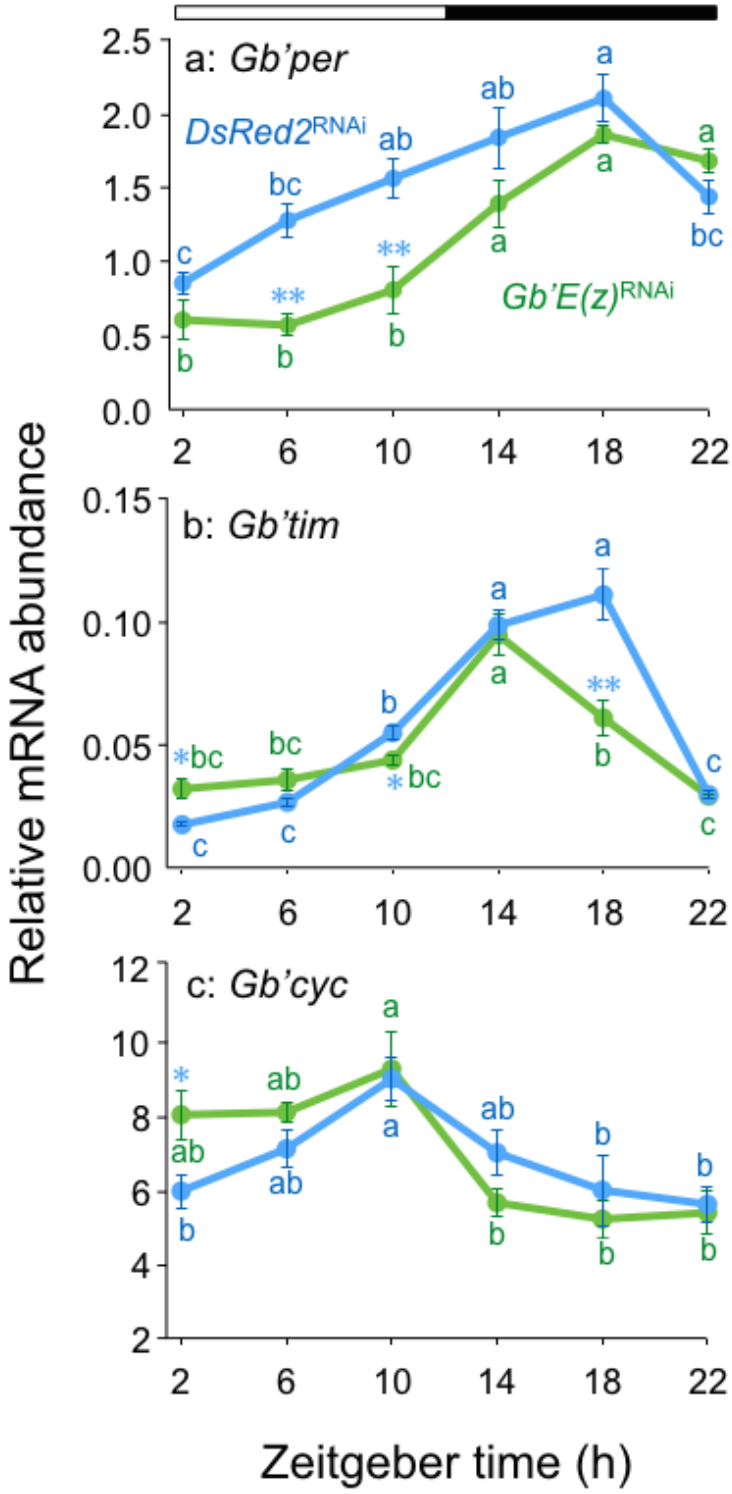

Fig. 3-3. Daily mRNA expression profiles of clock genes in the optic lobe of crickets under LD 12:12. Blue and green symbols indicate mRNA levels of *DsRed2*^{RNAi} and *Gb'E(z)*^{RNAi} crickets, respectively. The abundance of mRNA of *Gb'per* (a), *Gb'tim* (b), and *Gb'cyc* (c) was measured by qPCR, with total RNA extracted from the optic lobes, which were collected 7 days after dsRNA injection. Data collected from 3 to 15 independent measurements were averaged and plotted as mean ± SEM relative to the abundance of *Gb'rpl18a* mRNA, which was used as an internal reference. *$P < 0.05$, **$P < 0.01$, *t*-test vs *DsRed2*^{RNAi}. The mRNA of the three genes showed clear oscillation in both *DsRed2*^{RNAi} and *Gb'E(z)*^{RNAi} crickets (ANOVA, $P < 0.01$). Values with different lowercase letters differ significantly from each other (Tukey-test, $P < 0.05$).

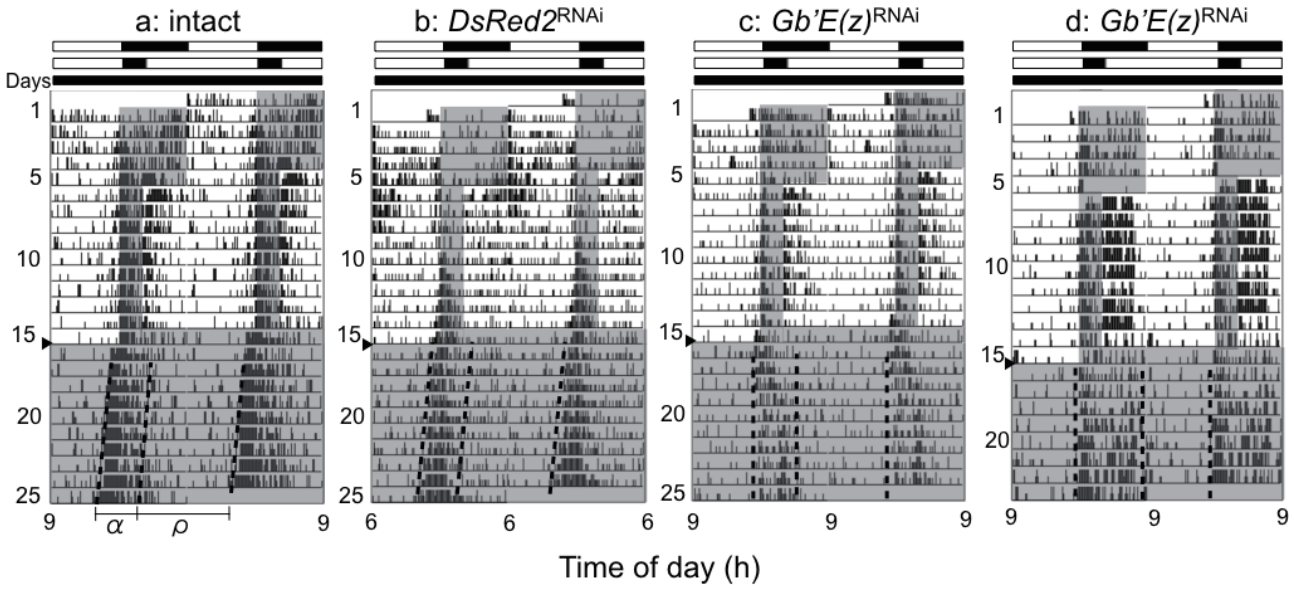

Fig. 3-4. Double-plotted actograms of locomotor activity of adult male crickets under LD 12:12, LD 20:4, and DD. a: intact cricket, b: cricket treated with ds*DsRed2*, c and d: crickets treated with ds*Gb'E(z)*. Crickets were exposed to LD 12:12 for the first 5 days, then in LD 20:4 for 10 days, and transferred to DD on the day indicated by an arrowhead, at a constant temperature of 25 ± 0.5 °C. α and ρ indicate active phase and rest phase, respectively. Dotted lines indicate onset and offset of the active phase. White and black bars above the actogram indicate the light and dark phases, respectively. Gray area in the actogram indicates the dark phase.

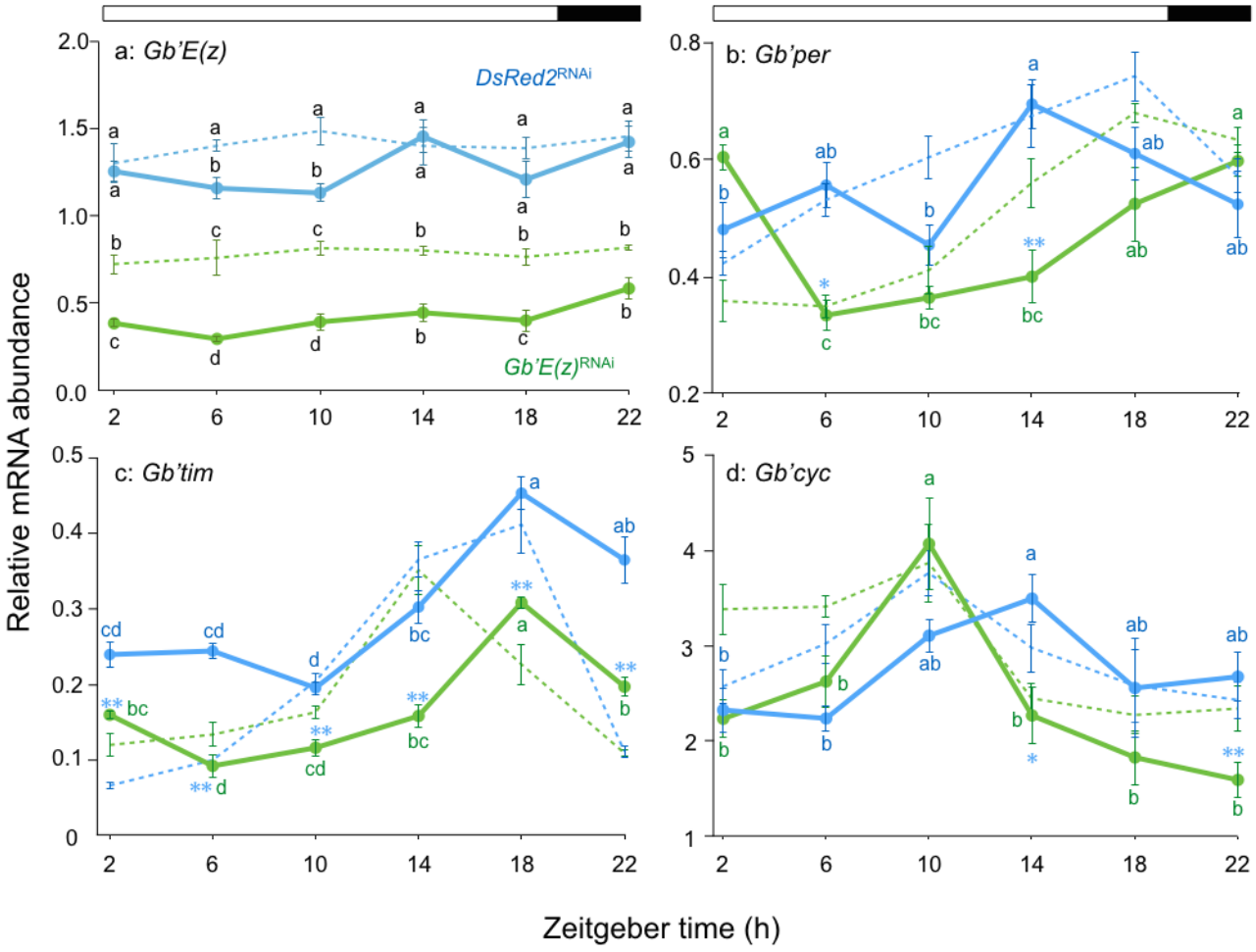

Fig. 3-5. Daily expression profiles of *Gb'E(z)* and clock genes in the cricket optic lobe under LD 20:4. Blue and green symbols with solid lines indicate the mRNA levels of *Gb'E(z)* (a), *Gb'per* (b), *Gb'tim* (c), and *Gb'cyc* (d) in *DsRed2*^{RNAi} and *Gb'E(z)*^{RNAi} crickets, respectively. For reference, data for LD 12:12 are shown by broken lines (blue, *DsRed2*^{RNAi} crickets; green, *Gb'E(z)*^{RNAi} crickets). mRNA abundance was measured by qPCR, with total RNA extracted from the optic lobes collected 7 days after transfer to LD 20:4. Data collected from 3 to 10 independent measurements were averaged and plotted as mean ± SEM. The values shown are relative to those of *Gb'rpl18a* mRNA, which was used as an internal reference. In LD 20:4, *Gb'E(z)* mRNA showed no significant daily oscillation in *DsRed2*^{RNAi} crickets (ANOVA, $P > 0.05$) but a significantly lower level at ZT 10 in comparison with that in LD 12:12 (a). *Gb'E(z)*^{RNAi} reduced the *Gb'E(z)* levels which were even lower than those of *Gb'E(z)* crickets in LD 12:12 at ZT 2-10 (Tukey-test, $P < 0.01$). The values with different lower case letter at each ZT significantly differ from each other (Tukey-test, $P < 0.01$, except between *DsRed2*^{RNAi} in LD 20:4 and *Gb'E(z)*^{RNAi} in LD 12:12 at ZT 10 and ZT 18 where $P < 0.05$). The mRNA levels of *Gb'per* (b), *Gb'tim* (c), and *Gb'cyc* (d) showed clear oscillatory profiles in both *DsRed2*^{RNAi} and *Gb'E(z)*^{RNAi} crickets (ANOVA, $P < 0.05$ for *Gb'cyc* in *DsRed2*^{RNAi}, and $P < 0.01$ for all other combinations). Values with different lowercase letters differ significantly from each other (Tukey-test, $P < 0.05$). *$P < 0.05$, **$P < 0.01$, *t*-test vs *DsRed2*^{RNAi} crickets in LD 20:4.

Chapter 4.
General discussion

Histone H3K27 methylation plays a role in leg regeneration patterning and photoperiodic responses of the circadian clock

It is known that epigenetics is defined as heritable changes in gene expression that are not caused by changes in the DNA sequence (Lan *et al*., 2007; Stewart *et al*., 2009; Wyngaarden *et al*., 2011). The relationship between epigenetic regulation and broad biological phenomena such as development, regeneration, tumor development, aging, profile of stem cell, and circadian rhythm, has been extensively studied (Brunet and Berger, 2014; Cridge *et al*., 2015; Dawson and Kouzarides, 2012; Herb, 2014; Hochedlinger and Plath, 2009; Yamanaka, 2009). This study focused on the epigenetic regulation by methylation on histone H3K27. E(z) and Utx methylate or demethylate histone H3K27, respectively, to induce heterochromatin or euchromatin formation for gene expression repression or activation of gene expression in insects (Hamada *et al*., 2015; Hamon and Cossart, 2008; Kawaguchi *et al*., 2012; Matsuoka *et al*., 2015). In this study, I analyzed the regulatory mechanism of gene expression by H3K27 methylation in leg regeneration and photoperiodic modulation circadian rhythms using the two-spotted cricket, *Gryllus bimaculatus* as a model animal.

When hind leg was amputated at tibia, normal control crickets regenerate tibia with tibial spur, tarsomere1/2/3 with tarsal spur and clow. In *Gb'E(z)*^{RNAi} and *Gb'Utx*^{RNAi} crickets, the regenerated leg showed abnormal structure which had ectopic tibia with tibial spur, lacking tarsal spur due to fused tarsomere1 and 2. These phenotypes were induced by ectopic expression of leg patterning genes with expanded *Gb'dac* expression in tarsus by RNAi against *Gb'E(z)* and disappearance of *Gb'Egfr* expression in mid tarsus by RNAi against *Gb'Utx* (Hamada *et al*., 2015).

As to circadian rhythms, the control crickets showed a nocturnal rhythm with activity concentrated in short dark phase. The circadian expression pattern of clock genes was altered by photoperiodic change from LD12:12 to LD20:4. However, *Gb'E(z)*^{RNAi} prevented photoperiod dependent changes in activity rhythms and circadian gene expressions, in that activity did not concentrate in short dark phase, and the peak phase of the circadian clock gene expression retained

the phase in LD12:12. These results suggested that *Gb'E(z)* modulates circadian rhythms in gene expression depending on photoperiodic changes to regulate the circadian locomotor rhythm.

In summary, this study revealed that the epigenetic regulation of gene expression by histone H3K27 methylation plays a key role in both leg regeneration and photoperiodic response of circadian rhythms in the cricket. It was shown that the same epigenetic control regulates expression of genes in a tissue and event dependent manner. The difference probably depends on the trigger and location by which the epigenetic factor E(z) is induced (Fig. 4-1). Recently, EzH2/E(z), a vertebrate homolog of E(z), has been elucidated to be involved in repression of allergy (Tumes *et al*., 2013) cancer development (Yoo and Hennighausen, 2012), and regulation of Hox genes during embryonic development (Lan et al., 2007; Matsuoka *et al*., 2015; Wyngaarden *et al*., 2011). *In situ* hybridization and qRT-PCR demonstrated that *Gb'E(z)* is expressed in whole developing embryo (Matsuoka *et al*., 2015), regenerating leg (Hamada *et al*., 2015), and the optic lobe. These findings suggest constant expression of E(z) in whole body from embryo to adult.

Accordingly, the epigenetic regulator E(z) controls various biological phenomena such as allergy repression, embryonic development, leg regeneration, cancer development, and circadian rhythms, through histone H3K27 methylation which in turn regulates expression of genes specifically involved in those phenomena in a tissue and/or event specific manner (Aguilar-Arnal and Sassone-Corsi, 2013; Aguilar-Arnal and Sassone-Corsi, 2015; Asher *et al*., 2008; Bellet and Sassone-Corsi, 2010; Brunet and Berger, 2014; Cridge *et al*., 2015; Dawson and Kouzarides, 2012; Doi *et al*., 2006; Etchegaray *et al*., 2006; Hamada *et al*., 2015; Hayashi *et al*., 2015a; Herb, 2014; Hochedlinger and Plath, 2009; Lan *et al*., 2007; Matsuoka *et al*., 2015; Ripperger and Merrow, 2011; Taylor and Hardin, 2008; Tumes *et al*., 2013; Wyngaarden *et al*., 2011; Yakushiji *et al*., 2007; Yakushiji *et al*., 2009; Yakushiji-Kaminatsui *et al*., 2016; Yung *et al*., 2015). Elucidation of the detailed mechanism of epigenetic regulation of specific gene expression might be applied to clinical studies on various diseases related to epigenetic control, including cancer, tissue/organ regeneration, and seasonal depression.

Figure and Figure legend

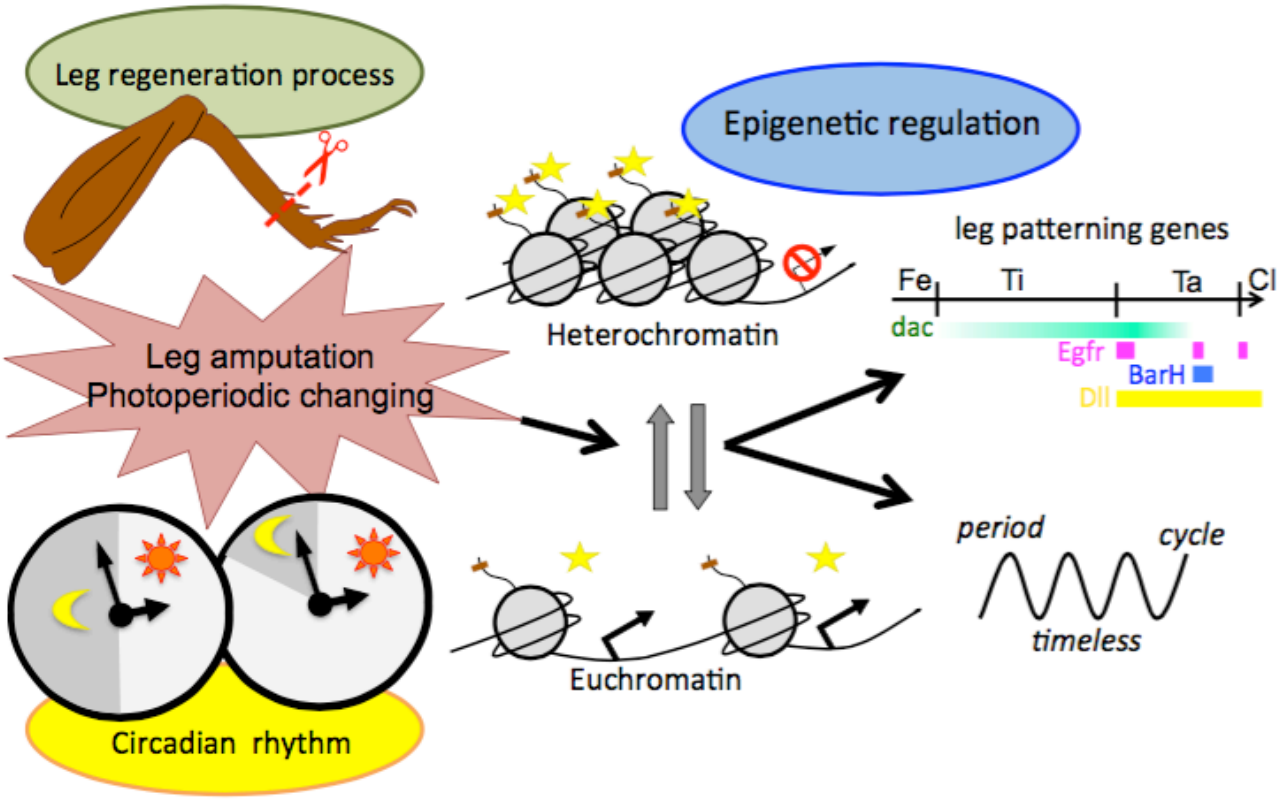

Fig. 4-1. The epigenetic regulation was induced by enviromental cues

Epigenetic regulation on leg patterning genes and clock component genes via chromatin structure was induced by leg amputation or photoperiodic changing.

References

Agata, K. and Inoue, T. (2012). Survey of the differences between regenerative and non-regenerative animals. *Dev Growth Differ* **54**, 143-152.

Agata, K., Saito, Y. and Nakajima, E. (2007). Unifying principles of regeneration I: Epimorphosis versus morphallaxis. *Dev Growth Differ* **49**, 73-78.

Aguilar-Arnal, L. and Sassone-Corsi, P. (2013). The circadian epigenome: how metabolism talks to chromatin remodeling. *Curr Opin Cell Biol* **25**, 170-176.

Aguilar-Arnal, L. and Sassone-Corsi, P. (2015). Chromatin landscape and circadian dynamics: Spatial and temporal organization of clock transcription. *Proc Natl Acad Sci U S A* **112**, 6863-6870.

Aguilar-Roblero, R., Díaz-Muñoz, M. and Fanjul-Moles, M. L. (2015). Mechanisms of Circadian Systems in Animals and Their Clinical Relevance. *Springer Cham Heidelberg New York Dordrecht London*.

Allada, R., White, N. E., So, W. V., Hall, J. C. and Rosbash, M. (1998). A mutant *Drosophila* homolog of mammalian *Clock* disrupts circadian rhythms and transcription of *period* and *timeless*. *Cell* **93**, 791-804.

Asher, G., Gatfield, D., Stratmann, M., Reinke, H., Dibner, C., Kreppel, F., Mostoslavsky, R., Alt, F. W. and Schibler, U. (2008). SIRT1 regulates circadian clock gene expression through PER2 deacetylation. *Cell* **134**, 317-328.

Bando, T., Hamada, Y., Kurita, K., Nakamura, T., Mito, T., Ohuchi, H. and Noji, S. (2011). Lowfat, a mammalian Lix1 homologue, regulates leg size and growth under the Dachsous/Fat signaling pathway during tissue regeneration. *Dev Dyn* **240**, 1440-1453.

Bando, T., Ishimaru, Y., Kida, T., Hamada, Y., Matsuoka, Y., Nakamura, T., Ohuchi, H., Noji, S. and Mito, T. (2013). Analysis of RNA-Seq data reveals involvement of JAK/STAT signalling during leg regeneration in the cricket *Gryllus bimaculatus*. *Development* **140**, 959-964.

Bando, T., Mito, T., Maeda, Y., Nakamura, T., Ito, F., Watanabe, T., Ohuchi, H. and Noji, S. (2009). Regulation of leg size and shape by the Dachsous/Fat signalling pathway during regeneration. *Development* **136**, 2235-2245.

Barrero, M. J. and Izpisua, B., J. C. (2011). Regenerating the epigenome. *EMBO Rep* **12**, 208-215.

Barrett, R. K. and Page, T. L. (1989). Effects of light on circadian pacemaker development. *Journal of Comparative Physiology A* **165**, 41-49.

Bellet, M. M. and Sassone-Corsi, P. (2010). Mammalian circadian clock and metabolism - the epigenetic link. *J Cell Sci* **123**, 3837-3848.

Borgens, R. B. (1982). Mice Regrow the Tips of Their Foretoes. *Science* **217**, 747-750.

Brunet, A. and Berger, S. L. (2014). Epigenetics of aging and aging-related disease. *J Gerontol A Biol Sci Med Sci* **69 Suppl 1**, S17-20.

Bryant, P. J. (1975). Pattern formation in the imaginal wing disc of *Drosophila melanogaster*: fate map, regeneration and duplication. *The Journal of experimental zoology* **193**, 49-77.

Campbell, G. and Tomlinson, A. (1995). Initiation of the proximodistal axis in insect legs. *Development* **121**, 619-628.

Collins, B. H., Rosato, E. and Kyriacou, C. P. (2004). Seasonal behavior in *Drosophila melanogaster* requires the photoreceptors, the circadian clock, and phospholipase C. *Proceedings of the National Academy of Sciences* **101**, 1945-1950.

Cridge, A. G., Leask, M. P., Duncan, E. J. and Dearden, P. K. (2015). What do studies of insect polyphenisms tell us about nutritionally-triggered epigenomic changes and their consequences? *Nutrients* **7**, 1787-1797.

Crosio, C., Cermakian, N., Allis, C. D. and Sassone-Corsi, P. (2000). Light induces chromatin modification in cells of the mammalian circadian clock. *Nat Neurosci* **3**, 1241-1247.

Dawson, M. A. and Kouzarides, T. (2012). Cancer epigenetics: from mechanism to therapy. *Cell* **150**, 12-27.
Ding, X., Wang, X., Sontag, S., Qin, J., Wanek, P., Lin, Q. and Zenke, M. (2014). The Polycomb Protein Ezh2 Impacts on Induced Pluripotent Stem Cell Generation. *Stem Cells and Development* **23**, 931-940.
Doi, M., Hirayama, J. and Sassone-Corsi, P. (2006). Circadian regulator CLOCK is a histone acetyltransferase. *Cell* **125**, 497-508.
Dubruille, R., Murad, A., Rosbash, M. and Emery, P. (2009). A constant light-genetic screen identifies KISMET as a regulator of circadian photoresponses. *PLoS Genet* **5**, e1000787.
Dunlap, J. C. (1999). Molecular bases for circadian clocks. *Cell* **96**, 271-290.
Dunlap, J. C., Loros, J. and DeCoursey, P. J. (2004). Chronobiology: Biological Timekeeping. *Journal of Heredity* **95**, 91-92.
Endo, T., Bryant, S. V. and Gardiner, D. M. (2004). A stepwise model system for limb regeneration. *Dev Biol* **270**, 135-145.
Etchegaray, J. P., Yang, X., DeBruyne, J. P., Peters, A. H., Weaver, D. R., Jenuwein, T. and Reppert, S. M. (2006). The polycomb group protein EZH2 is required for mammalian circadian clock function. *J Biol Chem* **281**, 21209-21215.
French, V. (1976). Leg regeneration in the cockroach, *Blatella germanica*. II. Regeneration from a non-congruent tibial graft/host junction. *J Embryol Exp Morphol* **35**, 267-301.
Fustin, J. M., Doi, M., Yamaguchi, Y., Hida, H., Nishimura, S., Yoshida, M., Isagawa, T., Morioka, M. S., Kakeya, H., Manabe, I. and Okamura, H. (2013). RNA-methylation-dependent RNA processing controls the speed of the circadian clock. *Cell* **155**, 793-806.
Gibson, M. C. and Schubiger, G. (1999). Hedgehog is required for activation of *engrailed* during regeneration of fragmented *Drosophila* imaginal discs. *Development* **126**, 1591-1599.
Glastad, K. M., Hunt, B. G., Yi, S. V. and Goodisman, M. A. (2011). DNA methylation in insects: on the brink of the epigenomic era. *Insect Mol Biol* **20**, 553-565.
Goto, S. G. (2013). Roles of circadian clock genes in insect photoperiodism. *Entomological Science* **16**, 1-16.
Hamada, Y., Bando, T., Nakamura, T., Ishimaru, Y., Mito, T., Noji, S., Tomioka, K. and Ohuchi, H. (2015). Leg regeneration is epigenetically regulated by histone H3K27 methylation in the cricket *Gryllus bimaculatus*. *Development* **142**, 2916-2927.
Hamon, M. A. and Cossart, P. (2008). Histone modifications and chromatin remodeling during bacterial infections. *Cell Host Microbe* **4**, 100-109.
Handberg-Thorsager, M., Fernandez, E. and Salo, E. (2008). Stem cells and regeneration in planarians. *Frontiers in bioscience : a journal and virtual library* **13**, 6374-6394.
Handler, A. M. and Konopka, R. J. (1979). Transplantation of a circadian pacemaker in *Drosophila*. *Nature* **279**, 236-238.
Hardin, P. E. (2009). Molecular mechanisms of circadian timekeeping in *Drosophila*. *Sleep and Biological Rhythms* **7**, 235-242.
Hayashi, S., Kawaguchi, A., Uchiyama, I., Kawasumi-Kita, A., Kobayashi, T., Nishide, H., Tsutsumi, R., Tsuru, K., Inoue, T., Ogino, H., Agata, K., Tamura, K. and Yokoyama, H. (2015a). Epigenetic modification maintains intrinsic limb-cell identity in *Xenopus* limb bud regeneration. *Dev Biol* **406**, 271-282.
Hayashi, S., Yokoyama, H. and Tamura, K. (2015b). Roles of Hippo signaling pathway in size control of organ regeneration. *Dev Growth Differ* **57**, 341-351.
Hayashi, T., Yokotani, N., Tane, S., Matsumoto, A., Myouga, A., Okamoto, M. and Takeuchi, T. (2013). Molecular genetic system for regenerative studies using newts. *Dev Growth Differ* **55**, 229-236.
Helfrich, C., Cymborowski, B. and Engelmann, W. (1985). Circadian activity rhythm of the house fly continues after optic tract severance and lobectomy. *Chronobiol Int* **2**, 19-32.
Herb, B. R. (2014). Epigenetics as an answer to Darwin's "special difficulty". *Front Genet* **5**, 321.

Herz, H. M., Madden, L. D., Chen, Z., Bolduc, C., Buff, E., Gupta, R., Davuluri, R., Shilatifard, A., Hariharan, I. K. and Bergmann, A. (2010). The H3K27me3 demethylase dUTX is a suppressor of Notch- and Rb-dependent tumors in *Drosophila*. *Mol Cell Biol* **30**, 2485-2497.

Hirose, K., Shimoda, N. and Kikuchi, Y. (2013). Transient reduction of 5-methylcytosine and 5-hydroxymethylcytosine is associated with active DNA demethylation during regeneration of zebrafish fin. *Epigenetics* **8**, 899-906.

Hochedlinger, K. and Plath, K. (2009). Epigenetic reprogramming and induced pluripotency. *Development* **136**, 509-523.

Hubert, A., Henderson, J. M., Ross, K. G., Cowles, M. W., Torres, J. and Zayas, R. M. (2014). Epigenetic regulation of planarian stem cells by the SET1/MLL family of histone methyltransferases. *Epigenetics* **8**, 79-91.

Hwang-Verslues, W. W., Chang, P. H., Jeng, Y. M., Kuo, W. H., Chiang, P. H., Chang, Y. C., Hsieh, T. H., Su, F. Y., Lin, L. C., Abbondante, S., Yang, C. Y., Hsu, H. M., Yu, J. C., Chang, K. J., Shew, J. Y., Lee, E. Y. and Lee, W. H. (2013). Loss of corepressor PER2 under hypoxia up-regulates OCT1-mediated EMT gene expression and enhances tumor malignancy. *Proc Natl Acad Sci U S A* **110**, 12331-12336.

Inoue, Y., Mito, T., Miyawaki, K., Matsushima, K., Shinmyo, Y., Heanue, T. A., Mardon, G., Ohuchi, H. and Noji, S. (2002). Correlation of expression patterns of *homothorax*, *dachshund*, and *Distal-less* with the proximodistal segmentation of the cricket leg bud. *Mechanisms of Development* **113**, 141-148.

Ishimaru, Y., Nakamura, T., Bando, T., Matsuoka, Y., Ohuchi, H., Noji, S. and Mito, T. (2015). Involvement of *dachshund* and *Distal-less* in distal pattern formation of the cricket leg during regeneration. *Sci Rep* **5**, 8387.

Kalantry, S. (2011). Recent advances in X-chromosome inactivation. *J Cell Physiol* **226**, 1714-1718.

Katsuyama, T. and Paro, R. (2011). Epigenetic reprogramming during tissue regeneration. *FEBS Lett* **585**, 1617-1624.

Kawaguchi, A., Ochi, H., Sudou, N. and Ogino, H. (2012). Comparative expression analysis of the H3K27 demethylases, JMJD3 and UTX, with the H3K27 methylase, EZH2, in *Xenopus*. *Int J Dev Biol* **56**, 295-300.

Koga, M., Ushirogawa, H. and Tomioka, K. (2005). Photoperiodic modulation of circadian rhythms in the cricket *Gryllus bimaculatus*. *J Insect Physiol* **51**, 681-690.

Kojima, T. (2004). The mechanism of *Drosophila* leg development along the proximodistal axis. *Dev Growth Differ* **46**, 115-129.

Konopka, R. J. and Benzer, S. (1971). Clock mutants of *Drosophila melanogaster*. *Proc Natl Acad Sci U S A* **68**, 2112-2116.

Konstantinides, N. and Averof, M. (2014). A Common Cellular Basis for Muscle Regeneration in Arthropods and Vertebrates. *Science* **343**, 788-791.

Kwok, R. S., Li, Y. H., Lei, A. J., Edery, I. and Chiu, J. C. (2015). The Catalytic and Non-catalytic Functions of the *Brahma* Chromatin-Remodeling Protein Collaborate to Fine-Tune Circadian Transcription in *Drosophila*. *PLoS Genet* **11**, e1005307.

Kyriacou, C. P. and Rosato, E. (2000). Squaring up the E-box. *J Biol Rhythms* **15**, 483-490.

Lan, F., Bayliss, P. E., Rinn, J. L., Whetstine, J. R., Wang, J. K., Chen, S., Iwase, S., Alpatov, R., Issaeva, I., Canaani, E., Roberts, T. M., Chang, H. Y. and Shi, Y. (2007). A histone H3 lysine 27 demethylase regulates animal posterior development. *Nature* **449**, 689-694.

Lee, N., Maurange, C., Ringrose, L. and Paro, R. (2005). Suppression of Polycomb group proteins by JNK signalling induces transdetermination in *Drosophila* imaginal discs. *Nature* **438**, 234-237.

Lyko, F. and Maleszka, R. (2011). Insects as innovative models for functional studies of DNA methylation. *Trends Genet* **27**, 127-131.

Majercak, J., Chen, W. F. and Edery, I. (2004). Splicing of the *period* Gene 3'-Terminal Intron Is Regulated by Light, Circadian Clock Factors, and Phospholipase C. *Molecular and Cellular Biology* **24**, 3359-3372.

Majercak, J., Sidote, D., Hardin, P. E. and Edery, I. (1999). How a circadian clock adapts to seasonal decreases in temperature and day length. *Neuron* **24**, 219-230.

Makanae, A., Mitogawa, K. and Satoh, A. (2014a). Co-operative Bmp- and Fgf-signaling inputs convert skin wound healing to limb formation in urodele amphibians. *Dev Biol* **396**, 57-66.

Makanae, A., Mitogawa, K. and Satoh, A. (2014b). Implication of two different regeneration systems in limb regeneration. *Regeneration* **1**, 1-9.

Mansour, A. A., Gafni, O., Weinberger, L., Zviran, A., Ayyash, M., Rais, Y., Krupalnik, V., Zerbib, M., Amann-Zalcenstein, D., Maza, I., Geula, S., Viukov, S., Holtzman, L., Pribluda, A., Canaani, E., Horn-Saban, S., Amit, I., Novershtern, N. and Hanna, J. H. (2012). The H3K27 demethylase Utx regulates somatic and germ cell epigenetic reprogramming. *Nature* **488**, 409-413.

Mao, Y., Kucuk, B. and Irvine, K. D. (2009). *Drosophila lowfat*, a novel modulator of Fat signaling. *Development* **136**, 3223-3233.

Matsuoka, Y., Bando, T., Watanabe, T., Ishimaru, Y., Noji, S., Popadic, A. and Mito, T. (2015). Short germ insects utilize both the ancestral and derived mode of Polycomb group-mediated epigenetic silencing of Hox genes. *Biol Open* **4**, 702-709.

McCusker, C. D. and Gardiner, D. M. (2013). Positional information is reprogrammed in blastema cells of the regenerating limb of the axolotl (*Ambystoma mexicanum*). *PLoS One* **8**, e77064.

Meinhardt, H. (1982). Theory of regulatory functions of the genes in the bithorax complex. *Progress in clinical and biological research* **85 Pt A**, 337-348.

Meissner, A. (2010). Epigenetic modifications in pluripotent and differentiated cells. *Nat Biotechnol* **28**, 1079-1088.

Menet, J. S., Pescatore, S. and Rosbash, M. (2014). CLOCK:BMAL1 is a pioneer-like transcription factor. *Genes Dev* **28**, 8-13.

Mito, T., Inoue, Y., Kimura, S., Miyawaki, K., Niwa, N., Shinmyo, Y., Ohuchi, H. and Noji, S. (2002). Involvement of *hedgehog*, *wingless*, and *dpp* in the initiation of proximodistal axis formation during the regeneration of insect legs, a verification of the modified boundary model. *Mech Dev* **114**, 27-35.

Mito, T. and Noji, S. (2008). The Two-Spotted Cricket *Gryllus bimaculatus*: An Emerging Model for Developmental and Regeneration Studies. *CSH protocols* **2008**, pdb.emo110.

Mitogawa, K., Hirata, A., Moriyasu, M., Makanae, A., Miura, S., Endo, T. and Satoh, A. (2014). Ectopic blastema induction by nerve deviation and skin wounding: a new regeneration model in *Xenopus laevis*. *Regeneration* **1**, 26-36.

Mitogawa, K., Makanae, A., Satoh, A. and Satoh, A. (2015). Comparative Analysis of Cartilage Marker Gene Expression Patterns during Axolotl and *Xenopus* Limb Regeneration. *PLoS One* **10**, e0133375.

Miura, S., Takahashi, Y., Satoh, A. and Endo, T. (2015). Skeletal callus formation is a nerve-independent regenerative response to limb amputation in mice and *Xenopus*. *Regeneration* **2**, 202-216.

Morales Torres, C., Laugesen, A. and Helin, K. (2013). Utx is required for proper induction of ectoderm and mesoderm during differentiation of embryonic stem cells. *PLoS One* **8**, e60020.

Moriyama, Y., Sakamoto, T., Karpova, S. G., Matsumoto, A., Noji, S. and Tomioka, K. (2008). RNA interference of the clock gene *period* disrupts circadian rhythms in the cricket *Gryllus bimaculatus*. *J Biol Rhythms* **23**, 308-318.

Muneoka, K., Allan, C. H., Yang, X., Lee, J. and Han, M. (2008). Mammalian regeneration and regenerative medicine. *Birth Defects Res C Embryo Today* **84**, 265-280.

Nakamura, T., Mito, T., Bando, T., Ohuchi, H. and Noji, S. (2008a). Dissecting insect leg regeneration through RNA interference. *Cell Mol Life Sci* **65**, 64-72.
Nakamura, T., Mito, T., Miyawaki, K., Ohuchi, H. and Noji, S. (2008b). EGFR signaling is required for re-establishing the proximodistal axis during distal leg regeneration in the cricket *Gryllus bimaculatus* nymph. *Dev Biol* **319**, 46-55.
Nakamura, T., Mito, T., Tanaka, Y., Bando, T., Ohuchi, H. and Noji, S. (2007). Involvement of canonical Wnt/Wingless signaling in the determination of the positional values within the leg segment of the cricket *Gryllus bimaculatus*. *Dev Growth Differ* **49**, 79-88.
Nakamura, T., Yoshizaki, M., Ogawa, S., Okamoto, H., Shinmyo, Y., Bando, T., Ohuchi, H., Noji, S. and Mito, T. (2010). Imaging of transgenic cricket embryos reveals cell movements consistent with a syncytial patterning mechanism. *Curr Biol* **20**, 1641-1647.
Neufeld, D. A. and Zhao, W. (1995). Bone regrowth after digit tip amputation in mice is equivalent in adults and neonates. *Wound Repair Regen* **3**, 461-466.
Niwa, N., Akimoto-Kato, A., Sakuma, M., Kuraku, S. and Hayashi, S. (2013). Homeogenetic inductive mechanism of segmentation in polychaete tail regeneration. *Dev Biol* **381**, 460-470.
Nye, H. L., Cameron, J. A., Chernoff, E. A. and Stocum, D. L. (2003). Regeneration of the urodele limb: a review. *Dev Dyn* **226**, 280-294.
Page, T. L. (1982). Transplantation of the cockroach circadian pacemaker. *Science* **216**, 73-75.
Page, T. L. (1983). Effects of optic-tract regeneration on internal coupling in the circadian system of the cockroach. *j comp Physiol* **153**, 353-363.
Page, T. L., Caldarola, P. C. and Pittendrigh, C. S. (1977). Mutual Entrainment of Bilaterally Distributed Circadian Pacemakers. *Proceedings of the National Academy of Sciences of the United States of America* **74**, 1277-1281.
Refinetti, R. (2002). Compression and expansion of circadian rhythm in mice under long and short photoperiods. *Integrative Physiological & Behavioral Science* **37**, 114-127.
Repiso, A., Bergantinos, C., Corominas, M. and Serras, F. (2011). Tissue repair and regeneration in *Drosophila* imaginal discs. *Dev Growth Differ* **53**, 177-185.
Ripperger, J. A. and Merrow, M. (2011). Perfect timing: epigenetic regulation of the circadian clock. *FEBS Lett* **585**, 1406-1411.
Robb, S. M. and Sanchez, A., A. (2014). Histone modifications and regeneration in the planarian *Schmidtea mediterranea*. *Current topics in developmental biology* **108**, 71-93.
Roberts, S. K. d. F. (1960). Circadian activity rhythms in cockroaches. I. The free-running rhythm in steady-state. *Journal of Cellular and Comparative Physiology* **55**, 99-110.
Rutila, J. E., Suri, V., Le, M., So, W. V., Rosbash, M. and Hall, J. C. (1998). CYCLE is a second bHLH-PAS clock protein essential for circadian rhythmicity and transcription of *Drosophila period* and *timeless*. *Cell* **93**, 805-814.
Sakamoto, T., Uryu, O. and Tomioka, K. (2009). The clock gene *period* plays an essential role in photoperiodic control of nymphal development in the cricket *Modicogryllus siamensis*. *J Biol Rhythms* **24**, 379-390.
Satoh, A., Mitogawa, K. and Makanae, A. (2015). Regeneration inducers in limb regeneration. *Dev Growth Differ* **57**, 421-429.
Saunders, D. S. (2012). Insect photoperiodism: seeing the light. *Physiological Entomology* **37**, 207-218.
Schmid, B., Helfrich-Forster, C. and Yoshii, T. (2011). A new ImageJ plug-in "ActogramJ" for chronobiological analyses. *J Biol Rhythms* **26**, 464-467.
Shah, M. V., Namigai, E. K. and Suzuki, Y. (2011). The role of canonical Wnt signaling in leg regeneration and metamorphosis in the red flour beetle *Tribolium castaneum*. *Mech Dev* **128**, 342-358.

Shaw, T. and Martin, P. (2009). Epigenetic reprogramming during wound healing: loss of polycomb-mediated silencing may enable upregulation of repair genes. *EMBO Rep* **10**, 881-886.

Shpargel, K. B., Starmer, J., Yee, D., Pohlers, M. and Magnuson, T. (2014). KDM6 demethylase independent loss of histone H3 lysine 27 trimethylation during early embryonic development. *PLoS Genet* **10**, e1004507.

Sokolove, P. G. and Bushell, W. N. (1978). The chi square periodogram: Its utility for analysis of circadian rhythms. *Journal of Theoretical Biology* **72**, 131-160.

Stanewsky, R. (2003). Genetic analysis of the circadian system in *Drosophila melanogaster* and mammals. *Journal of Neurobiology* **54**, 111-147.

Stewart, S., Tsun, Z. Y. and Izpisua Belmonte, J. C. (2009). A histone demethylase is necessary for regeneration in zebrafish. *Proc Natl Acad Sci U S A* **106**, 19889-19894.

Strub, S. (1979). Leg regeneration in insects. An experimental analysis in *Drosophila* and a new interpretation. *Dev Biol* **69**, 31-45.

Sun, G. and Irvine, K. D. (2014). Control of growth during regeneration. *Current topics in developmental biology* **108**, 95-120.

Syrova, Z., Dolezel, D., Saumann, I. and Hodkova, M. (2003). Photoperiodic regulation of diapause in linden bugs: are *period* and *Clock* genes involved? *Cell Mol Life Sci* **60**, 2510-2515.

Tajiri, R., Misaki, K., Yonemura, S. and Hayashi, S. (2011). Joint morphology in the insect leg: evolutionary history inferred from *Notch* loss-of-function phenotypes in *Drosophila*. *Development* **138**, 4621-4626.

Takayama, K., Shimoda, N., Takanaga, S., Hozumi, S. and Kikuchi, Y. (2014). Expression patterns of *dnmt3aa*, *dnmt3ab*, and *dnmt4* during development and fin regeneration in zebrafish. *Gene expression patterns : GEP* **14**, 105-110.

Tamaki, S., Takemoto, S., Uryu, O., Kamae, Y. and Tomioka, K. (2013). Opsins are involved in nymphal photoperiodic responses in the cricket *Modicogryllus siamensis*. *Physiological Entomology* **38**, 163-172.

Tamura, K., Ohgo, S. and Yokoyama, H. (2010). Limb blastema cell: a stem cell for morphological regeneration. *Dev Growth Differ* **52**, 89-99.

Taniguchi, N. and Tomioka, K. (2003). Duration of development and number of nymphal instars are differentially regulated by photoperiod in the cricket *Modicogryllus siamensis* (Orthoptera : Gryllidae). *European Journal of Entomology* **100**, 275-281.

Tataroglu, O. and Emery, P. (2015). The molecular ticks of the *Drosophila* circadian clock. *Curr Opin Insect Sci* **7**, 51-57.

Tauber, T. J., Tauber, C. A. and Masaki, S. (1986). Seasonal Adaptations of Insects. *New York, Oxford University Press*.

Taylor, P. and Hardin, P. E. (2008). Rhythmic E-box binding by CLK-CYC controls daily cycles in *per* and *tim* transcription and chromatin modifications. *Mol Cell Biol* **28**, 4642-4652.

Tomioka, K. (2014). Chronobiology of crickets: a review. *Zoolog Sci* **31**, 624-632.

Tomioka, K. and Chiba, Y. (1982). Persistence of Circadian ERG Rhythm in the Cricket with Optic Tract Severed. *Naturwissenschaften* **69**, 395-396.

Tomioka, K. and Chiba, Y. (1984). Effects of Nymphal Stage Optic-Nerve Severance or Optic Lobe Removal on the Circadian Locomotor Rhythm of the Cricket, *Gryllus bimaculatus*. *Zoological Science* **1**, 375-382.

Tomioka, K. and Chiba, Y. (1989a). Light cycle during post-embryonic development affects adult circadian parameters of the cricket (*Gryllus bimaculatus*) optic lobe pacemaker. *Journal of Insect Physiology* **35**, 273-276.

Tomioka, K. and Chiba, Y. (1989b). Photoperiod during Post-Embryonic Development Affects Some Parameters of Adult Circadian-Rhythm in the Cricket, *Gryllus bimaculatus*. *Zoological Science* **6**, 565-571.

Tomioka, K. and Chiba, Y. (1992). Characterization of an optic lobe circadian pacemaker by *in situ* and *in vitro* recording of neural activity in the cricket, *Gryllus bimaculatus*. *Journal of Comparative Physiology A* **171**, 1-7.

Truby, P. R. (1985). Separation of wound healing from regeneration in the cockroach leg. *J Embryol Exp Morphol* **85**, 177-190.

Truman, J. W. (1974). Physiology of Insect Rhythms
IV. Role of the Brain in the Regulation of the Flight Rhythm of the Giant Silkmoths. *Journal of Comparative Physiology* **95**, 281-296.

Tsutsumi, R., Inoue, T., Yamada, S. and Agata, K. (2015). Reintegration of the regenerated and the remaining tissues during joint regeneration in the newt *Cynops pyrrhogaster*. *Regeneration* **2**, 26-36.

Tumes, D. J., Onodera, A., Suzuki, A., Shinoda, K., Endo, Y., Iwamura, C., Hosokawa, H., Koseki, H., Tokoyoda, K., Suzuki, Y., Motohashi, S. and Nakayama, T. (2013). The polycomb protein Ezh2 regulates differentiation and plasticity of CD4(+) T helper type 1 and type 2 cells. *Immunity* **39**, 819-832.

Tweedell, K. S. (2010). The urodele limb regeneration blastema: the cell potential. *ScientificWorldJournal* **10**, 954-971.

Umesono, Y., Tasaki, J., Nishimura, Y., Hrouda, M., Kawaguchi, E., Yazawa, S., Nishimura, O., Hosoda, K., Inoue, T. and Agata, K. (2013). The molecular logic for planarian regeneration along the anterior-posterior axis. *Nature* **500**, 73-76.

Uryu, O., Karpova, S. G. and Tomioka, K. (2013). The clock gene cycle plays an important role in the circadian clock of the cricket *Gryllus bimaculatus*. *J Insect Physiol* **59**, 697-704.

Watanabe, T., Ochiai, H., Sakuma, T., Horch, H. W., Hamaguchi, N., Nakamura, T., Bando, T., Ohuchi, H., Yamamoto, T., Noji, S. and Mito, T. (2012). Non-transgenic genome modifications in a hemimetabolous insect using zinc-finger and TAL effector nucleases. *Nat Commun* **3**, 1017.

Williams, J. A. and Sehgal, A. (2001). Molecular components of the circadian system in *Drosophila*. *Annu Rev Physiol* **63**, 729-755.

Worley, M. I., Setiawan, L. and Hariharan, I. K. (2012). Regeneration and transdetermination in *Drosophila* imaginal discs. *Annu Rev Genet* **46**, 289-310.

Wright, K. P., Lowry, C. A. and Lebourgeois, M. K. (2012). Circadian and wakefulness-sleep modulation of cognition in humans. *Front Mol Neurosci* **5**, 50.

Wyngaarden, L. A., Delgado-Olguin, P., Su, I. H., Bruneau, B. G. and Hopyan, S. (2011). Ezh2 regulates anteroposterior axis specification and proximodistal axis elongation in the developing limb. *Development* **138**, 3759-3767.

Yakushiji, N., Suzuki, M., Satoh, A., Sagai, T., Shiroishi, T., Kobayashi, H., Sasaki, H., Ide, H. and Tamura, K. (2007). Correlation between *Shh* expression and DNA methylation status of the limb-specific *Shh* enhancer region during limb regeneration in amphibians. *Dev Biol* **312**, 171-182.

Yakushiji, N., Yokoyama, H. and Tamura, K. (2009). Repatterning in amphibian limb regeneration: A model for study of genetic and epigenetic control of organ regeneration. *Semin Cell Dev Biol* **20**, 565-574.

Yakushiji-Kaminatsui, N., Kondo, T., Endo, T. A., Koseki, Y., Kondo, K., Ohara, O., Vidal, M. and Koseki, H. (2016). RING1 proteins contribute to early proximal-distal specification of the forelimb bud by restricting *Meis2* expression. *Development* **143**, 276-285.

Yamanaka, S. (2009). Elite and stochastic models for induced pluripotent stem cell generation. *Nature* **460**, 49-52.

Yoo, K. H. and Hennighausen, L. (2012). EZH2 methyltransferase and H3K27 methylation in breast cancer. *Int J Biol Sci* **8**, 59-65.

Yung, P. Y., Stuetzer, A., Fischle, W., Martinez, A. M. and Cavalli, G. (2015). Histone H3 Serine 28 Is Essential for Efficient Polycomb-Mediated Gene Repression in *Drosophila*. *Cell Rep* **11**, 1437-1445.